# MATHEMATICAL MODELLING OF PHASE TRANSFORMATION IN A PLAIN CARBON EUTECTOID STEEL

By

IYER JAYARAMAN RAJAGOPALAN

B. Tech. (Metallurgical Engineering), Indian Institute of Technology, Bombay, India, 1974

M.B.A., Indian Institute of Management, Ahmedabad, India, 1979

A THESIS SUBMITTED IN PARTIAL FULFILLMENT OF THE REQUIREMENTS FOR THE DEGREE OF MASTER OF APPLIED SCIENCE

in

THE FACULTY OF GRADUATE STUDIES

Department of Metallurgical Engineering

We accept this thesis as conforming to the required standard

THE UNIVERSITY OF BRITISH COLUMBIA

October 1983

In presenting this thesis in partial fulfilment of the requirements for an advanced degree at the University of British Columbia, I agree that the Library shall make it freely available for reference and study. I further agree that permission for extensive copying of this thesis for scholarly purposes may be granted by the head of my department or by his or her representatives. It is understood that copying or publication of this thesis for financial gain shall not be allowed without my written permission.

Department of METALLURGICAL ENGINEERING

The University of British Columbia
1956 Main Mall
Vancouver, Canada
V6T 1Y3

Date 14-10-1983

# ABSTRACT

With the ultimate objective of quantitatively predicting the mechanical properties of steels, a mathematical model has been developed to compute the transient temperature distribution and austenite-pearlite transformation in an eutectoid steel rod during controlled cooling. The model is based on one-dimensional, unsteady-state heat conduction and incorporates empirical TTT data in the form of the parameters n and b(T) from the Avrami equation and the CCT start time, $t_{AV-CCT}$. This data was obtained using a diametral dilatometer for an eutectoid steel of composition 0.82% C - 0.82% Mn - 0.26% Si and a grain size of 5-7 ASTM. CCT kinetics are predicted from the TTT data by the additivity principle originally proposed by Scheil.

The adequacy of the model was checked by comparing model predictions of the centre-line temperature of 9 and 10 mm diameter rods to measurements made during air cooling from an initial temperature between 840 and 870°C. The agreement obtained was good. Also the conditions determined by Avrami and Cahn for the additivity principle to hold were checked. Even though model predictions of CCT from TTT data generally were good, the application restrictions were not satisfied. Thus a new sufficient condition has been proposed which holds

for the steel under study and establishes a firm theoretical foundation for model calculations. The condition, termed "effective site saturation", indicates that for growth dominated reactions, wherein the rate of reaction is governed by the growth of nuclei nucleated very early in the reaction, the kinetics can be considered additive due to the relative unimportance of subsequent nucleation. This condition suggests that the additivity rule may have a much broader range of applicability than was originally supposed.

The calculation of TTT from CCT has been studied and a new method, involving an interative procedure using the additivity rule, has been derived. Agreement between calculated and measured TTT data is good.

Finally the model has been employed to study the effect of centre segregation of manganese on the transformation behaviour of eutectoid steel rods and also to predict the mechanical properties of the same steel. Calculations indicate that segregation can lead to the formation of martensite at the centre of the rods with faster cooling rates. The calculation of mechanical properties is based on published relationships between pearlite spacing, undercooling and mechanical properties.

# TABLE OF CONTENTS

Chapter | Page

APPENDICES

# LIST OF TABLES

Chapter 6



Chapter 7

# LIST OF FIGURES

Chapter 6

| Symbol | Description |
|---|---|
| $N$ | Nucleation rate (constant) |
| $N(T)$ | Nucleation rate (function of temperature) |
| $G$ | Growth rate (constant) |
| $G(T)$ | Growth rate (function of temperature) |
| $t$ | Time |
| $t_x$ | Time for x% volume transformed |
| $V_{ex}$ | Extended volume transformed |
| $V$ | Real volume transformed (extended volume corrected for impingement) |
| $V_{ex}^{t_x}$ | Extended volume transformed at $t_x$ |
| $V_{ex_{0/t_y}}^{t_x}$ | Extended volume transformed at time $t_x$ of nuclei nucleating between time = 0 and time = $t_y$ |
| $X$ | Volume fraction transformed |
| $\rho$ | Density |
| $C_p$ | Specific heat |
| $K$ | Thermal conductivity |
| $T$ | Temperature |
| $Z$ | Dummy variable representing time |

# ACKNOWLEDGEMENT

I would like to thank Professors J. K. Brimacombe and E. B. Hawbolt for their help and guidance during the course of the project. Thanks are also due to Mr. Binh Chau, Mr. Baha Kuban, Mr. S. Chattopadhyay, Mr. Ramaprasad and Mr. Neil Walker for all the help rendered. Financial assistance was received in the form of a research grant from the American Iron and Steel Institute.

# Chapter 1

## 1.1 INTRODUCTION

The mechanical properties of steels depend on their composition, grain size and structure. The latter is normally controlled by applying specific cooling conditions in the last stage of processing. An example is the production of steel rods in which after the last rolling pass, the rods are control cooled from about 900°C by forced air on a Stelmor line. By adjusting the residence time of rods and the air velocity in individual cooling zones, the desired structure, e.g. fraction pearlite and ferrite, can be obtained. Because the structure has a strong influence on the mechanical properties, it is important that the link between structure for each steel and process variables such as, in the case of the Stelmor process, rod diameter, air velocity and line speed is well established. Up to the present time, such links have been determined empirically. Practices have been developed in this way, for example, to control rod cooling and achieve specific pearlite spacings which govern the mechanical properties.[1-10] However this approach, on a plant scale, is time consuming and expensive. There is

considerable incentive, therefore, for the development of a predictive capability, such as a mathematical model, which can predict mechanical properties of a given steel as a function of process variables. This is the subject of the present study.

Development of a mathematical model to predict mechanical properties, however, is a difficult task owing to the complexity of the processes which determine structure in steels. One major problem is that heat flow and phase transformation kinetics are coupled. In a controlled cooling process, the steel undergoes a continuous change of temperature, the rate of which depends on the location within the steel. At the same time, as phase transformation takes place heat is evolved which frequently causes recalescence. Thus the changing temperature field is affected by heat extraction from, and conduction within, the rod as well as heat generation which depends on the kinetics of the phase transformation. The transformation kinetics, in turn are dependent on temperature.

A second problem is that the transformation kinetics have been characterized empirically in isothermal tests (TTT) and experiments in which the cooling rate is constant (CCT). But neither condition holds at a given location within the steel shape during cooling. Thus the question

becomes how data obtained in the laboratory can be applied to the complex non-isothermal situation of controlled cooling.

Thus the mathematical model must incorporate heat conduction within the steel, heat extraction from the surface of the steel and recalescence which is dependent on the coupled phase-transformation kinetics. The heat-extraction part of the model is relatively straightforward compared to the transformation kinetics; the latter must be determined empirically for each steel composition and austenite grain size. Moreover, as mentioned above, once the transformation data have been measured, usually under isothermal conditions, a valid procedure must be developed to apply the data in the prediction of non-isothermal transformation. The fundamental inter-relationships between the process variables and the cooling rate are developed in Chapter 3.

In the present study it was decided to model the austenite-pearlite reaction in a plain-carbon eutectoid steel. This material transforms from austenite to pearlite at the $AC_1$ temperature under equilibrium conditions and does not exhibit any other phases, like ferrite or cementite, and hence is simplest to model. The model, which is described in Chapter 4, has been written to predict the

temperature response of a cylindrical rod, since the heat transfer and boundary conditions are well defined for such a shape. Such a shape also has wide industrial applicability and is simple to use in experiments under controlled conditions. The model integrates CCT and TTT data for the steel as measured in experiments described in Chapter 5 and easily measurable process variables such as initial temperature and cooling parameters. The model has been validated by comparing predictions of centreline temperature to measurements described in Chapter 6. The effect of centre segregation on transformation has been studied by modifying the model. Calculations were done to predict the effect of centre segregation (of composition 0.80% C - 1.88% Mn in a matrix of composition 0.82% C - 0.82% Mn) in an air cooled rod, described in Chapter 6. Finally, calculations were done to derive mechanical properties of steel rods under different cooling conditions using the model generated data and are described in Chapter 6.

# Chapter 2

# LITERATURE SURVEY

## 2.1 Kinetics of the Austenite-Pearlite Reaction.

A systematic study of the austenite-pearlite reaction was made by Bain.[11] Subsequently several other studies, based on measurements of temperature, dilation and hardness as well as metallographic techniques, were conducted.[12-18]

The most important works, which advanced the understanding of reaction kinetics, are those of Johnson-Mehl,[19] Avrami[20-22] and Scheil.[17] Johnson-Mehl gave a comprehensive mathematical treatment of the austenite-pearlite reaction kinetics. They derived an equation for kinetics of nucleation and growth reactions under the following assumptions:

i) Constant nucleation and growth rates

ii) Random nucleation

iii) The reaction product forms true spheres except when during growth, impingement on other growing spheres occur.

With the above assumptions the volume fraction transformed, X, is related to the nucleation rate, N, and the

growth rate, G, by the following relationship:

$$X = 1 - \exp\left(-\frac{\pi}{3} N G^3 t^4\right) \qquad (2.1)$$

However there is some question that the assumptions are valid. Even for an isothermal reaction it is doubtful that the nucleation rate remains constant. Undercooling is the driving force for the nucleation process, and for an isothermal reaction, it may seem possible that N may remain constant. But this is too simplistic a view which neglects the effect of composition, structure and the transformation product on the phenomenon of nucleation. Brown and Ridley[36] have shown that it is possible to have a decreasing nucleation rate after about 20% transformation. Other evidence also exists to suggest that nucleation may decrease as the reaction proceeds.[19] However, the growth rate of pearlite is constant at a given temperature.[36] The assumption of random nucleation is also questionable, especially in commercial steels which are prone to some degree of segregation of elements like Mn and P. Also nonuniformity in grain size may have an effect. The assumption of completely spherical growth is, likewise, questionable in the light of micrographic studies conducted by Kuban.[37] A further difficulty in using Eq. (2.1) is the required determination of N and G by conducting controlled experiments. Moreover, reactions of industrial importance are

usually non-isothermal. Since Eq. (2.1) cannot be used for non-isothermal reactions, its use is very restricted.

Avrami's formulation is more useful in this regard. Like Johnson-Mehl, Avrami derived an equation for austenite-pearlite reactions as:

$$X = 1 - \exp(-bt^n) \qquad (2.2)$$

where n is a constant and b is a temperature dependent parameter.

Clearly Eq. (2.2) is a more general form of Eq. (2.1). Though b and n are empirical constants, Avrami used sound theoretical principles to derive Eq. (2.2). His treatment of nucleation rate is superior to that of Johnson and Mehl and he derived a simpler formula for including the effect of impingement during growth in the volume calculation. Avrami also showed that his equation included those of previous authors, like Austin and Rickett,[18] Zener,[14] Johnson and Mehl[19] as special cases.

## 2.2 The Additivity Rule

Scheil[17] first enunciated the additivity rule, which links the isothermal kinetics to non-isothermal reactions. This rule simplified the problem of studying non-isothermal

reaction kinetics. Christian[25] gave an up-to-date version of this rule, which states that

$$\int_0^t \frac{dt}{t_a(T)} = 1 \qquad (2.3)$$

(See Appendix 1 for derivation.)

where:

$t$ = time for a non-isothermal reaction to reach a specific amount of transformation.

$t_a(T)$ = time to reach the same transformation isothermally at temperature T.

This rule holds true for reactions for which the instantaneous reaction rate is only a function of the temperature and the amount transformed, irrespective of the previous thermal history. Avrami's derivation is very important in this regard. He showed that Eq. (2.2) describes the kinetics of additive reactions provided the ratio $\frac{N}{G}$ remains constant over the temperature range of the reaction. He defined this temperature range as the "Isokinetic Range". However, because the change in N with temperature is much more rapid than that of G for many austenite-pearlite transformations in steel, the existence of such a range is doubtful.[36,37] The advantage of Eq. (2.2) over Eq. (2.1) is that Avrami directly addressed the problem of additivity and provided

at least one sufficient condition for additivity to hold.

Despite the questionability of the isokinetic range, the Avrami Equation, (2.2) with empirically determined values of b and n, predicts the nature of the austenite-pearlite reaction kinetics quite accurately. The difficulty lies in determining the appropriate values of b and n.

## 2.3 Formulation of Nucleation and Growth

In order to derive ways of finding b and n, and to describe the theoretical importance and basis of these, several attempts have been made to formulate the nucleation and growth phenomena in fundamental terms. Equations have been derived for plate-like growth, needle-like growth, grain-broundary nucleated growth etc. by several workers; a comprehensive treatment of all of these can be found in reference (35). The resulting equations, essentially, are extensions of the Johnson-Mehl type of calculations and are subject to similar assumptions. These methods ultimately result in the formulation of an equation like Eq. (2.2) with different values for the constant n. Since the validity of the assumptions made are questionable, a closer examination of the reaction kinetics is in order.

## 2.4 Kinetics of Additive Reactions

In 1956, Cahn[23,24] proposed that reaction kinetics which

can be described by:

$$\frac{dX}{dt} = \frac{h(T)}{g(X)} \qquad (2.4)$$

where:

X = volume fraction transformed

t = time

h(T) = a function of temperature

g(X) = a function of volume fraction transformed.

can be expected to be additive. It can be shown that the Avrami equation can be modified to be of the same form as Eq. (2.4) (provided 'n' is a constant independent of T and X) such that

$$h(T) = n(-b)^{\frac{1}{n}} \qquad (2.5)$$

and

$$g(X) = \frac{1}{1-X}\left\{\frac{1}{\log\ (1-X)}\right\}^{\frac{n-1}{n}} \qquad (2.6)$$

(See Appendix 2 for derivation.)

Hence the Avrami equation describes the kinetics of additive reactions. Several authors have shown that, despite the questionable assumptions, the additivity rule holds true for austenite-pearlite and bainite reactions.[26,29,39,44] An important feature of all these works is the assumption that, irrespective of the reaction conditions (i.e. isothermal

or non-isothermal), the transformation of austenite to pearlite begins at the equilibrium transformation temperature. Hawbolt et al.,[35] in a very recent work have derived a different method for determining the "start" of the transformation under non-equilibrium reaction conditions. This procedure is discussed in detail in Chapter 6, and may contrast with the published TTT or CCT diagrams which show the "start" line as 0.1% or 1% transformed. In the new procedure, for assessing the kinetic data, the incubation time is neglected and the Avrami equation is applied only to describe the nucleation and growth phenomenon. The start of the transformation occurs after an incubation time $t_{AV}$ (for $t_{AVRAMI}$). In the present work, this time has been used as the "start" time. This is a major departure from the conventional methods of studying the kinetics. The results from the present work confirm that the use of $t_{AV}$ for additivity calculations gives better agreement with experimental observations.

## 2.5 Alternative Approaches to the Study of Non-isothermal Reaction Kinetics

In 1941, Grange and Keifer[28] described a simple and elegant method of deriving CCT from TTT data. This method was empirical in nature and involved assumptions regarding the kinetics. Though these were simplistic assumptions,

and hence the results approximate, the method is easy to use. But it did not employ additivity. However, since this method could not be justified on sound theoretical grounds, it has not found much application.

Another method, employed by Manning and Lorig,[16] used the experimental determination of the "start" of transformation during continuous cooling by conducting controlled-cooling experiments. These are time consuming procedures and the results generated do not lend themselves useful for general application.

A new approach to the problem of non-isothermal kinetics was given by Cahn[23,24] in 1956. He showed that since the isokinetic range is only a sufficient condition for additivity, the rule of additivity could also be applied to reactions under a condition called "site saturation". He deduced this from micrographs from experiments on eutectoid alloy steels having a large austenite grain size. In such steels, the reaction is initiated at grain boundaries where the nucleation event is so rapid that in the very early stages of transformation (10-20%) the grain boundaries are saturated with the growing new phase. Nucleation is therefore complete in the early stages of the reaction and plays no further role. The ensuing transformation is then controlled by the growth rate. Since the growth rate is a

temperature dependent parameter, additivity must be expected to hold. This was a definite new direction in the work on kinetics of reactions. By eliminating nucleation as a variable, Cahn simplified the process of characterising the kinetics by the growth rate alone, thereby eliminating the assumptions regarding the nucleation rate.

Though the condition of "site saturation" increased the number of transformations for which the additivity principle could be applied, this is not a universal phenomenon. In the work by Kuban,[37] where a plain carbon eutectoid steel was studied, micrographs unambiguously reveal the absence of grain boundary saturation. It is possible, however, that site saturation is more probable in the case of alloy steels due to the presence of alloying elements which may encourage grain boundary nucleation. Also the effect of grain size on site saturation needs to be examined. Intuitively, it would appear grain boundary site saturation is more probable in larger grain size material due to the reduced amount of grain boundary area per unit volume. Cahn's method differs from other empirical methods in that it has a firm theoretical basis. This is evident when comparing Cahn's work with Sakamoto[27] and Tzitzelkov.[39] These and other workers[26,29,30] have employed curve-fitting methods, aided by computer-based calculations, to derive CCT

from TTT. Since these are not based on theoretical considerations they cannot be considered as contributions to the understanding of the reaction kinetics. They find their use in specific situations.

## 2.6 Mathematical Modelling of Phase Transformations

Calculation of CCT from TTT by using the additivity principle is complex and laborious.[15,16,28] Such calculations are normally done to plot the CCT diagram for a material of a given chemistry and grain size. They can also be used to calculate reaction kinetics in a material undergoing processing in industrial situations, e.g., an infinitely long rod of circular cross-section in a wire rod mill. To study reactions taking place in such shapes, under different processing conditions, e.g., cooling rates, the kinetics must be related to the thermal history, which is in turn governed by the material properties and process conditions. Developments in the fields of heat transfer, solution of differential equations by finite-difference methods and rapid computer-aided calculations have resulted in the formulation of mathematical models to study such phoneomena as phase transformations, stress fields, temperature fields, etc.[31,32,33]

A mathematical model to study reaction kinetics in a plain carbon eutectoid steel rod was first attempted by

Agarwal and Brimacrombe.[31] They solved the second-order differential equation for heat transfer in an infinitely long circular cross-section rod by using an implicit finite-difference procedure. The kinetics of transformation were incorporated into the model by using published TTT data and additivity. They compared their model-predicted results with the experimental work of Takeo et al.[40] and found that agreement was relatively poor. It was thought that this might have been due to the TTT data used in the model and also the assumption that the transformation, under non-equilibrium conditions, began at the equilibrium transformation temperature. Though the agreement with experimental results was not good, the work demonstrated the feasibility of the use of models to study phase transformations. Their study indicated the need for the use of appropriate transformation data for successful model application.

## 2.7 Scope of Present Work

The present work was undertaken primarily to develop a mathematical model of heat flow and transformation in eutectoid wire rods using carefully measured TTT and CCT data. Also, it was decided to conduct experiments to validate model calculations. These were to be accomplished by measuring centre-line temperature of air-cooled steel rods

under controlled conditions of chemistry, grain size and cooling rate.

Since model calculations would involve the use of additivity, it was decided to examine the fundamental quantities involved, like the nucleation and growth rates. This work was carried out independently, by Kuban,[37] on a material very similar to the one used in the present work. The results from the study by Kuban were examined to check whether the conditions needed for additivity, like isokinetic range, site saturation etc., did exist in the material under study. As mentioned earlier, from Kuban's work, the following observations were made:

i) N and G, for isothermal reactions, are constant upto about 20% transformation.

ii) N and G vary with temperature. An isokinetic range, as defined by Avrami, does not exist.

iii) There is no evidence of site saturation, as revealed by metallographs.

iv) Calculations, using N and G values as found experimentally, reveal that the isothermal reaction kinetics are much slower than would be predicted by the Johnson-Mehl equation.

v) Growth of grains is not truly spherical, especially for large grain size, nor is nucleation random.

Since the steels used in the present work and that of Kuban are virtually the same (plain carbon eutectoid), the same kinetic conditions apply in both cases. Since it was found that the conditions required for the additivity rule to hold, the isokinetic range and site saturation, did not exist, but that the model calculations using additivity agreed well with experimental results, it was decided to re-examine the conditions needed for additivity. In addition, alternative conditions satisfying the additivity rule were also investigated. As a result, a new condition for additivity, a sufficient condition, has been proposed to explain the successful application of additivity in the present context. Finally since it is experimentally more difficult to obtain TTT data than CCT, due to limitations of the experimental apparatus, it was decided to investigate the possibility of devising a simple mathematical procedure to derive TTT from CCT.

## 2.8 Objectives

The objectives of this study can be summarized as follows:

i) To develop a procedure for quantitative prediction of mechanical properties of plain carbon steel rods control cooled in a Stelmor-type process.

ii) To develop a computer-based mathematical model to calculate the heat flows and austenite-pearlite reaction kinetics in a plain carbon eutectoid steel rod.

iii) To test the adequacy of the mathematical model by comparing model predictions with measurements of the centre-line temperature of rods under different cooling conditions.

iv) To examine the theory of additivity and explain its applicability to the kinetics of the experimentally determined austenite-pearlite reaction.

v) To devise a procedure for calculating TTT from CCT data.

vi) To use the model to examine the effect of segregation on reaction kinetics and transformation behaviour in plain carbon eutectoid steel rods.

vii) To predict mechanical properties by using the information generated by the model.

# Chapter 3

## THEORY OF ADDITIVE REACTIONS

As described in Chapter 2, the conditions necessary for additivity to hold for the austenite-pearlite reaction, i.e. Avrami's isokinetic range and Cahn's early site saturation, do not obtain for the reactions observed in the present work. However model calculations using additivity (described in Chapters 5 and 6), show good agreement with experimental results. Therefore it is necessary to examine alternate conditions under which the additivity principle will become applicable.

In this chapter, two new sufficient conditions for additivity are examined. These are:

i) the additivity range

ii) effective site saturation.

These two conditions have been derived after a careful theoretical analysis of the fundamental aspects of reaction kinetics - the nucleation rate and the growth rate. The additivity range, as will be shown in Section 3.1, is an extension of the isokinetic range. The effective site saturation criterion, described in Section 3.2, is similar to Cahn's early site saturation principle. The derivation

of the effective site saturation criterion has been done in three stages:

i) It is first derived for a homogeneous reaction with constant N and G (section 3.2.1).

ii) It is extended to cover homogeneous reactions with a constant G and a variable nucleation rate, which includes (i) as a special case (section 3.2.2).

iii) It is then derived for a heterogeneous reaction with constant N and G. It is also indicated that the results for a heterogeneous reaction with a variable nucleation rate and a constant G would yield the same results as obtained in (ii) (section 3.2.3).

The applicability of the criterion to the present work is described and by using experimental results, it has been shown that the reactions encountered in the present work are additive (section 3.3).

Finally, a new method has been devised, using additivity, to derive TTT data from CCT (section 3.4). A short summary of the work done in this regard is also included in this section to describe the context and relevance of this procedure.

It must be pointed out that the derivations leading to the additivity range, effective site saturation and the method of obtaining $t_{AV-TTT}$ from $t_{AV-CCT}$ are original and must be considered as fresh contributions to knowledge in this field.

## 3.1 Reaction Kinetics in the Additivity Range

As per Avrami,[21] the extended volume fraction transformed, $V_{ex}$, for a nucleation and growth reaction is:

$$V_{ex} = \sigma \int_0^{\tau} \overline{N}^4 \beta^3 (\tau - z)^3 e^{-z} dz \qquad (3.1)$$

where

$\sigma$ = shape factor ($= \frac{4\pi}{3}$ for spherical particle growth)

$\overline{N}$ = number of germ nuclei at the start of transformation

$\beta$ = G/N

$\tau$ = characteristic time

Since $\overline{N}$ is independent of time,

$$V_{ex} = \sigma \overline{N}^4 \int_0^{\tau} \beta^3 (\tau - z)^3 e^{-z} dz \qquad (3.2)$$

If N and G are functions of temperature alone, then

$$V_{ex} = \sigma \overline{N}^4 \beta^3 \int_0^{\tau} (\tau - z)^3 e^{-z} dz \qquad (3.3)$$

On integrating Eq. (3.3) and correcting for impingement,

$$V = 1 - \exp(-V_{ex})^{21} \qquad (3.4)$$

where

V = real volume fraction transformed,

we obtain,

$$V = 1 - \exp(-bt^n)^{21} \qquad (3.5)$$

where

n = constant

b = function of temperature.

Eq. (3.5) is the Avrami equation which has been shown in (Appendix 1) to describe the kinetics of additive reactions. The temperature range over which Eq. (3.5) holds is the "additivity range".

The Johnson-Mehl equation (Eq. 2.1) is a specific case of the more general Avrami equation of reaction kinetics. For an isothermal reaction, for which there is evidence that N and G are constant for some nucleation and growth reactions,[36] the Johnson-Mehl equation can be applied to study the kinetics. But by using the concept of the additivity range, it can be shown that the Johnson-Mehl equation, with slight modifications, can be used to describe the kinetics of non-isothermal reactions which are additive.

Consider a non-isothermal reaction (a nucleation and growth reaction) occurring between the temperatures $T_0$ and $T_{100}$. In this temperature range, let

$N(T)$ = nucleation rate (a function of temperature alone)

$G(T)$ = growth rate (a function of temperature alone)

$V^t$ = real volume fraction transformed at time 't'.

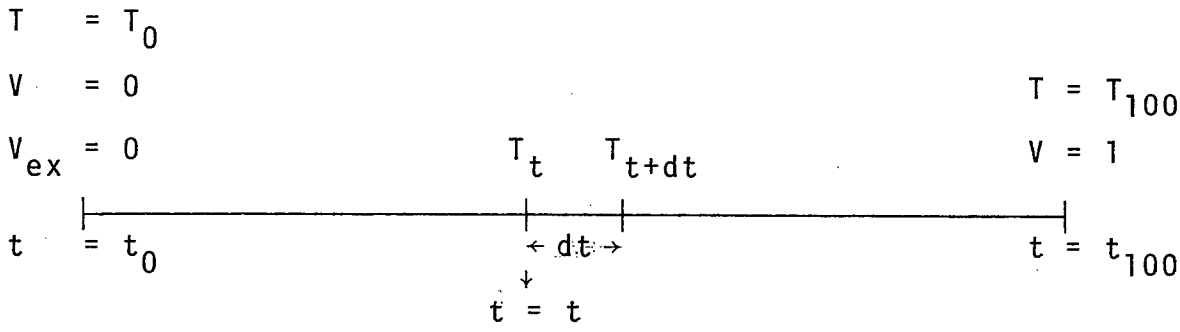


During the infinitesimally small time step 'dt', the number of nuclei that nucleate = $N'(T)dt$.

$N'(T)$ = temperature averaged nucleation rate over the time interval dt

Consider the growth of one nucleus which starts its growth during dt. The extended volume of this nucleus at time '$t_{100}$' is:

$$V_{ex} = \left\{ \frac{1}{T_{100} - T_t} \int_{T_t}^{T_{100}} G(T)dT \; (t_{100} - t) \right\}^3 \qquad (3.6)$$

where:

$$\frac{1}{T_{100} - T_t} \int_{T_t}^{T_{100}} G(T)dT$$

is the temperature averaged growth rate between times t and $t_{100}$.

Hence the volume of all nuclei nucleating between t and t+dt at $t_{100}$ is:

$$\sigma \int_{t}^{t+dt} \left\{ \frac{1}{T_{100} - T_t} \int_{T_t}^{T_{100}} G(T)dT(t_{100}-t) \right\}^3 \left\{ \frac{1}{dT} \int_{T_t}^{T_{t+dt}} N(T)dT \right\} dt \qquad (3.7)$$

Therefore, the total extended volume of growth of all nuclei nucleating between $t_0$ and $t_{100}$ at time $t_{100}$ is:

$$V_{ex}^{t_{100}} = \sigma \int_{t_0}^{t_{100}} \left\{ \frac{1}{T_{100}-T_t} \int_{T_0}^{T_{100}} G(T)dT \; (t_{100}-t) \right\}^3 \left\{ \frac{1}{T_{100}-T_0} \int_{T_0}^{T_{100}} N(T)dT \right\} dt \qquad (3.8)$$

Let

$$G_1(T) = \frac{1}{T_{100} - T_0} \int_{T_0}^{T_{100}} G(T)dT \qquad (3.9)$$

$$N_1(T) = \frac{1}{T_{100} - T_0} \int_{T_0}^{T_{100}} N(T)dT \qquad (3.10)$$

$N_1(T)$ and $G_1(T)$ are the temperature averaged growth rates for the reaction. Then, Eq. (3.8) can be written as

$$V_{ex}^{t_{100}} = \sigma \int_{t_0}^{t_{100}} G_1^3(T) \cdot N_1(T) \cdot (t_{100}-t)^3 \, dt \qquad (3.11)$$

$G_1(T)$ and $N_1(T)$ are functions independent of time. This is illustrated in Appendix 3. Because of this independence, $G_1(T)$ and $N_1(T)$ can be taken out of the integral in Eq.(3.11).

$$\therefore V_{ex}^{t_{100}} = \sigma G_1^3(T) N_1(T) \int_{t_0}^{t_{100}} (t_{100}-t)^3 \, dt \qquad (3.12)$$

Considering this transformation to have occurred in a unit volume, at any time "$\tau$" during the reaction,

$$V_{ex}^{\tau} = \sigma \cdot G_\tau^3(T) \cdot N_\tau(T) \cdot \int_0^{\tau} (\tau-t)^3 \, dt \qquad (3.13)$$

where

$$G_\tau(T) = \frac{1}{T_\tau - T_0} \int_{T_0}^{T_\tau} G(T) \, dT \qquad (3.14)$$

$$N_\tau(T) = \frac{1}{T_\tau - T_0} \int_{T_0}^{\bar{T}_\tau} N(T)\, dT \tag{3.15}$$

$$\therefore \quad V_{ex}^{\tau} = \sigma\, G_\tau^3(T)\, N_\tau^3(T)\, \frac{\tau^4}{4} \tag{3.16}$$

For spherical particle growth,

$$V_{ex}^{\tau} = \frac{\pi}{3}\, N_\tau(T)\, G_\tau^3(T)\, \tau^4 \tag{3.17}$$

Since

$$V^t = 1 - \exp\left\{-V_{ex}^t\right\} \tag{3.18}$$

$$\therefore \quad V^t = 1 - \exp\left\{-\frac{\pi}{3}\, N_t(T)\, G_t^3(T)\, t^4\right\} \tag{3.19}$$

For an isothermal reaction, Eq. (3.19) can be written as

$$V^t = 1 - \exp\left(-\frac{\pi}{3}\, NG^3\, t^4\right) \tag{3.20}$$

which is the Johnson-Mehl equation. Eq. (3.20) is of the same form as the Avrami equation with

$$b = \frac{\pi}{3}\, N_t(T)\, G_t^3(T) \tag{3.21}$$

$$n = 4 \tag{3.22}$$

Hence Eq. (3.19) also describes the kinetics of additive

reactions. It holds under the following assumptions:

i) N and G are functions of temperature alone for non-isothermal reactions.

ii) Random nucleation.

iii) Spherical particle growth until impingement.

The temperature range for which Eq. (3.19) holds is the "additivity range".

### 3.1.1 Definition of Additivity Range

The additivity range is the temperature range, for a nucleation and growth reaction, in which the nucleation and growth rates are dependent only on the temperature. Reactions occurring in such a range obey Scheil's additivity principle.

## 3.2 Kinetics of Nucleation and Growth Reactions and the Criterion of Effective Site Saturation

Isothermal reactions which do not follow the Johnson-Mehl equation due to the violation of any one or all of the assumptions made in deriving the equation can be termed non-homogeneous reactions. Such reactions are not covered by Eq. (3.19). Hence it is necessary to derive a sufficient condition of additivity for such reactions. Since the

austenite-pearlite reaction, studied in the present work, is heterogeneous, it becomes all the more essential. In order to study heterogeneous reaction kinetics, it is important to understand the kinetics of homogeneous reactions.

### 3.2.1 Kinetics of Isothermal Homogeneous Nucleation and Growth Reactions

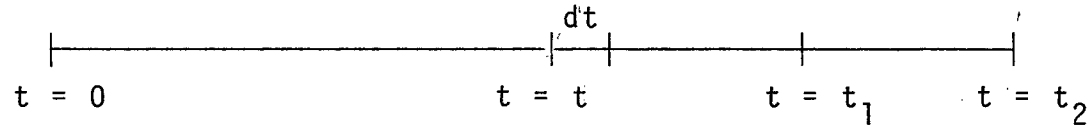


Assumptions:

i) Constant N and G

ii) Spherical particle growth

iii) Random nucleation.

Number of nuclei formed upto time t = Nt

Number of nuclei nucleating in an infinitesimally small time interval dt = Ndt

The extended growth volume of these nuclei at $t = t_1$ = $\sigma \int_t^{t_1} \left(G(t_1-t)\right)^3 N dt$

$\therefore$ The extended growth volume of all nuclei nucleating during the time interval 0 to $t_1$ is:

$$\int_0^{t_1} \sigma G^3 N (t_1-t)^3 \, dt$$

$$\therefore V_{ex}^{t_1} = \frac{\sigma N G^3 t_1^4}{4} \qquad (3.23)$$

The total number of sites consumed due to nucleation and the volumetric growth by the end of time $t = t_1$ is:

$$S_{ex}^{t_1} = Nt_1 + \frac{\sigma G^3 N\, t_1^4}{4} \cdot I_0 \tag{3.24}$$

where

$I_0$ = Initial number of available sites for nucleation.

The rate of site consumption is (obtained by differentiating Eq. (3.24))

$$\dot{S}_{ex}^{t_1} = N + \sigma N G^3 t_1^3 I_0 \tag{3.25}$$

Considering a unit volume of material, from Eq. (3.23),

$$V_{ex}^{t} = \frac{\sigma N G^3 t^4}{4} \tag{3.26}$$

Also,

$$S_{ex}^{t} = Nt + I_0 \cdot V_{ex}^{t} \tag{3.27}$$

$$\dot{S}_{ex}^{t} = N + I_0 \cdot \dot{V}_{ex}^{t} \tag{3.28}$$

For spherical growth ($\sigma = \frac{4\pi}{3}$),

$$V_{ex}^{t} = \frac{\pi}{3} N G^3 t^4 \tag{3.29}$$

Since

$$V^{t} = 1 - \exp\left(- V_{ex}^{t}\right) \tag{3.30}$$

$$S^{t} = 1 - \exp\left(- S_{ex}^{t}\right) \tag{3.31}$$

We have,

$$V^t = 1 - \exp\left(-\frac{\pi}{3} NG^3 t^4\right) \tag{3.32}$$

$$S^t = 1 - \exp -(Nt + I_0 \cdot V_{ex}^t) \tag{3.33}$$

$$\dot{S}^t = N+I_0 \cdot \frac{4\pi}{3} NG^3 t^3 \cdot \exp -(Nt+I_0 \cdot V_{ex}^t) \tag{3.34}$$

Eq. (3.32) to Eq. (3.34) are the three basic equations of homogeneous isothermal reaction kinetics. Eq. (3.32) is the Johnson-Mehl equation, which is the volume fraction transformed at any time t during the reaction. This volume growth is due to the growth of nuclei nucleated throughout the reaction. It is also possible to calculate the volumetric growth of nuclei nucleating during a specific time interval in the reaction. It is useful to calculate this quantity because it will indicate the relative importance of the growth of these nuclei to the total growth volume. If the volume contribution due to nuclei nucleating very early in the reaction to the total volumetric growth at a very late stage in the reaction is significantly high, then it can be postulated that the reaction is essentially growth dominated.

As before, the extended volume of growth from nuclei nucleating between times 0 and $t_1$ at time $t_2$ is:

$$V_{ex}^{t_2}{}_{0/t_1} = \int_0^{t_1} \sigma G^3 (t_2 - t)^3 N \, dt \tag{3.35}$$

$$= \sigma \frac{NG^3}{4} \left[ t_2^4 - (t_2 - t_1)^4 \right] \tag{3.36}$$

Also, the total extended volume of growth at $t_2$ is:

$$V_{ex}^{t_2} = \sigma \frac{NG^3 t_2^4}{4} \tag{3.37}$$

A more general form of Eq. (3.35) is:

$$V_{ex}^{\tau}{}_{t_i/t_j} = \int_{t_i}^{t_j} \sigma G^3 N (\tau - t)^3 \, dt \tag{3.38}$$

$$= \sigma \frac{NG^3}{4} \left[ (\tau - t_i)^4 - (\tau - t_j)^4 \right] \tag{3.39}$$

Hence, at any time t during the reaction, the fractional volume contributed by nuclei nucleating between the times $t_i$ and $t_j$ to the total extended volume transformed is:

$$\frac{V_{ex}^{t}{}_{t_i/t_j}}{V_{ex}^{t}} = \frac{(t - t_i)^4 - (t - t_j)^4}{t^4} \tag{3.40}$$

If

$$t_i = 0$$

$$t_j = t_{20}$$

$$t = t_{90}$$

then, from Eq. (3.41)

$$\frac{V_{ex_{0/t_{20}}}^{t_{90}}}{V_{ex}^{t_{90}}} = \frac{t_{90}^4 - (t_{90} - t_{20})^4}{t_{90}^4} \qquad (3.41)$$

Now if, for this reaction, the growth rate is the dominant feature (and consequently, the nucleation rate is relatively unimportant) then it can be expected that the fractional volume contributed by the nuclei nucleating in the very early stages of the reaction (say, up to 20% transformation) to the volume transformed at the final stages of the reaction (say, 90% transformation) must be close to unity.

If the ratio is close to unity, say 0.85, then the nucleation event after 20% transformation becomes unimportant and the reaction is growth rate dominated. Since it is known that the growth rate is a function of temperature only for austenite-pearlite reactions, these reactions can be considered additive. Hence, if

$$\frac{V_{ex_{0/t_{20}}}^{t_{90}}}{V_{ex}^{t_{90}}} = \frac{t_{90}^4 - (t_{90}-t_{20})^4}{t_{90}^4} \geq 0.85 \qquad (3.42)$$

$$\therefore\ t_{20} = \geq 0.38\ t_{90} \qquad (3.43)$$

holds for the reaction, it should be additive. It should be noted that Eq. (3.42) involves the ratio of extended volumes. It also can be shown, as described below, that

$$\frac{V_{0/t_{20}}^{t_{90}}}{V^{t_{90}}} > \frac{V_{ex_{0/t_{20}}}^{t_{90}}}{V_{ex}^{t_{90}}} \tag{3.44}$$

Since

$$V^{t_{90}} = 1 - \exp\left(-V_{ex}^{t_{90}}\right) \tag{3.45}$$

and

$$V_{0/t_{20}}^{t_{90}} = 1 - \exp\left(-V_{ex_{0/t_{20}}}^{t_{90}}\right) \tag{3.46}$$

$$\therefore \quad \frac{V_{0/t_{20}}^{t_{90}}}{V^{t_{90}}} = \frac{1 - \exp\left(-V_{ex_{0/t_{20}}}^{t_{90}}\right)}{1 - \exp\left(-V_{ex}^{t_{90}}\right)} \tag{3.47}$$

Also,

$$V^{t_{90}} = 0.90 \tag{3.48}$$

$$\therefore \quad 1 - \exp\left(-V_{ex}^{t_{90}}\right) = 0.90 \tag{3.49}$$

$$\therefore \quad V_{ex}^{t_{90}} = \ln 10 \tag{3.50}$$

From Eq. (3.43),

$$V_{ex_{0/t_{20}}}^{t_{90}} \geq 0.85\, V_{ex}^{t_{90}} \tag{3.51}$$

. . Eq. (3.48), combined with Eq. (3.44), can be written as:

$$\frac{V_{0/t_{20}}^{t_{90}}}{V^{t_{90}}} \geq \frac{1 - \exp(-0.85 \ln 10)}{0.9} \geq 0.95 \tag{3.52}$$

The relationship between the ratios of extended volumes and real volumes is shown in Fig. (3.1) and Fig. (3.2). Therefore, from Eq. (3.52), it can be concluded that the ratio of the real volumes is greater than the ratio of the extended volumes. Thus, Eq. (3.43), which is the "Effective Site Saturation" condition for constant nucleation and growth rate homogeneous reactions, can be used to study the applicability of additivity to such reactions. The criterion is so called because the nature of conclusions derived by it are essentially similar to Cahn's site saturation. But it does not require that nucleation sites saturate physically during the reaction. Also, the criterion requires only a knowledge of $t_{20}$ and $t_{90}$ for such reactions. Hence it is very easy to use.

The only restriction in using the effective site

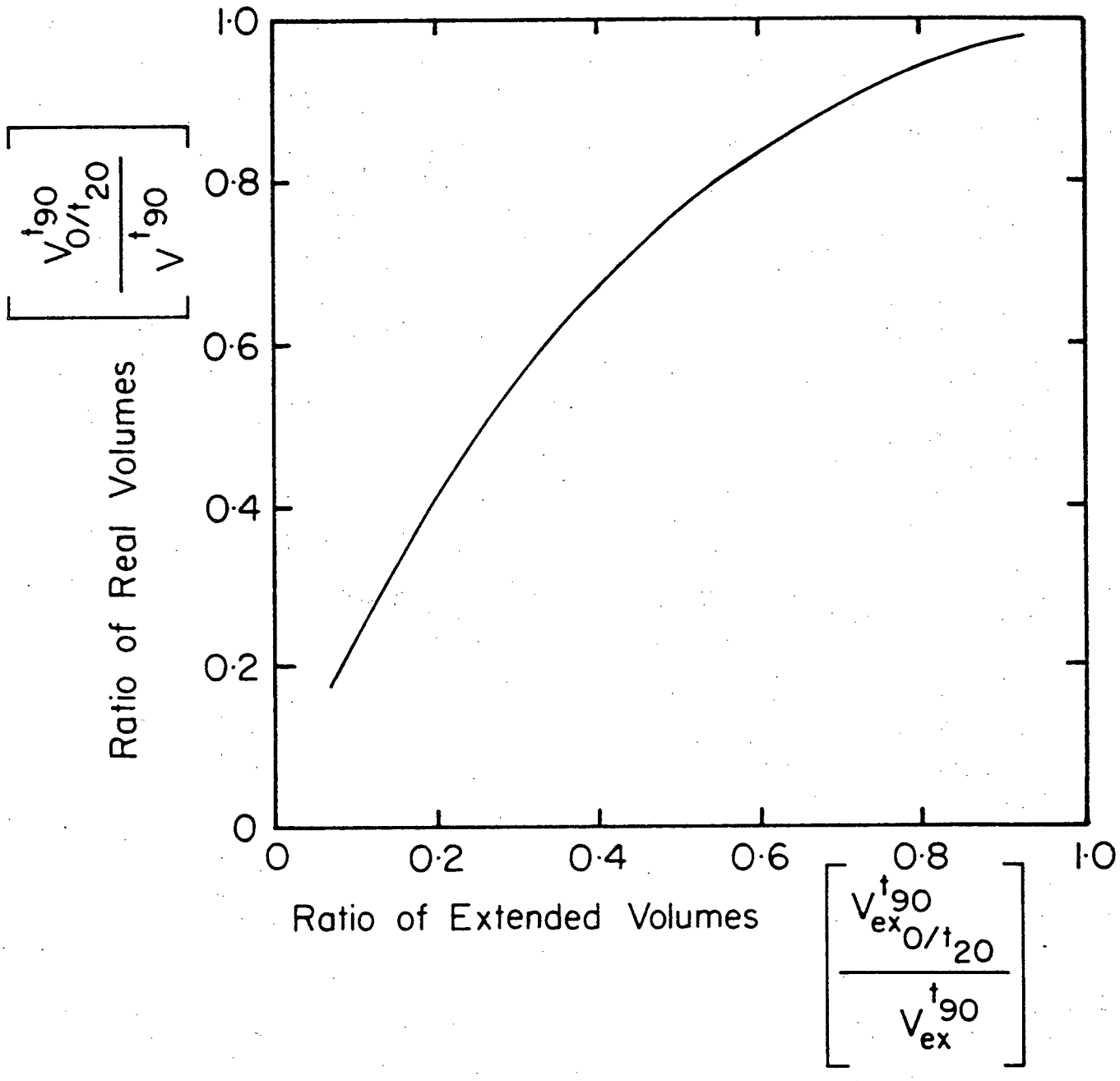


Fig. 3.1 Relationship between the ratios of extended volumes and real volumes.

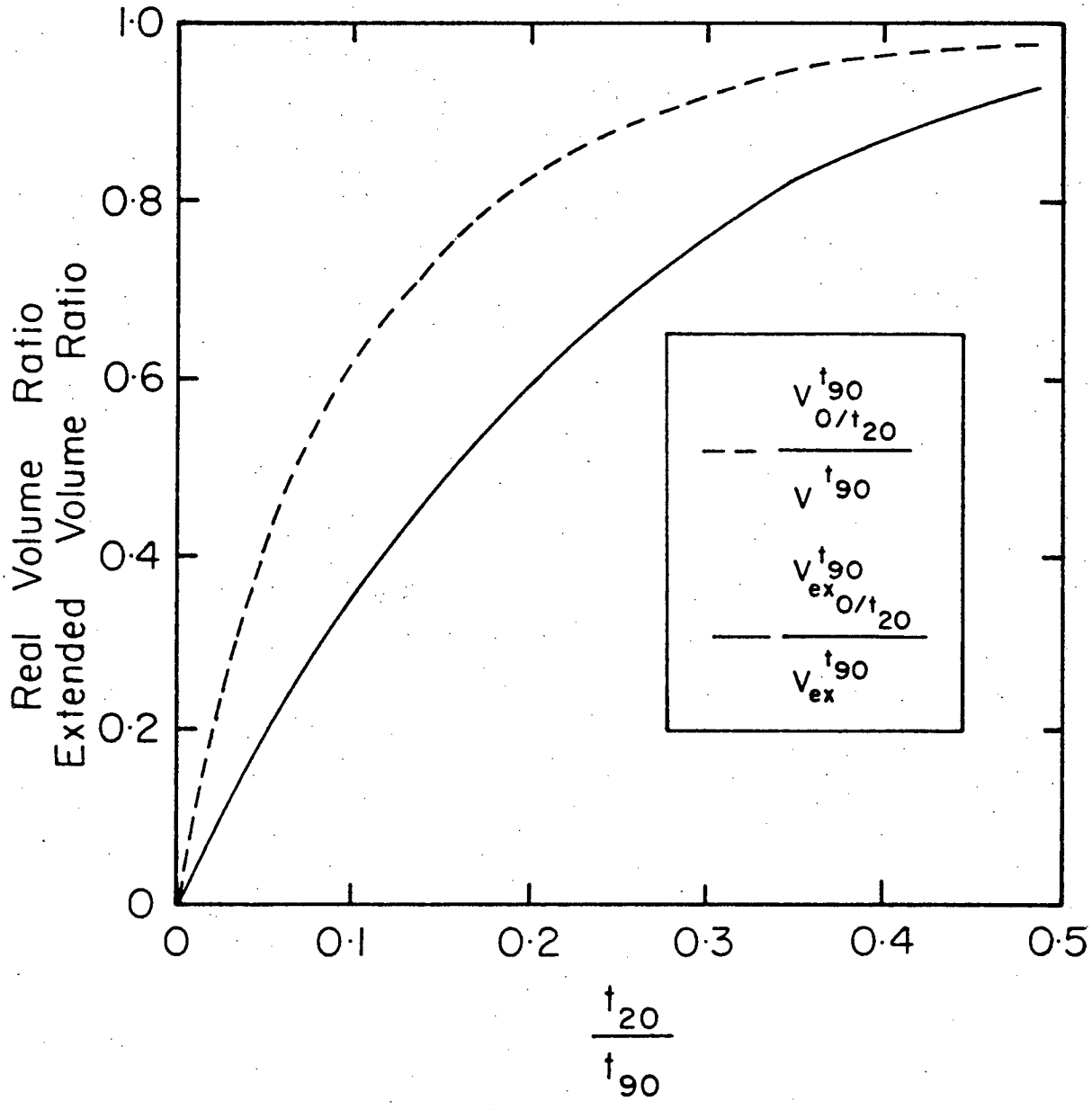


Figure 3.2 Relationship between the effective site saturation ratio and the real volumes and extended volumes ratios.

saturation condition, as derived in Eq. (3.43), is that N and G be constant. However, it can be extended to include reactions in which N varies with time.

### 3.2.2 Effective Site Saturation Criterion for Variable Nucleation Rate Isothermal Reactions

If we consider a reaction such that,

$$\begin{aligned} N &= N_0 \quad (t \leq t_N) \\ &= N(t) \quad (t > t_N) \end{aligned} \tag{3.53}$$

As before, upto $t = t_N$,

$$V_{ex}^{t_N} = \frac{\pi}{3} N_0 G^3 t_N^4 \tag{3.54}$$

Also,

$$V_{ex_{0/t_N}}^{t_1} = \frac{\pi}{3} N_0 G^3 \left\{ t_1^4 - (t_1 - t_N)^4 \right\} \quad (t_1 > t_N) \tag{3.55}$$

$$\begin{aligned} V_{ex_{t_N/t}}^{t_1} &= \frac{4\pi}{3} \int_{t_N}^{t_i} G^3 \, (t_1 - t)^3 \, N(t) \, dt \\ &= \frac{4\pi}{3} G^3 \int_{t_N}^{t_1} N(t) \, (t_1 - t)^3 \, dt \end{aligned} \tag{3.56}$$

Consider a decreasing nucleation rate,

$$N(t) = N_0 \left\{ \frac{t_{90} - t}{t_{90}} \right\}^m \tag{3.57}$$

which is the most probable form of equation based on evidence in the literature. Moreover, the application of Le Chatelier's principle points to the possibility that the nucleation rate should decrease with time due to the "back pressure" exerted by the transformed procuct. Eq. (3.57) also implies that the nucleation rate is negligibly small after $t_{90}$, which again is a reasonable assumption. 'm' is a co-efficient which will depend on factors like composition, temperature etc. Substituting Eq. (3.57) for N(t) in Eq. (3.56), we obtain

$$V_{ex_{t_N/t_{90}}}^{t_{90}} = \frac{4\pi}{3} N_0 G^3 \int_{t_N}^{t_{90}} (t_{90}-t)^3 \left\{ \frac{t_{90}-t}{t_{90}} \right\}^m dt \tag{3.58}$$

$$= \frac{4\pi}{3} \cdot \frac{N_0 G^3}{t_{90}^m} \cdot \frac{(t_{90}-t_N)^{m+4}}{(m+4)} \tag{3.59}$$

Hence,

$$\frac{V_{ex_{0/t_N}}^{t_{90}}}{V_{ex}^{t_{90}}} = \frac{\frac{\pi}{3} N_0 G^3 \; t_{90}^4 - (t_{90} - t_N)^4}{V_{ex_{t_N/t_{90}}}^{t_{90}} + V_{ex_{0/t_N}}^{t_{90}}} \tag{3.60}$$

$$= \frac{t_{90}^4 - (t_{90} - t_N)^4}{\frac{4}{t_{90}^m}\,\frac{(t_{90} - t_N)^{m+4}}{(m+4)} + t_{90}^4 - (t_{90} - t_N)^4} \qquad (3.61)$$

The effective site saturation criterion is:

$$\frac{V_{ex_{0/t_N}}^{t_{90}}}{V_{ex}^{t_{90}}} \geq 0.85 \qquad (3.62)$$

$$\therefore\ t_N \geq t_{90}\left[1 - \frac{1}{\sqrt[4]{\frac{36}{(m+4)}\left\{1 - \frac{t_N}{t_{90}}\right\}^m + 1}}\right] \qquad (3.63)$$

Eq. (3.63) is the general statement of the effective site saturation criterion which includes Eq. (3.43). Eq. (3.63) considerably expands the scope of reactions covered by the effective site saturation condition.

However, in practice, homogeneous reactions are not common. This is especially true of the austenite-pearlite reaction, which is heterogeneous. Micrographic evidence also exists to show that grain growth may not be spherical.[37] In the work by Kuban,[37] the reaction kinetics calculated by using experimentally determined N and G in the Johnson-Mehl

equation for isothermal reactions, predicted much faster rates of transformation than those experimentally observed. Thus, for the effective site saturation criterion to be useful for heterogeneous reactions, it must be extended to cover the conditions obtained in such reactions.

### 3.2.3 Effective Site Saturation Criterion for Heterogeneous Isothermal Reactions

The Johnson-Mehl equation represents the kinetics of homogeneous reactions.

$$V^t_{Hom} = 1 - \exp\left(-\frac{\pi}{3} NG^3 t^4\right) \qquad (3.64)$$

Due to heterogeneity, the reaction kinetics are slower than that predicted by Eq. (3.64). These kinetics can be represented as

$$V^t_{Het} = 1 - \exp\left(- bt^n\right) \qquad (3.65)$$

where b and n represent the effect of heterogeneity. We can define a factor, called the "Inhomogeneity Co-efficient", as:

$$I_t = \frac{V^t_{Hom}}{V^t_{Het}} \qquad (3.66)$$

It is not possible, at this stage, to speculate upon the precise nature of $I_t$. Values of $I_t$ calculated from the work of Kuban[37] are shown in Figs. 3.3 and 3.4.

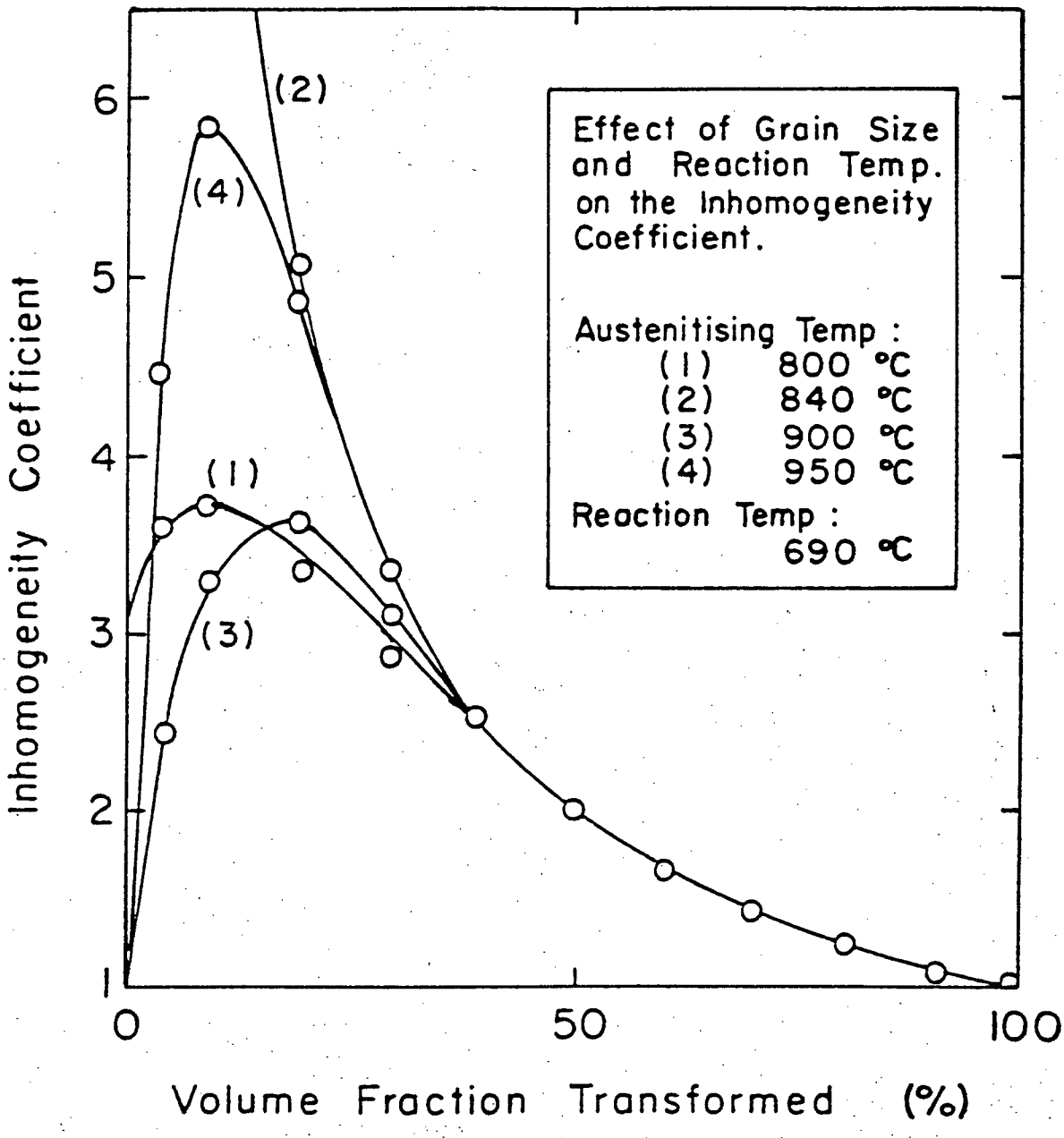


Figure 3.3 Effect of grain size and reaction temperature on the Inhomogeneity co-efficient.

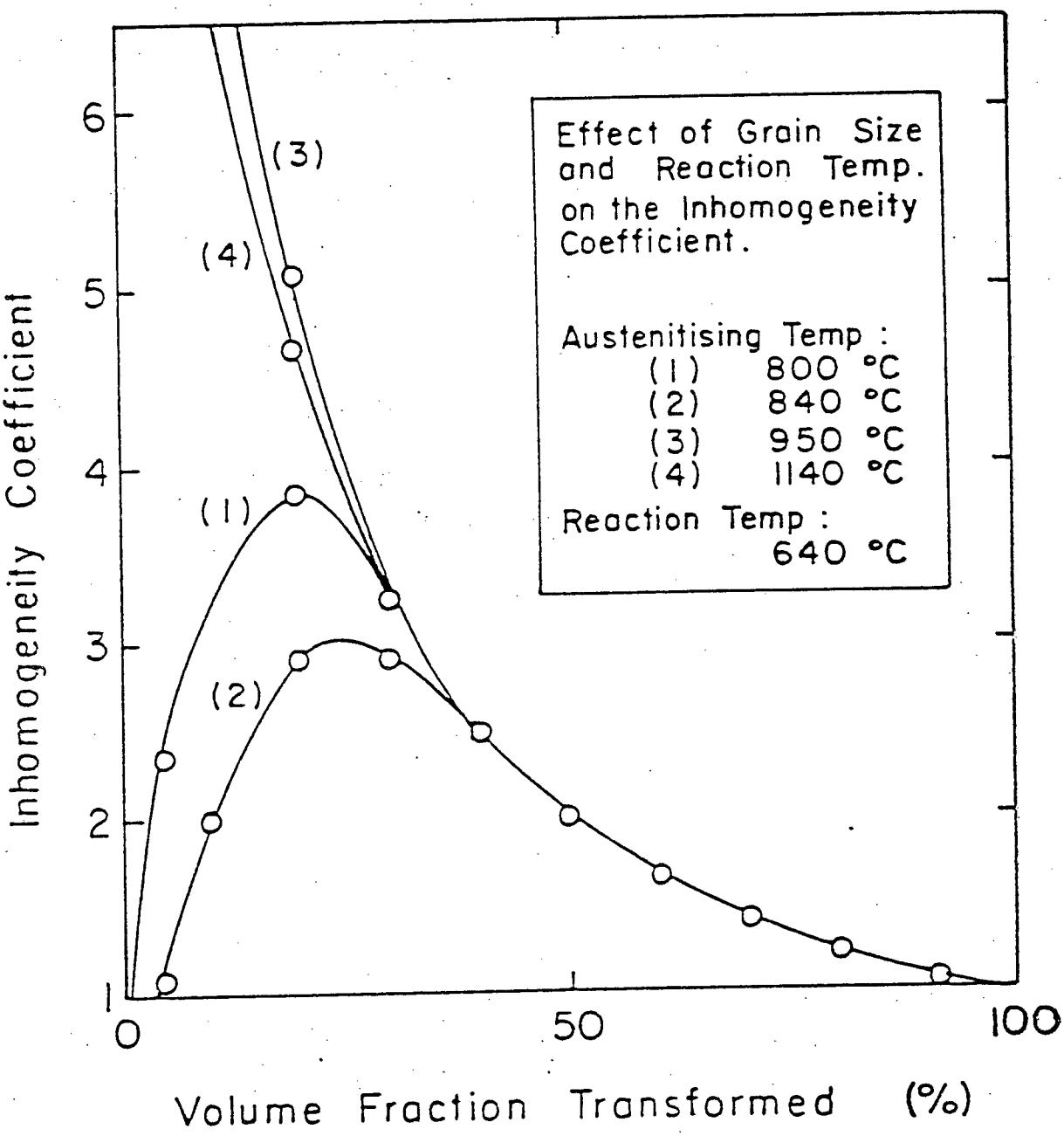


Fig. 3.4 Effect of grain size and reaction temperature on the Inhomogeneity co-efficient.

The inhomogeneity co-efficient, $I_t$, helps to characterize the degree of inhomogeneity of a reaction, but complicates the derivation of a criterion of the form of Eq. (3.43). Introducing $I_t$ in a slightly modified form, as $H_t$, the "heterogeneity co-efficient", helps accomplish this objective.

$$V^t_{Het} = \frac{V^t_{Hom}}{I_t} = \frac{1 - \exp - V^t_{ex_{Hom}}}{I_t}$$

$$= 1 - \exp - H_t \cdot V^t_{ex_{Hom}} \qquad (3.67)$$

Since

$$H_t \cdot V^t_{ex_{Hom}} = H_t \cdot \frac{\pi}{3} NG^3 t^4 = bt^n \qquad (3.68)$$

$$\therefore \quad H_t = \frac{b}{\frac{\pi}{3} NG^3} t^{n-4} \qquad (3.69)$$

As for $I_t$, it is difficult to predict the nature of $H_t$ for different reactions. Values of $H_t$ for the reactions studied by Kuban are summarized in Table 3.1. As can be seen from this table, the value of $H_t$ is constant for some reactions and varying for others.

For a heterogeneous reaction with constant N and G, we have,

Table 3.1 Summary of Heterogeneity Co-efficient Calculations

| Reaction Temperature (°C) | Austenitising Temperature (°C) | Range of $H_t$ | Average $H_t$ |
|---|---|---|---|
| 640 | 800 | 0.04 to 0.26 | 0.10 |
| 640 | 840 | 0.04 to 0.48 | 0.15 |
| 640 | 950 | 0.07 to 0.09 | 0.08 |
| 640 | 1100 | 0.03 to 0.035 | 0.033 |
| 690 | 800 | 0.13 to 0.23 | 0.17 |
| 690 | 840 | 0.0018 to 0.0034 | 0.0024 |
| 690 | 900 | 0.05 to 0.027 | 0.17 |
| 690 | 950 | 1.4 to 12.3 | 4.42 |

$$V_{ex_{Het}}^{t_{90}} = H_{t_{90}} \frac{\pi}{3} NG^3 t_{90}^4 \tag{3.70}$$

$$V_{ex_{Het_{t_{20}/t_{90}}}}^{t_{90}} = H_{t_{90}} \frac{\pi}{3} NG^3 (t_{90}-t_{20})^4 \tag{3.71}$$

$$V_{ex_{Het_{0/t_{20}}}}^{t_{90}} = H_{t_{90}} \frac{\pi}{3} NG^3 \left[t_{90}^4-(t_{90}-t_{20})^4\right] \tag{3.72}$$

Since the effective site saturation condition is:

$$\frac{V_{ex_{0/t_{20}}}^{t_{90}}}{V_{ex}^{t_{90}}} \geq 0.85$$

for a heterogeneous reaction,

$$\frac{t_{90}^4 - (t_{90}-t_{20})^4}{t_{90}^4} \geq 0.85 \tag{3.73}$$

$$\therefore t_{20} \geq 0.38 \ t_{90} \tag{3.74}$$

Eq. (3.74) is the same as Eq. (3.43). The same derivations can be done for a variable nucleation rate reaction with the same results as obtained in Eq. (3.63). Thus, the effective site saturation criterion remains unaltered for homogeneous and heterogeneous reactions.

## 3.3 Validation of the Effective Site Saturation Criterion by Experimental Results

The effective site saturation criterion was applied to experimental results to check its validity. The model predictions, using additivity, show very good agreement with experimental results in the present work, indicating that additivity holds under the experimental conditions encountered. The material used and experimental conditions are virtually the same in the present work and that of Kuban[37] and hence comparable in terms of kinetic behaviour. The results of volume contribution calculations for experiments conducted by Kuban[37] are summarized in Table 3.2 and show very good agreement with the result expected from Eq. (3.74). Table 3.3 shows the calculation of the ratio $\frac{t_{20}}{t_{90}}$ for the experiment conducted by Kuban.[37] Table 3.4 shows the same ratio calculated for experiments conducted in the present study and others.[30,43,50] The values indicate very good agreement with the effective site saturation criterion. The above results validate the use of the effective site saturation criterion to ensure additivity in reactions. They also establish a firm theoretical framework for using additivity in the model calculations.

## 3.4 Application of Additivity to Derive TTT from CCT by the Additivity Method

An important application of the additivity rule is the

Table 3.2 Summary of Effective Site Saturation Calculations

| Reaction Temperature (°C) | Austenitising Temperature (°C) | Volume Contribution* (%) | |
|---|---|---|---|
| | | Extended Volume | Real Volume |
| 640 | 800 | 86 | 95 |
| 640 | 840 | 82 | 94 |
| 640 | 950 | 96 | 98 |
| 640 | 1100 | 97 | 99 |
| 690 | 800 | 94 | 98 |
| 690 | 840 | 93 | 97 |
| 690 | 899 | 88 | 96 |
| 690 | 950 | 85 | 95 |

*Volume contributed by nuclei nucleating between 0 and 20% transformation to the total volume transformed at 90% transformation.

Table 3.3. Effective Site Saturation Criterion Values

| Steel Chemistry: 0.78 C Eutectoid (plain carbon) | | | | |
|---|---|---|---|---|
| Reaction Temperature (°C) | Austenitising Temperature (°C) | $t_{20}$ (s) | $t_{90}$ (s) | $\frac{t_{20}}{t_{90}}$ |
| 640 | 800 (9.1 ASTM) | 3.22 | 8.38 | 0.38 |
| 640 | 840 (7.8 ASTM) | 3.08 | 8.93 | 0.34 |
| 640 | 950 (7.3 ASTM) | 6.8 | 12.7 | 0.53 |
| 640 | 1100 ( 3 ASTM) | 31.76 | 55.14 | 0.58 |
| 690 | 800 (9.1 ASTM) | 51.1 | 101.4 | 0.51 |
| 690 | 840 (7.8 ASTM) | 119 | 243 | 0.49 |
| 690 | 900 (7.5 ASTM) | 918 | 2275 | 0.40 |
| 690 | 950 (7.3 ASTM) | 847 | 2301 | 0.37 |

(Data from Reference 37.)

Table 3.4 Effective Site Saturation Criterion Values

| Experimental Conditions | Reaction Temperature (°C) | $t_{20}$ (s) | $t_{90}$ (s) | $\frac{t_{20}}{t_{90}}$ | Reference No. |
|---|---|---|---|---|---|
| 0.82 C Eutectoid Steel | 660 | 32.4 | 72 | 0.45 | |
| Austenitised at 850°C for 5 mts | 650 | 13.5 | 25.9 | 0.52 | * |
| 5-7 ASTM | 630 | 5.6 | 9.8 | 0.57 | |
| | 615 | 3.25 | 5.4 | 0.62 | |
| | 603 | 3.15 | 5.4 | 0.58 | |
| 0.78 C Eutectoid Steel | 500 | 4.20 | 5.5 | 0.76 | |
| Austenitised at 875°C for 30 mts | 540 | 4.8 | 6.5 | 0.74 | 43 |
| 5.25 ASTM | 600 | 6.4 | 10.0 | 0.64 | |
| 0.80 C Eutectoid Steel | 630 | 8.0 | 20.0 | 0.40 | |
| Austenitised at 875°C for 30 mts | 650 | 23.0 | 42.0 | 0.54 | 43 |
| 4.25 ASTM | 690 | 700.0 | 1100.0 | 0.63 | |
| 1.10 C Eutectoid 5 ASTM | 662 | 4.7 | 6.5 | 0.72 | |
| 0.57 C Eutectoid 5 ASTM | 691 | 80.0 | 200.0 | 0.40 | |
| 0.93 C Eutectoid 1 ASTM | 689 | 35.0 | 46.0 | 0.75 | 43 |
| All Steels Austenitised at 875°C for 30 mts | | | | | |
| SKD-6 | 715 | 95 | 200 | 0.475 | 30 |
| | 670 | 340 | 830 | 0.410 | |
| SKS-5 | 632 | 31 | 55 | 0.56 | |
| Austenitised at 1100°C for 15 mts | 622 | 24 | 42 | 0.57 | 50 |
| | 612 | 19 | 34 | 0.56 | |
| | 601 | 16.5 | 30 | 0.55 | |

* Present work.

determination of CCT from TTT. In the literature, several attempts have been made in this direction.[15,16] The derivation of CCT from TTT is possible only after the experimental determination of the TTT data. But the experimental determination of TTT is very difficult. To determine the TTT, the specimen must be cooled from the austenitising temperature (usually around 850-900 °C) to the isothermal test temperature (usually around 650 °C) in a very short period of time, usually a second or two. This must be done in order to ensure that the transformation does not begin before the test temperature is reached. This calls for cooling rates of the order of 100 to 150 °C/s or more which are very difficult to achieve. In a salt pot, which has been the medium used by several workers in the literature to achieve such cooling rates, it is impossible to do so. Hence this introduces an error in the experimental measurements. Also it is impossible to ensure equal cooling rates at all locations even in a thin disc-shaped specimen in a salt pot quench. On the other hand, CCT data is much simpler to determine experimentally and more accurate. Thus a method for determining TTT from CCT is very much needed to check experimental TTT results. The present study enumerates a simple iterative procedure called the "additivity method", for deriving the TTT from the CCT. This procedure is easy to use and much less time consuming when compared to the lengthy calculations suggested by others.[15,16]

## 3.5 Derivation of TTT from CCT by the Additivity Method

The TTT curve can be expressed by a mathematical equation.

$$t_{AV\text{-}TTT} = a\, b^{x}\, e^{cx} \qquad (3.75)$$

where

$t_{AV\text{-}TTT}$ = TTT start time at the temperature T

a, b, c = constants

$x = T_{A1} - T$

$T_{A1}$ = equilibrium transformation termperature of the material

The CCT start can also be expressed in a similar form as

$$T_{AV\text{-}CCT} = a_1\, b_1^{x}\, e^{c_1 x} \qquad (3.76)$$

The constants $a_1$, $b_1$, $c_1$ in Eq. (3.76) can be calculated by using a multiple-regression procedure by using experimentally determined $t_{AV\text{-}CCT}$ values. By using additivity and the iterative procedure to be described, the constants a,b,c in Eq. (3.75) can be determined.

To start the iterative procedure, an estimate of a,b and c must be made. This can be done by using published TTT diagrams as a guide or can be determined on any arbitrary basis. A proper estimation of these constants results in a reduction of the number of iterations needed to determine

the correct TTT start curve. Hence the estimation of these constants is not crucial to the success of the method. The TTT start curve determined by the estimated constants a, b and c is the first approximation to the correct $t_{AV\text{-}TTT}$.

Consider a cooling rate A °C/s. The principle of additivity states that

$$\int_0^{t_{AV\text{-}CCT}} \frac{dt}{t_{AV\text{-}TTT}} = 1 \qquad (3.77)$$

for a constant cooling rate, Eq. (3.77) can be written as:

$$\frac{1}{A} \int_0^{t_{AV\text{-}CCT}} \frac{dT}{t_{AV\text{-}TTT}} = 1 \qquad (3.78)$$

$$\therefore \int_0^{t_{AV\text{-}CCT}} \frac{dT}{t_{AV\text{-}TTT}} = A \qquad (3.79)$$

The Eq. (3.79) can be approximated by

$$\sum_0^{t_{AV\text{-}CCT}} \frac{\Delta T}{t_{AV\text{-}TTT}} = A \qquad (3.80)$$

As $\Delta T \to 0$, Eq. (3.80) becomes the same as Eq. (3.79). For the cooling rate A, the $T_{AV\text{-}CCT}$ can be found from the CCT curve. Using $t_{AV\text{-}TTT}$ Calculated at each temperature, from $T_{A1}$ to the $T^{A}_{AV\text{-}CCT}$ in steps of $\Delta T$, by using the Eq. (3.75), the LHS of Eq. (3.80) can be calculated. If this is greater than the RHS, the first approximation of the TTT upto $T_{AV\text{-}CCT}$ is to the left of the correct $t_{AV\text{-}TTT}$. If the LHS value is $A_1$, then by multiplying all the $t_{AV\text{-}TTT}$ values upto $T^{A}_{AV\text{-}CCT}$ by $A_1/A$, the identity expressed in Eq. (3.80) will hold true upto $T_{AV\text{-}CCT}$. Now, using these values of $t_{AV\text{-}CCT}$ upto $T_{AV\text{-}CCT}$, the constants a, b and c in Eq. (3.75) are recalculated by using a multiple regression procedure. This equation is used in the next iteration for calculating the LHS in Eq. (3.81). A cooling rate $A_1$ °C/s is now chosen such that $A_1 > A$. The calculations, as done during the first iteration, are repeated, now upto a new $T^{A_1}_{AV\text{-}CCT}$. This procedure is carried on until the correct $t_{AV\text{-}TTT}$ is obtained. The iterations can be stopped, when required, depending upon the needed accuracy.

The theoretical justification for the iterative procedure is as follows. For a cooling rate A, for an additive reaction, Eq. (3.80) must hold. If the LHS of Eq. (3.80), calculated using the first approximation for $t_{AV\text{-}TTT}$, is $A_1$, then

$$\sum_{0}^{t_{AV\text{-}CCT}} \frac{\Delta T}{t_{AV\text{-}TTT}} = A_1 \qquad (3.81)$$

$$\therefore \frac{1}{A_1} \sum_{0}^{t^A_{AV\text{-}CTT}} \frac{\Delta T}{t_{AV\text{-}TTT}} = 1 \qquad (3.82)$$

$$\therefore \frac{A}{A_1} \sum_{0}^{t^A_{AV\text{-}CCT}} \frac{\Delta T}{t_{AV\text{-}TTT}} = A \qquad (3.83)$$

$$\therefore \sum_{0}^{t^A_{AV\text{-}CCT}} \frac{\Delta T}{\frac{A_1}{A} \cdot t_{AV\text{-}TTT}} = A \qquad (3.84)$$

$\therefore$ by multiplying $t_{AV\text{-}TTT}$ upto $T^A_{AV\text{-}CCT}$ by $\frac{A_1}{A}$, we can ensure that Eq. (3.79) will hold. Fig. 3.5 is a pictorial representation of this procedure.

This iterative method was used to predict the $t_{AV\text{-}TTT}$ for the material used in the present work. The $t_{AV\text{-}TTT}$ and $t_{AV\text{-}CCT}$ are, respectively, the incubation periods for isothermal and continuous cooling rransformations. The details of the

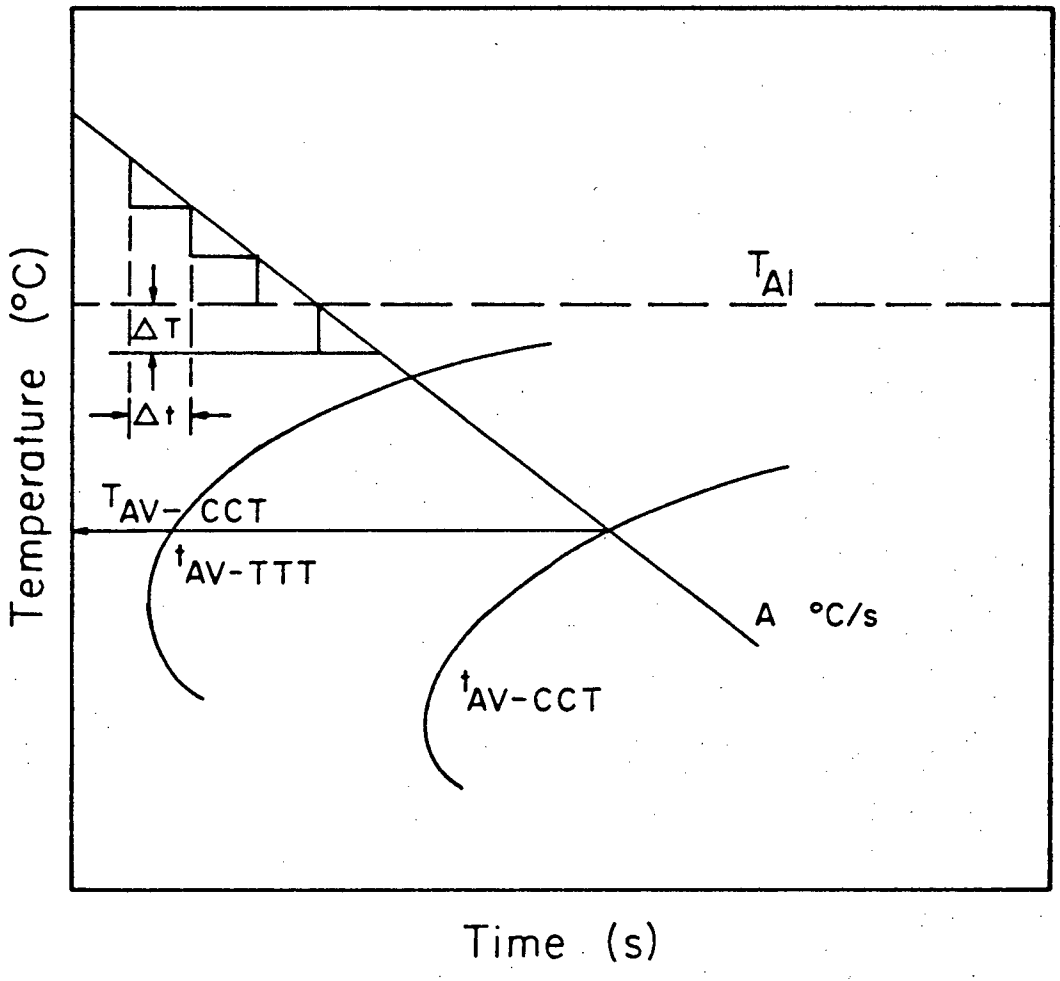


Figure 3.5 Nomenclature of parameters used to characterize isothermal and continuous cooling reactions.

calculations are shown in Appendix 4. The $t_{AV-TTT}$ values calculated by the iterative procedure and that found by experiments are compared in Table 3.5. As can be seen from this table, the agreement between predicted and calculated values is quite good. B. Hawbolt et al.[5] have reported that, in their experiments, the additivity rule did not work well in the incubation period. This is contrary to the observations in the present work. Since the nature of the reactions in the incubation period (growth of embryo to nucleus) is essentially the same as in the region beyond the incubation period, it is possible to expect the additivity rule to work in the incubation period as well. Calculations to find the values of the LHS of Eq. (3.80) have been accomplished by a FORTRAN computer program. A listing of this program is shown in Appendix 5.

Table 3.5 Comparison of Experimentally Determined and Calculated (by the Additivity Method) $t_{AV-TTT}$

| Temperature (°C) | $t_{AV-TTT}$ (s) | |
|---|---|---|
| | Experimental | Calculated |
| 680 | 43 | 41.3 |
| 670 | 5.6 | 12.9 |
| 660 | 6.2 | 5.7 |
| 650 | 3.0 | 3.2 |
| 630 | 1.8 | 1.8 |
| 623 | 1.6 | 1.7 |
| 615 | 1.5 | 1.6 |
| 603 | 1.9 | 1.8 |

# Chapter 4

# DEVELOPMENT OF A MATHEMATICAL MODEL TO STUDY PHASE TRANSFORMATION

## 4.1 Introduction

In this chapter, a description is given of the mathematical model developed to predict the phase transformation of austenite to pearlite in a plain carbon eutectoid steel. The model is based on experimentally measured TTT and CCT data. To characterize the non-isothermal austenite-pearlite reaction kinetics, the principle of additivity has been used, the theoretical justification for which has been given in Chapter 3. The model, in its present form, can be used to predict the temperature response in an "infinitely" long plain carbon eutectoid steel rod of circular cross-section being cooled in air.

## 4.2 Model Formulation

For a cylindrical rod cooling in air, heat flow to the surroundings is governed by heat conduction within the rod and heat transfer from the surface of the rod. The heat conduction in a rod undergoing cooling in a medium is given in quantitative terms by the following equation:

$$\frac{\partial}{\partial r}\left(K\frac{\partial T}{\partial r}\right) + \frac{K}{r}\frac{\partial T}{\partial r} + \dot{q}_{AP} = \rho C_p \frac{\partial T}{\partial t} \qquad (4.1)$$

where:

$K$ = thermal conductivity of the rod material

$r$ = radial distance from the centre of the rod

$T$ = temperature of the rod

$C_p$ = specific heat of the rod material

$\rho$ = density of the rod material

$t$ = time

$\dot{q}_{AP}$ = volumetric rate of latent heat liberated due to the austenite-pearlite transformation. This term is zero when there is no transformation taking place.

Eq. (4.1) is valid under the following assumptions:

i) Infinitely long rod.

ii) Negligible axial heat flow.

iii) Radial symmetry of temperature

iv) Uniform initial temperature

v) Uniform circular cross-section.

These conditions apply to a wire rod undergoing cooling in a controlled cooling process such as Stelmor cooling. The boundary conditions are:

i) $t > 0,\ r = 0,\ -K \frac{\partial T}{\partial r} = 0$

ii) $t > 0,\ r = r_a,\ -K \frac{\partial T}{\partial r} = h\ (T_{r_a} - T_a)$

where

$r_a$ = radius of the rod

$h$ = surface heat transfer co-efficient

$T_a$ = atmospheric temperature

$T_{r_a}$ = surface temperature of the rod.

The initial condition is:

$t = 0,\ 0 \leq r \leq r_a,\ T = T_i$

$T_i$ = uniform initial temperature.

Solution of Eq. (4.1) with the proper constants will give the thermal history of the rod under a given cooling condition. Incorporation of the latent-heat liberation term in the heat-transfer equation requires a knowledge of the kinetics of the austenite-pearlite reaction. This term can be calculated as:

$$\dot{q}_{AP} = \rho H \frac{\Delta F_{AP}}{\Delta t} \qquad (4.2)$$

where

$H$ = enthalpy of the austenite-pearlite reaction

$\Delta F_{AP}$ = volume fraction transformed during the time $\Delta t$.

Calculation of $\Delta F_{AP}$ must be done by using $t_{AV\text{-}CCT}$ and the principle of additivity, as described in Section 4.4. Owing to the complexity and the amount of calculations

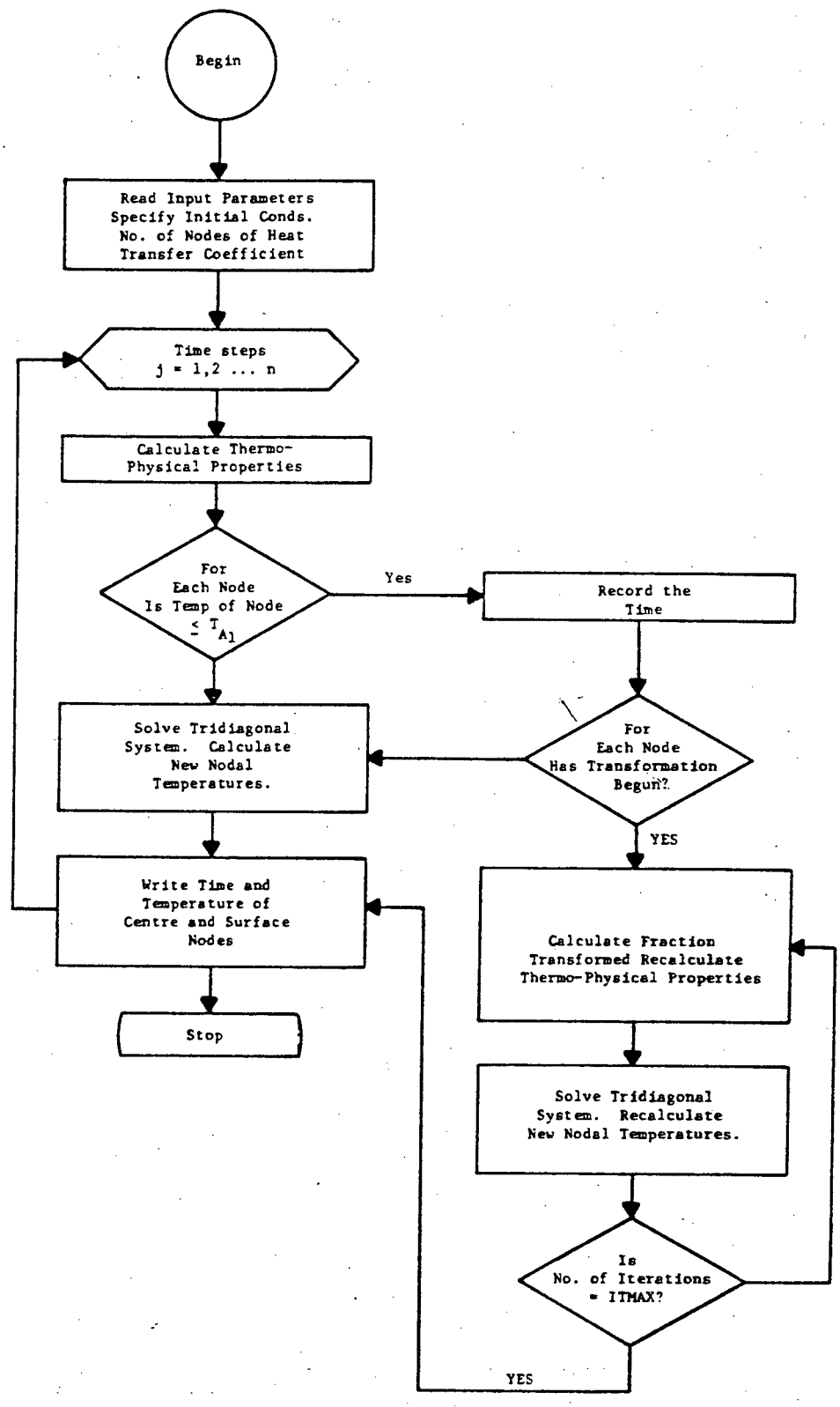


Fig. 4.1 Computer program flow-chart.

involved, it is appropriate to solve Eq. (4.1) subject to the boundary and initial conditions with the aid of a digital computer.

## 4.3 Computer Program

Solution of Eq. (4.1) can be accomplished by using a one-dimensional implicit finite-difference approximation. (The diagonal system of equations is shown in Appendix 6.) The node arrangement, the finite difference equations and the tri-diagonal system of equations was solved by using the Gaussian elimination method. A flow chart of the computer program is shown in Fig. 4.1. Some important features of the program are:

i) Thermal conductivity and specific heat have been considered as functions of temperature.[46]

ii) Density is assumed constant to keep the node size constant.

iii) The $t_{AV-CCT}$ has been used as a function of temperature. The relationship between $t_{AV-CCT}$ and time can be found from the equation

$$t_{AV-CCT} = A\, x^B\, e^{Cx} \qquad (4.3)$$

where

A,B,C = constants

$x = T_{Al} - T$

T = Temperature.

The constants A, B and C were found by a multiple-regression procedure.

iv) Because of the relationship between $\dot{q}_{AP}$ and $\Delta F_{AP}$, Eq. (4.2), an iterative procedure was required at each time step, after the start of transformation, to check for convergence. It was found that within 3 to 4 iterations, the temperature values at the nodes converged to give a difference less than $10^{-4}$ °C for successive temperature approximations.

v) The number of nodes and the time step must be chosen carefully, depending on the rod size and the cooling rate. The node size must be not more than 0.25 mm. The time-step interval could be 1.s for slow cooling rates (less than 10 °C/s) and should be approximately 0.1s for faster cooling rates.

vi) n and b in the Avrami equation, Eq. (2.2) have been incorporated as functions of temperature. These functions are calculated in separate subroutines.

The program was checked for internal consistency by comparing the solution generated by assuming $\dot{q}_{AP} = 0$ and

constant thermophysical properties for an eutectoid steel with an analytical solution of Eq. (4.1). The results agreed to within 2% of error and are shown in Appendix 7. A comparison was also made for the case of small diameter rods with negligible internal resistance. The above checks confirmed that the program is free of logical and other errors. A complete listing of the program is given in Appendix 8. The model calculates the temperature profiles at all locations inside the rod undergoing cooling. The model output consists of:

i) Temperature of surface and central nodes and the corresponding time.

ii) Start time and temperature of transformation at surface and central nodes.

iii) Volume fraction transformed at surface and central nodes at each time step.

By plotting the time-temperature data generated by model, for a given cooling condition, the amount of recalescence can be calculated and the temperature range over which the transformation takes place can be determined. By plotting the volume fraction transformed-time predictions, the course of the reaction during the process of cooling can be charted. Typical time-temperature plots from model predictions for a steel rods of composition 0.82% C - 0.82% Mn - 0.26% Si (Grain size 5-7 ASTM) and diameters

5.5 mm, 20 mm and 25 mm at different cooling rates are shown in Figs. 4.2 and 4.3. Typical calculations from model predictions for the same material are shown in Table 4.1.

## 4.4 Program Logic

The rod diameter, number of nodes, initial temperature of the rod, ambient temperature (or the temperature of the cooling medium), the surface heat transfer co-efficient and the time-step are input to the program. In the pre-transformation period, say upto 700°C (this depends upon the rod diameter and the cooling rate for a given material) the tri-diagonal system of equations is solved at each time step, in the absence of transformational heat, to determine the new temperatures at all nodes. After these temperatures are determined, each node is checked, against $t_{AV-CCT}$, to determine whether the transformation has begun at that node. If the transformation "starts" at any node, the fraction transformed is calculated, for this node, by using the principle of additivity. In general, at the $j-1^{th}$ time step, for the $i^{th}$ node undergoing transformation,

$$F^i_{j-1} = 1 - \exp\left[-b(T^i_{j-1})\,\Theta^i_{j-1}{}^{n(T^i_{j-1})}\right] \qquad (4.4)$$

where

$F^i_{j-1}$ = volume fraction transformed at node i during the time step j-1

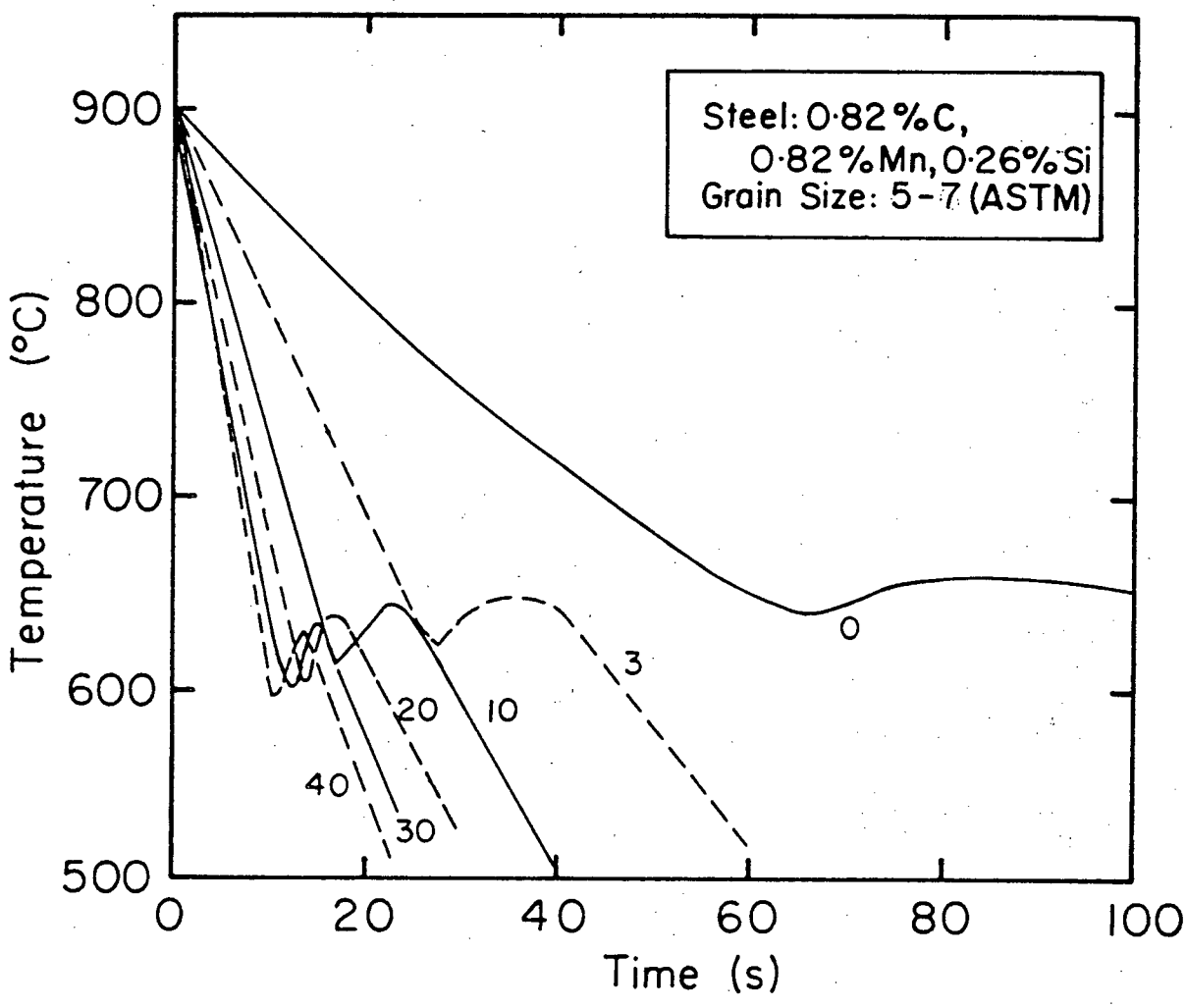


Fig. 4.2 Typical model-predicted centre-line temperature response for an air-cooled steel rod. (Rod diameter = 5.5 mm) (Figures on the curves indicate the air velocity in m/s.)

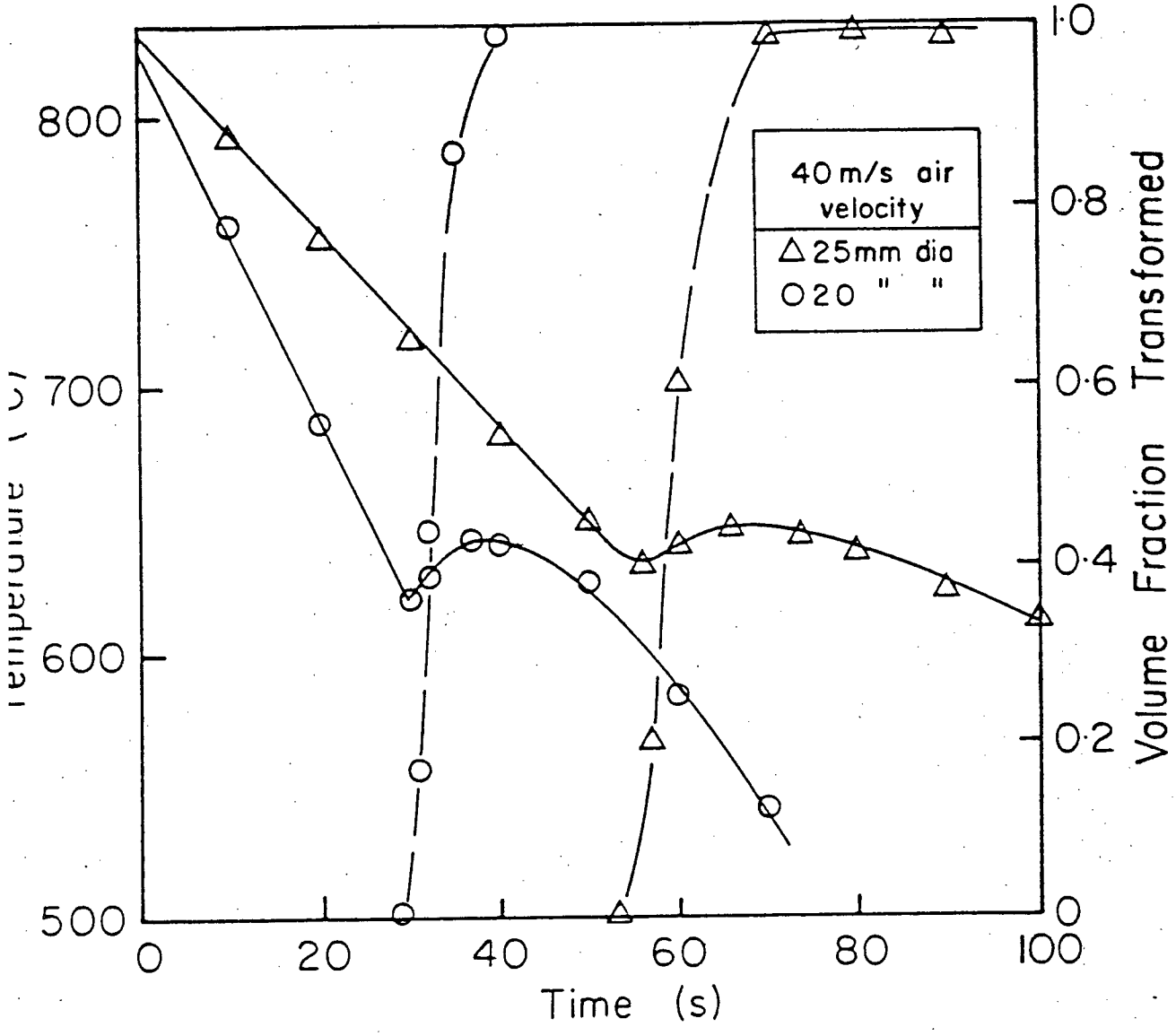


Fig. 4.3 Typical model-predicted centre-line temperature and transformation profiles for air-cooled steel rods.

Table 4.1 Typical Model Predictions of Undercooling and Recalescence at the Centre-line of Air Cooled Steel Rods

| Steel: 0.82% C - 0.82% Mn - 0.26% Si<br>Grain Size: 5 - 7 ASTM | | | | |
|---|---|---|---|---|
| Rod Diameter (mm) | | Air Velocity (m/s) | | |
| | | 0 | 20 | 40 |
| 5 | Minimum (°C) | 69 | 92 | - |
| | Maximum (°C) | 83 | 135 | - |
| | Recalescence (°C) | 14 | 43 | - |
| | Cooling Rate (°C/s) | 4.38 | 24.32 | - |
| 10 | Minimum (°C) | 60 | 76 | 81 |
| | Maximum (°C) | 81 | 103 | 109 |
| | Recalescence (°C) | 21 | 23 | 28 |
| | Cooling Rate (°C/s) | 1.9 | 8.5 | 12.6 |
| 20 | Minimum (°C) | 54 | 65 | 69 |
| | Minimum (°C) | 72 | 84 | 86 |
| | Recalescence (°C) | 18 | 19 | 17 |
| | Cooling Rate (°C/s) | 0.9 | 3.4 | 5.0 |

Note: Minimum = Minimum undercooling (= $T_{Al}$ - T)
Cooling rate at $T_{Al}$

$b(T^i_{j-1})$ = value of co-efficient b in the Avrami equation at the temperature of the $i^{th}$ node at time step j-1

$\theta^i_{j-1}$ = time taken to transform the cumulative fraction $F^i_{j-2}$ at the temperature $T^i_{j-1}$

$n(T^i_{j-1})$ = value of the co-efficient n in the Avrami equation at the $i^{th}$ node at temperature $T_{j-1}$.

For the $j^{th}$ time step,

$$F^i_j = 1 - \exp\left[-b(T^i_j)\,\theta^i_j\right]^{n(T^i_j)} \tag{4.5}$$

where

$$\theta^i_j = \Delta t + \left[\frac{\ln \dfrac{1}{1 - F^i_{j-1}}}{b(T^i_j)}\right]^{\frac{1}{n(T^i_j)}} \tag{4.6}$$

Then the additional fraction transformed during the time interval j to j-1 is:

$$\Delta F = F^i_j - F^i_{j-1} \tag{4.7}$$

and the corresponding latent heat liberated is:

$$\dot{q}_{AP,j} = \rho H \frac{\Delta F}{t_j} \tag{4.8}$$

Equation (4.6) is the mathematical statement of the additivity principle. This calculation, when ultimately used in Eq. (4.8) and subsequently as a term in the tridiagonal system of equations, provides for the effect of reaction kinetics on the time-temperature response of the rod. Thus, the difficulties encountered in the direct measurement of reaction kinetics by means of the nucleation and growth rates have been overcome by linking the kinetics to a more easily and accurately measurable variable, like the temperature.

Once the transformation is detected and the amount of transformation calculated, the co-efficients of the tridiagonal system are calculated. Then the new temperatures at all nodes are calculated for that time step, including the effect of the latent heat of transformation. Since the rate of the latent heat liberation is of the form given in Eq. (4.7), an iterative procedure is necessary to check for stability of temperature. This is done and it has been established that four iterations are needed to give stable temperatures. This procedure is repeated for subsequent time steps until transformation is complete at all nodes. The program execution is terminated after a predetermined total time value is reached, which depends on the diameter and cooling rate. At each time step, for each node, the temperature dependent properties (thermal conductivity and specific heat) are calculated. Since these also depend

upon the transformation, the properties for austenite and pearlite for eutectoid plain carbon steel have been incorporated into the program as temperature functions. During transformation, the program adjusts the values of these variables at all nodes, according to the amount of transformation and temperature.

In order to make the program efficient, several counters have been employed. These restrict the number of times a loop is used, thereby reducing program execution time. Since the $t_{AV-CCT}$, thermal conductivity and specific heat are material specific properties, the program, in its present form, can be used only for the 0.82% C - 0.82% Mn - 0.26% Si eutectoid steel of grain size 5 to 7 ASTM.

# Chapter 5

# EXPERIMENTAL

All experiments have been conducted on a plain carbon eutectoid steel having the composition shown in Table 5.1.

## 5.1 Objectives of Experiments

Experiments have been conducted in pursuit of the following objectives:

i) To determine the TTT "start" line and to charactize the kinetics of the austenite-pearlite reaction under isothermal conditions.

ii) To determine the CCT "start" line for a range of continuous cooling rates.

iii) To measure the time-temperature response at the centre-line of air cooled steel rods under different cooling conditions.

## 5.2 Experimental Procedures

### 5.2.1 TTT Tests

The isothermal kinetics of a eutectoid plain carbon steel were obtained in a nitrogen atmosphere using a diametral dilatometer and a thermocouple attached to the

Table 5.1 Steel Composition

| | |
|---|---|
| C | 0.82% |
| Mn | 0.82% |
| Si | 0.26% |
| S | 0.01% |
| P | 0.016% |
| Cu | Nil |
| Ni | < 0.004% |
| Cr | 0.02% |

(Plain Carbon Eutectoid)

centre of the outside surface of the specimen. The testing chamber was evacuated with a mechanical forepump, after which nitrogen was introduced to obtain a positive pressure. This was repeated 3 times to ensure a low oxygen content in the atmosphere. A complete description of the apparatus used can be found in reference 35.

The tests were conducted on tubular specimens of 8 mm OD x 6 mm ID x 75 mm long. These specimens were machined out of rods of 10 mm OD x 150 mm length. The solid rods were used in the centre-line temperature tests. This was done to ensure that the material characteristics in all the tests (i.e. the TTT, CCT and centre-line temperature tests) were identical.

To ensure uniform wall thickness of the tubular specimens throughout the length, a procedure developed by Hawbolt et al.[35] was employed. A Chromel-Alumel thermocouple was spot-welded to the surface of the specimen at the centre. A quartz tipped dilatometer was also attached at this same diametral plane on the specimen. The temperature and dilational history of the specimens were recorded on a continuous chart recorder, during each test.

Each specimen was mounted in the apparatus (Fig. 5.1)

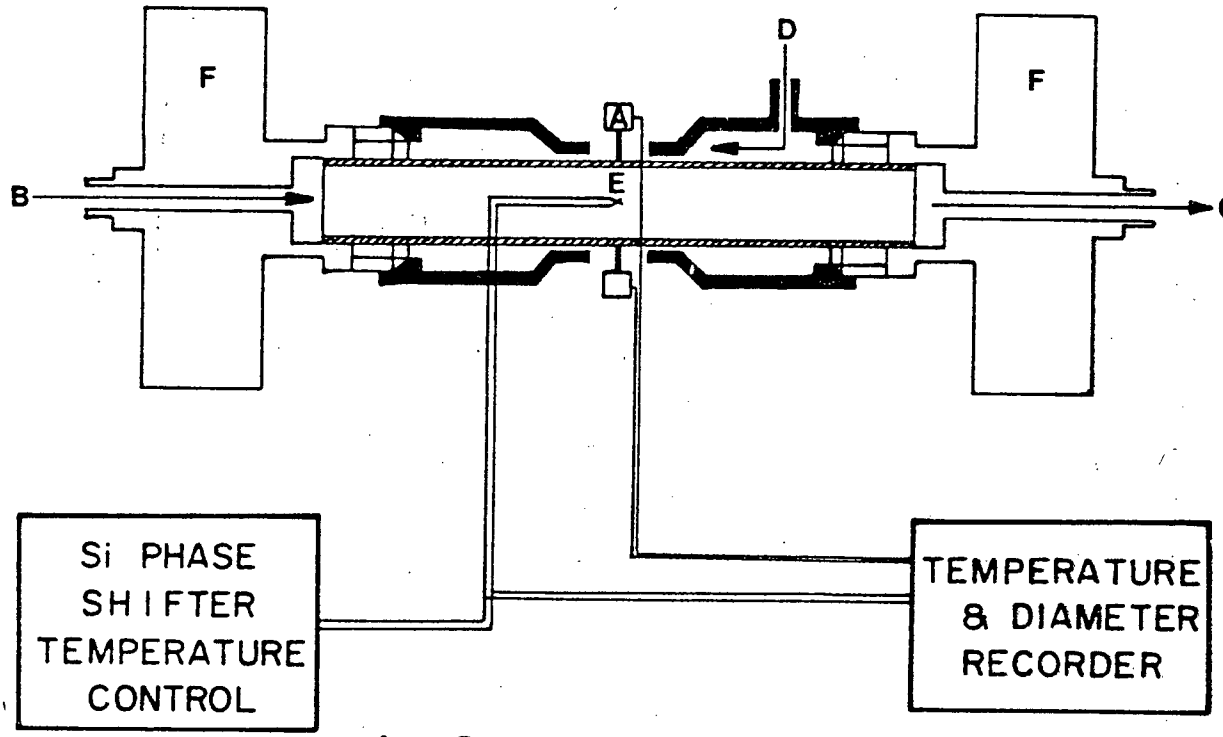


A Diametral Dilatometer
B Inlet for internal gas flow
C Outlet for internal gas flow
D Inlet for external gas flow
E Thermocouple on sample
F Support Structure

Fig. 5.1 Experimental apparatus for TTT and CCT tests.

and austenitised by resistance heating to 850°C and held for 5 minutes at this temperature. The specimen was then cooled to 740°C and held for 1 minute. Then it was cooled to the desired isothermal transformation temperature. A controlled flow of nitrogen gas over the external surface and through the internal core was used to cool the specimen to the test temperature. The maintenance of a nitrogen atmosphere in the specimen chamber tends to minimize the decarburization, though it does not eliminate it. Metallographic examinations revealed that decarb was less than 10% of the wall thickness and hence did not seriously affect the results.

The diameter of the specimen during the test was measured by the dilatometer. Due to the dimensional changes accompanying the austenite-pearlite transformation, the dilatometer measurements, in conjunction with the thermal history recorded by the thermocouple, could be used to chart the course of transformation during the tests. In all, eight TTT tests were conducted between 680°C and 603°C.

### 5.2.2 CCT Tests

The details of heating and cooling of the specimens are the same as for the TTT tests. The difference is only in the continuous cooling conditions employed. After heating each specimen to 850°C and holding for 5 minutes,

then cooling to 740°C and holding for an additional 1 minute, it was then cooled down at different cooling rates (varying from 2°C/s to 50°C/s). The different cooling rates were achieved by varying the amount of flow of nitrogen passed over the inside and the external surface of the specimen. As in the case of the TTT tests, the temperature and dilational history were recorded continuously during the tests. Sixteen CCT tests were conducted, some of which were duplicated. The reproducibility observed in these also reinforces the conclusion that the decarburization was minimal and did not seriously affect the test results.

### 5.2.3 Centre-line Temperature Measurements in Air-Cooling Tests

Solid rod specimens of at least 150 mm length were machined to 10 mm diameter from the original hot rolled 12.5 mm diameter rod stock obtained from a local supplier. A centre hole of 3 mm diameter and 5 mm depth was drilled and tapped to the centre of each rod along a radial line. A threaded plug, of the same steel, was made, with a 1.5 mm hole at its centre; this was screwed into the threaded hole in the rod. The specimen assembly is shown in Fig. 5.2. The hot junction of a 4 thou diameter Chromel-Alumel thermocouple was held in contact with the rod centre-line by the plug. The thermocouple wires were encased in a ciramic sheath. The OD of the sheath was 1.5 mm, thus fitting

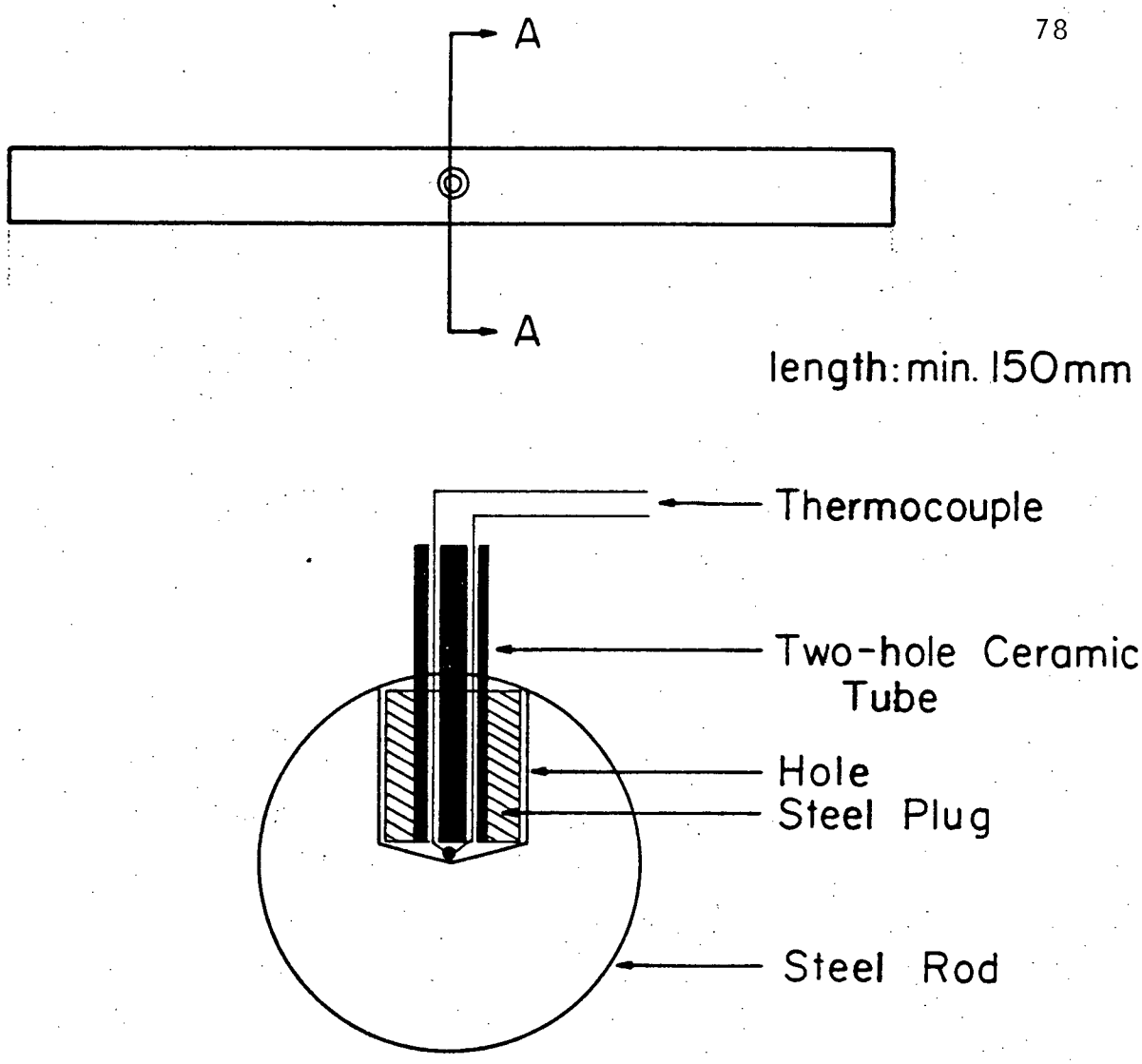


Fig. 5.2 Specimen assembly for centre-line temperature tests.

tightly into the hole at the centre of the plug. The cold junction of the thermocouple was maintained in an ice-water bath. The thermocouple leads were connected to a chart recorder to record the temperature of the centre-line of the specimen continuously during the cooling test.

The specimen, with the thermocouple firmly embedded in place, was placed in an electrically heated furnace maintained at a temperature of 850°C. The specimen attained the furnace temperature, typically, within 3 minutes. It was held at this temperature for 5 minutes, then withdrawn from the furnace and allowed to cool in air. In order to obtain different cooling conditions air was blown across the surface of the rod transverse to the axis. A schematic diagram of this procedure is shown in Fig. 5.3. By using different air velocities, a range of cooling rates, from 4°C/s to 70°C/s, was obtained. Each rod specimen was used once for a test and then discarded, thereby preventing decarburization from affecting the test results. Some of the specimens, after the completion of the tests, were examined under the microscope for grain size measurements and structure. The grain size measurements were done on specimens heated to 850°C, held for 5 minutes, and quenched in water. This procedure allows for some transformation of austenite to pearlite and the remainder transforms to martensite. On polishing and

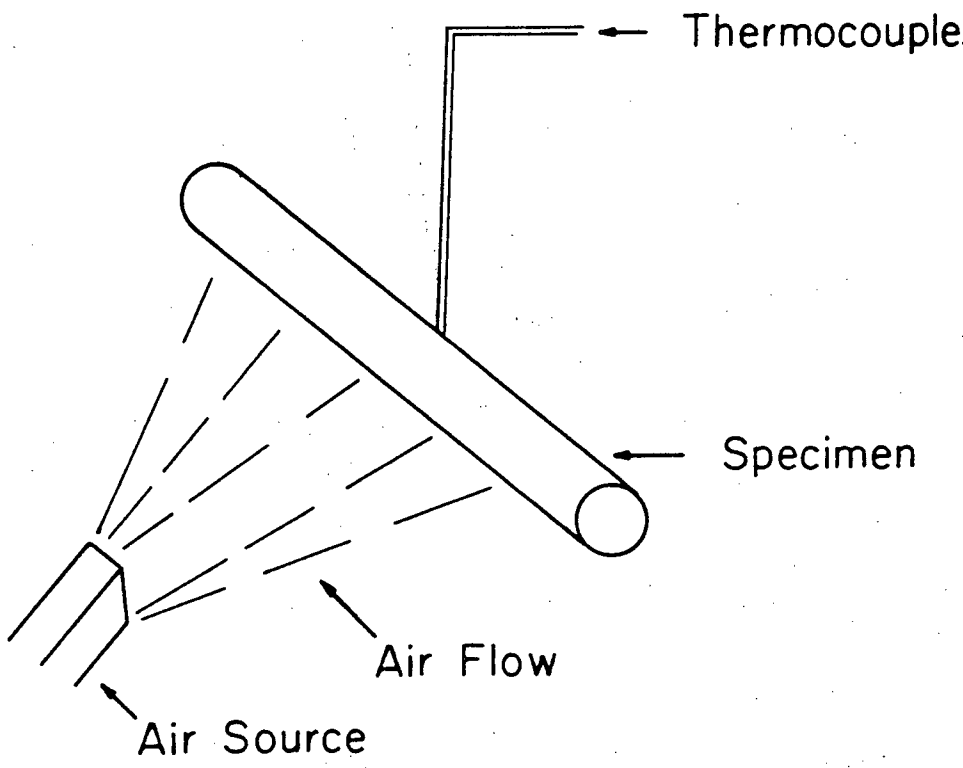


Fig. 5.3 Arrangement of air source and specimen during centre-line temperature measurement tests.

etching, the original austenite grain boundaries become visible. This micrograph was then compared with the standard ASTM grain size chart. The grain size so determined gave a range of 5 to 7 ASTM as the grain size for the material used in the tests. This was confirmed using another method of measuring grain size.[49] In this method, the number of grain intersections on a circle of a specific diameter superimposed on the micrograph are counted. The grain size (ASTM) is then given by the formula:

$$G(\text{ASTM}) = -10.0 - 6.64 \ln L_3$$

where

$$L_3 = \frac{L_T}{P \cdot M}$$

$P$ = number of grain intersections on the circumference of the superimposed circle

$M$ = magnification

$L_T$ = circumference of circle (cm)

The austenitising treatment and hence the grain size, the test conditions and the constancy of material characteristics obtained in the TTT, CCT and centre-line temperature measurement tests ensure that the experimental conditions were the same for all specimens.

# Chapter 6

## RESULTS AND DISCUSSION

During the TTT and CCT tests, the diametral response of the specimen and the temperature were recorded continuously. Typical results from these tests are shown in Figs. 6.1 and 6.2. Using these results, the $t_{AV-TTT}$ and the $t_{AV-CCT}$ have been calculated, as described in sections 6.1 and 6.2. A comparison between model predicted and experimental time-temperature profiles measured at the centre-line of air-cooled steel rods is discussed in section 6.3, followed by analysis and discussion of the experimental results.

### 6.1 TTT Test Results

To calculate the "start" of transformation, the data from the diametral dilatometer recordings was used. The fractional diameter change is equal to the fraction transformed. From the dilatometer response, a graph of $\ln \ln \left(\frac{1}{1-X}\right)$ versus ln time (X = volume fraction transformed) was plotted for each isothermal test. The empirical Avrami equation, Eq. (2.1), was then used to find the "start" of the transformation by the following procedure.

i) For values of X = 0.1, 0.2, 0.25, 0.30, 0.40, 0.50, 0.60, 0.70, 0.75, 0.80, and 0.90, the

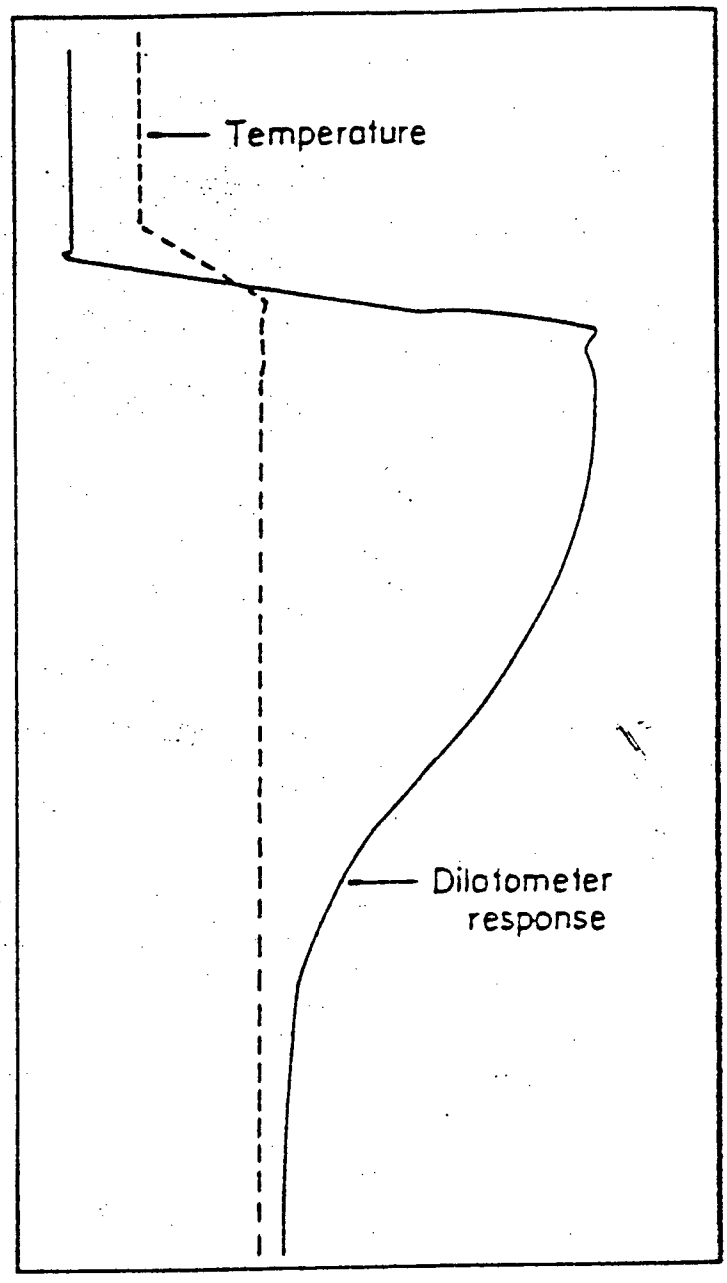


Fig. 6.1 Typical dilatometer and temperature response during a TTT test.

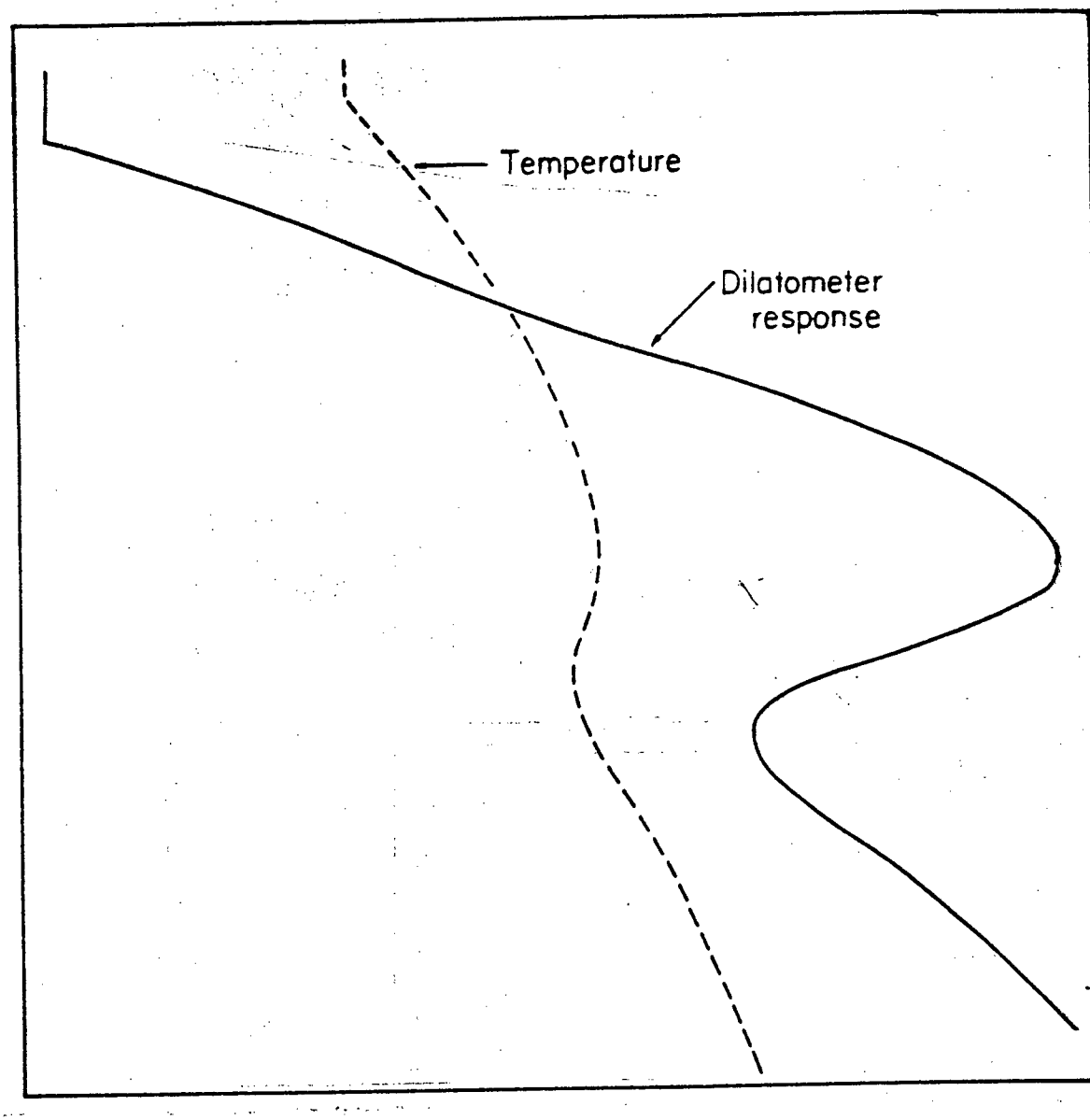


Fig. 6.2 Typical dilatometer and temperature response during a CCT test.

corresponding 't' values are obtained for each test from the dilatometer data. The 't' values are adjusted to correspond to t = 0 at 728°C ($T_{A1}$ temperature).

ii) These values of X and t are used as data for a computer program which calculates the coefficients of a linear regression line fitted to the Avrami equation, Eq. (2.2). The program uses a variable '$t_{AV}$', called "Avrami time", which is the "start" time of the transformation for a given test. During program execution, the value of '$t_{AV}$', starting with $t_{AV}$ = 0 at $T_{A1}$ and incremented in predetermined steps, is subtracted from all values of 't'. A linear regression is then done and the regression coefficients printed out along with the sum of differences. This procedure is repeated for each value of "$t_{AV}$". The regression fit which gives the least sum of differences of squares is the "best-fit" line for the data and the corresponding value of the "$t_{AV}$" is the "start" time of transformation for the given test temperature.

The TTT "start" time determined by the above procedure is different from the "start" times in conventional published

TTT diagrams. Traditionally, TTT diagrams were plotted by conducting TTT tests using salt pots and subsequent metallographic examinations of the transformed specimens. These "start" lines for either 0.1% or 1% transformed were determined assuming that the transformation started as soon as the temperature fell below the "$T_{A1}$" temperature; only the limitations of visual observations and experimental difficulties prevented the exact determination of the transformation product. The method adopted in the present work, first developed by Hawbolt et al.,[35] does not make this assumption. The "best-fit" line gives the "$t_{AV}$" for an isothermal temperature and it is assumed that the transformation starts at the time; the incubation period is not included in the determination of Avrami's co-efficients (during the test). The plots of X versus t are shown in Figs. 6.3 and 6.4. The $t_{AV-TTT}$ plot, obtained from calculations described above, is shown in Fig. 6.5. The values of the co-efficients n and b from the best-fit line are plotted in Fig. 6.6. In the model calculations, to find the appropriate values of n and b at various temperatures, curve-fit routines are used. These routines calculate the co-efficients of a polynomial of the form,

$$n(t) = a + bT + CT^2 + dT^3 \qquad (6.1)$$

$$b(T) = a_1 + b_1T + C_1T^2 + d_1T^3 \qquad (6.2)$$

where a, b, c etc. are co-efficients. In using this

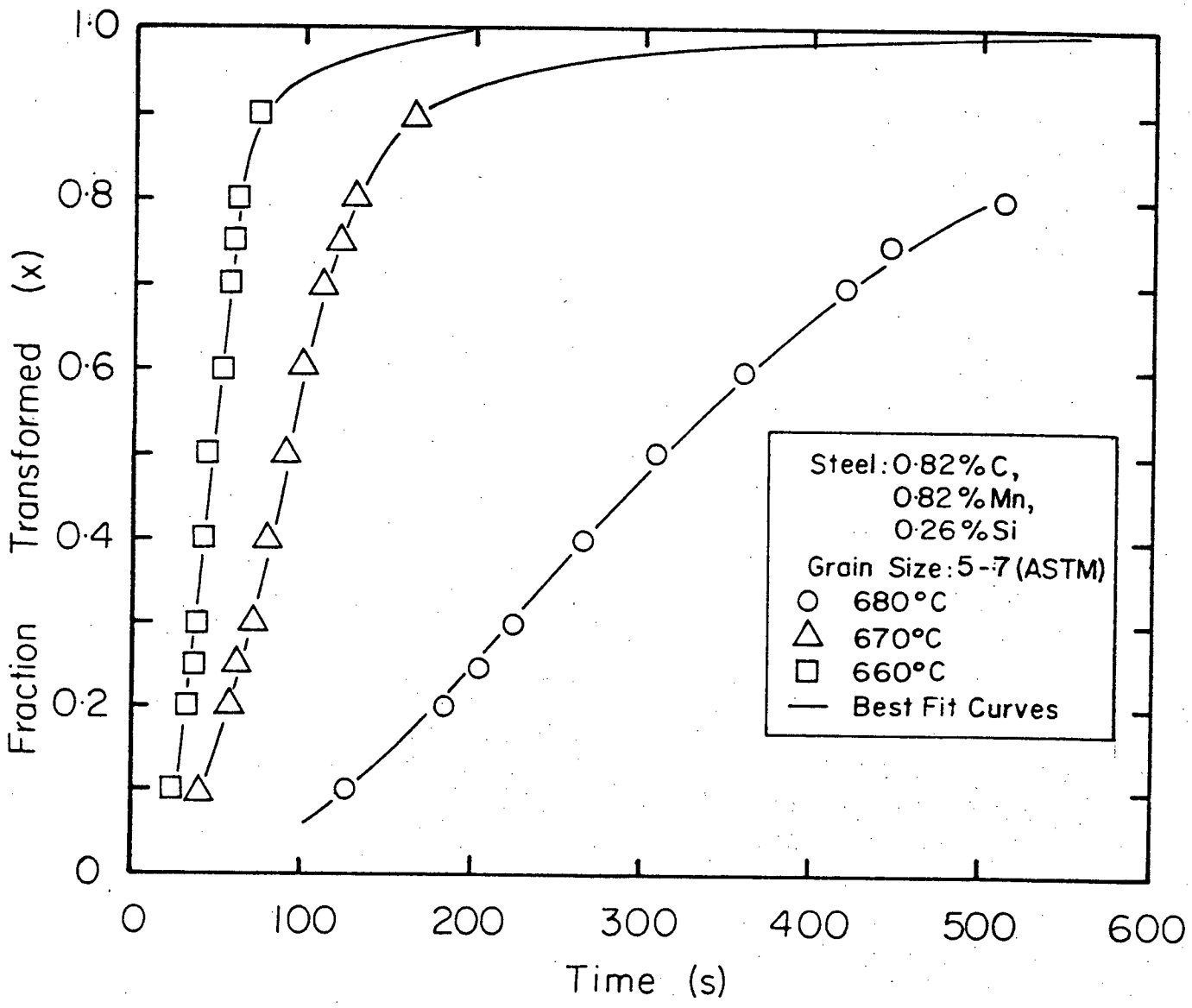


Fig. 6.3 Isothermal transformation kinetics.

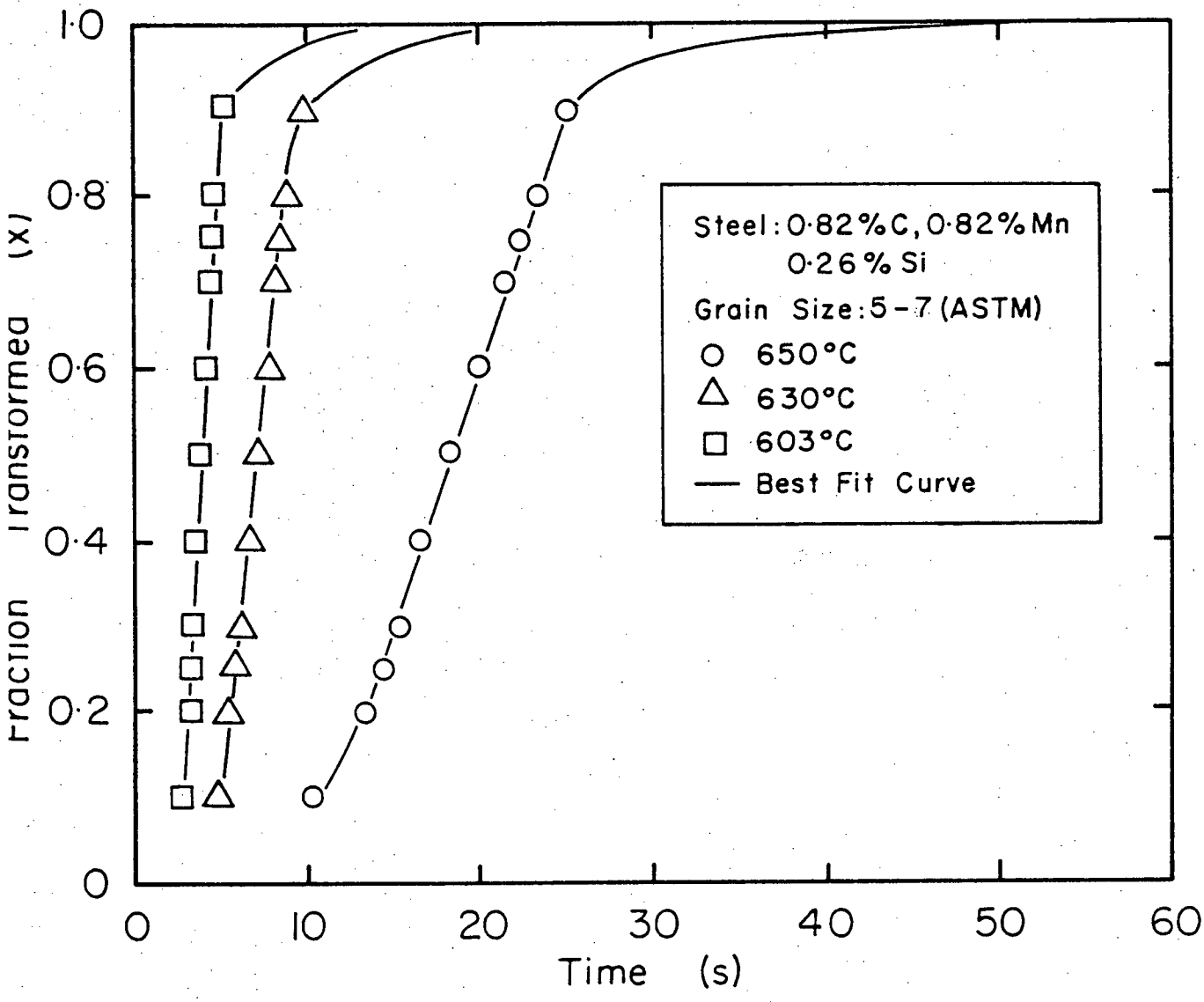


Fig. 6.4 Isothermal transformation kinetics.

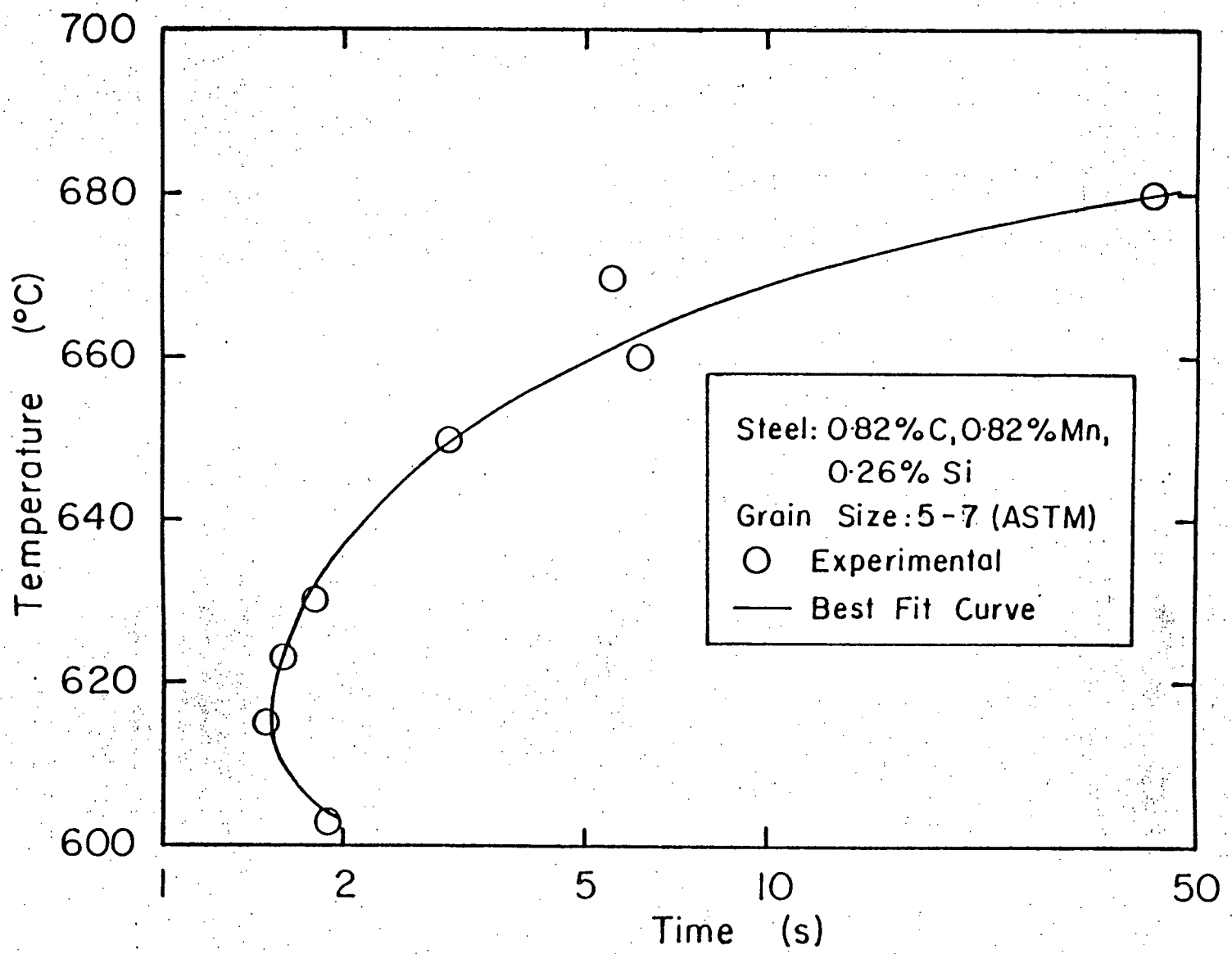


Fig. 6.5 $t_{AV-TTT}$

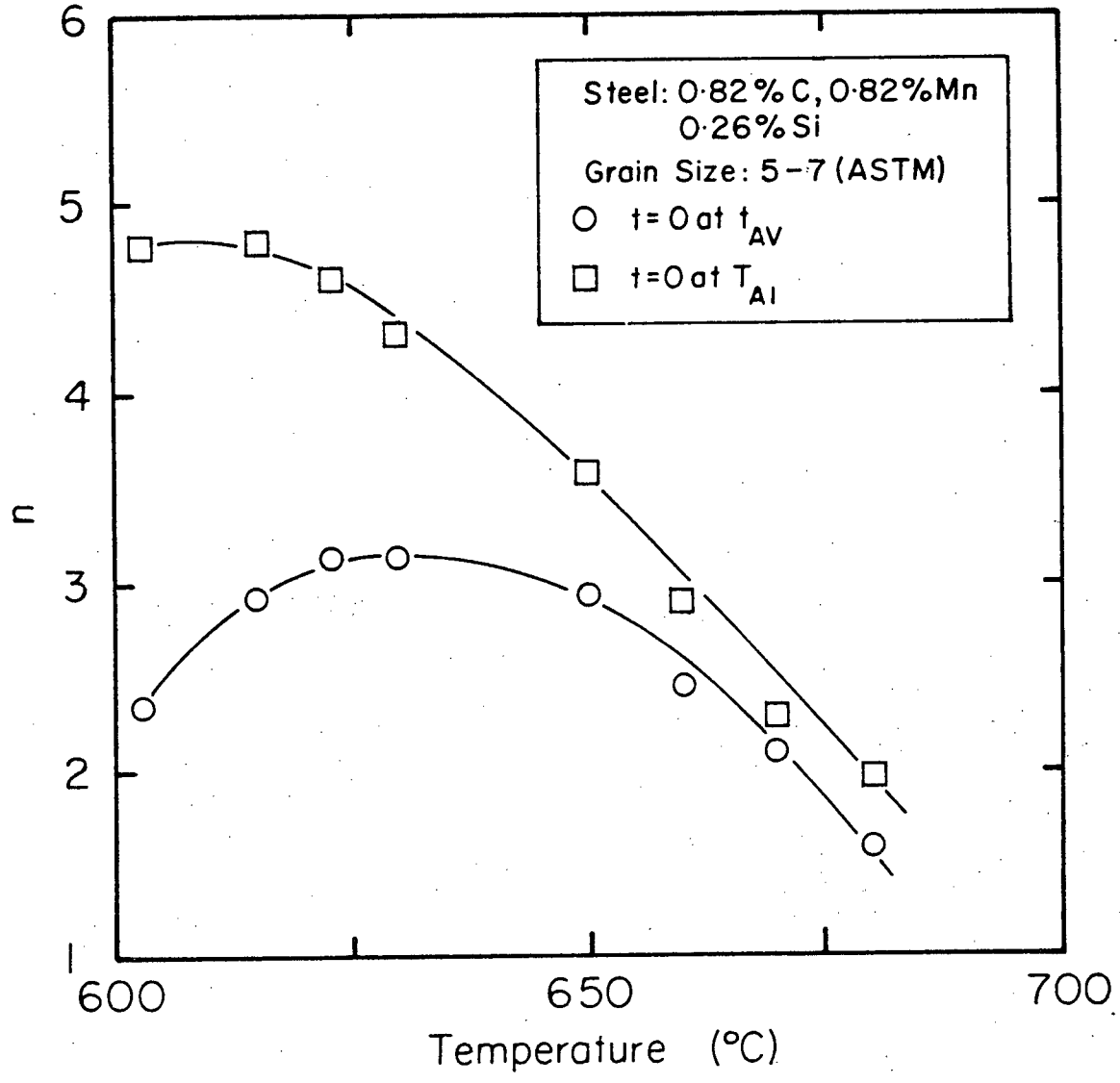


Fig. 6.6(a) Variation of n with temperature.

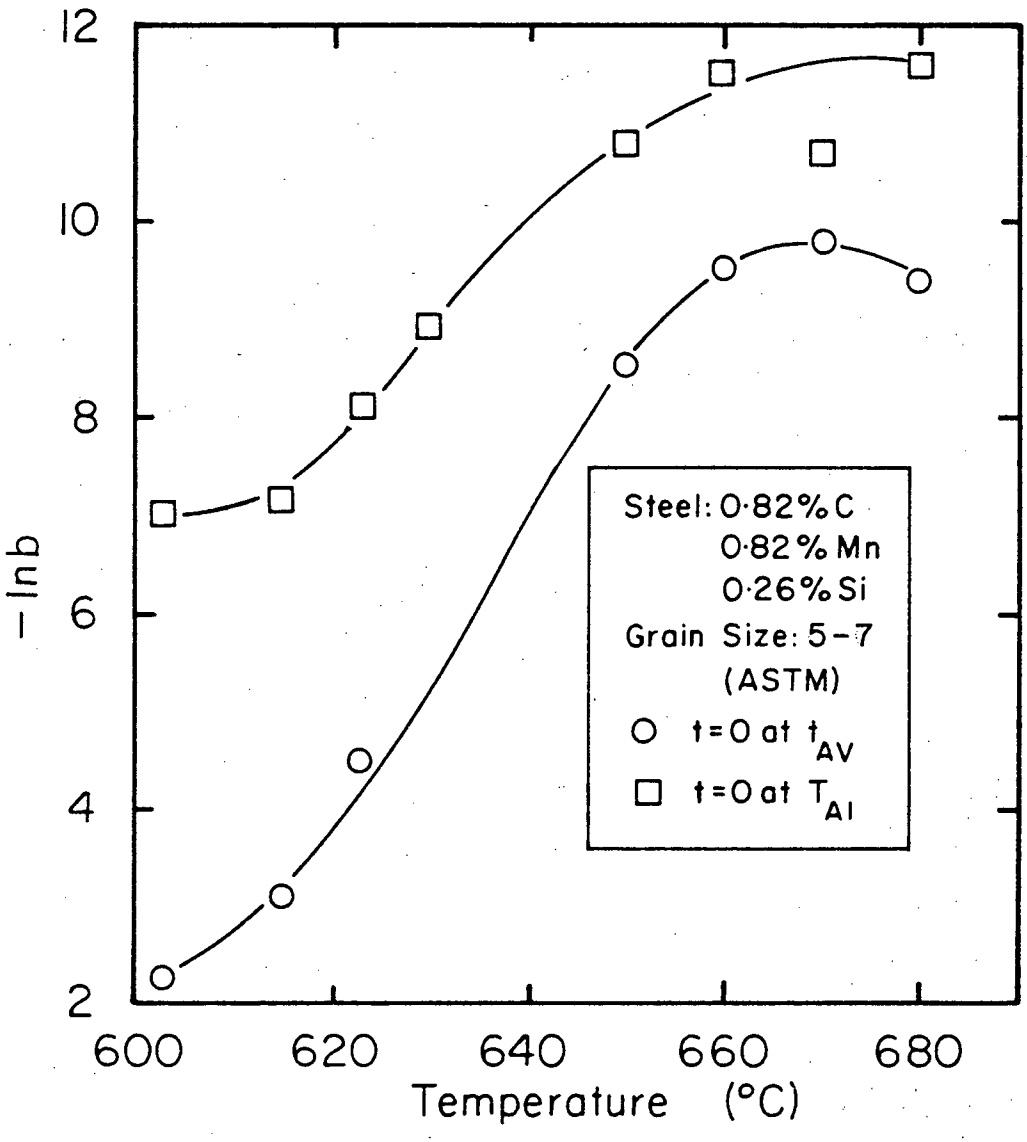


Fig. 6.6(b) Variation of b with temperature.

procedure, a small error may be introduced in the values of n and b as seen by comparing the polynomial calculated and the experimentally determined values of n and b (Table 6.1). However, values of n(T) and b(T) calculated from Eqs. (6.1) and (6.2) are within 3% of experimentally measured values. Even though the variation in n with temperature is small (between 2 and 3), it has been used as a function of temperature in model calculations.

## 6.2 CCT Test Results

A simple heat-transfer equation was used to find the "start" of transformation during continuous cooling, $t_{AV\text{-}CCT}$. For a body with negligible internal resistance undergoing cooling by convection,

$$\frac{T_t}{T_0} = \exp\left(-\frac{hA}{\rho V C_p}\, t\right) \qquad (6.3)$$

where

$T_t$ = $T(t) - T(\infty)$

$T_0$ = $T(0) - T(\infty)$

$T(t)$ = temperature of body at time 't' (°C)

$T(0)$ = initial temperature of body (°C)

$T(\infty)$ = temperature of the cooling medium (°C)

$h$ = convective heat transfer co-efficient ($W/m^2°C$)

$\rho$ = density of the body ($Kg/m^3$)

Table 6.1 Errors in n and b Values

| Temperature (°C) | n | | ln b | |
|---|---|---|---|---|
| | Experimental | Predicted | Experimental | Predicted |
| 680 | 2.125 | 2.102 | - 9.81 | - 9.83 |
| 670 | 1.619 | 1.619 | - 9144 | - 9.43 |
| 660 | 2.467 | 2.536 | - 9.47 | - 9.45 |
| 650 | 2.946 | 2.885 | - 8.39 | - 8.48 |
| 630 | 3.166 | 3.190 | - 5.73 | - 5.57 |
| 623 | 3.148 | 3.131 | - 4.51 | - 4.48 |
| 615 | 2.922 | 2.934 | - 3.14 | - 3.32 |
| 603 | 2.346 | 2.341 | - 2.04 | - 1.98 |

$V$ = volume of the body ($m^3$)

$C_p$ = specific heat of the body (W/Kg°C Sec)

$t$ = time (Sec)

From Eq. (6.3), taking the natural log of both sides,

$$\ln \left(\frac{T_t}{T_0}\right) = -Ht \tag{6.4}$$

where

$$H = \frac{hA}{VC_p} \tag{6.5}$$

$$\therefore \quad H = \frac{-\ln \frac{T_t}{T_0}}{t} \tag{6.6}$$

Since the cooling tests were conducted in a uniform nitrogen flow, the convective heat-transfer co-efficient can be expected to be nearly constant. At the time the transformation begins, the value of 'H' should change markedly, primarily due to the recalescence caused by the release of latent heat of transformation. For any given CCT test, the values of H were calculated for progressively increasing values of t. The time at which there is a sudden change in the value of H is then the $t_{AV\text{-}CCT}$. These values were also checked with the dilatometer data. The $t_{AV\text{-}CCT}$ thus calculated from experimental data are shown in Table 6.2. By using a multiple regression procedure, a curve for determining $t_{AV\text{-}CCT}$ at various temperatures, for use in

Table 6.2 Continuous Cooling Data ($t_{AV-CCT}$)

| Experiment # | $t_{AV}$ (s) | $T_{AV}$ (°C) |
|---|---|---|
| 1 | 3.2 | 585.50 |
| 2 | 3.7 | 606.75 |
| 3 | 4.1 | 605.50 |
| 4 | 4.6 | 607.50 |
| 5 | 4.9 | 611.50 |
| 6 | 5.1 | 612.75 |
| 7 | 3.1 | 589.50 |
| 8 | 4.0 | 594.00 |
| 9 | 5.1 | 613.75 |
| 10 | 3.8 | 570.50 |
| 11 | 3.3 | 591.50 |
| 12 | 4.3 | 607.00 |
| 13 | 12.0 | 629.00 |
| 14 | 14.0 | 636.00 |
| 15 | 19.8 | 642.00 |
| 16 | 38.0 | 649.50 |

model calculations, was obtained. The equation of the curve so obtained is

$$\ln (t_{AV-CCT}) = (62.7)\ (728-T)^{-15.4} \cdot \exp\ 0.1\ (728-T) \qquad (6.7)$$

The $t_{AV-CCT}$ calculated by Eq. (6.7) fits the experimental data quite well. A plot of $t_{AV-CCT}$ is shown in Fig. 6.7.

In order to check for consistency in the CCT tests, some of the tests were repeated. The consistency was found to be good as determined from the $t_{AV-CCT}$ calculations and the dilatometer responses (Fig. 6.8)

## 6.3 Comparison of Model Predicted and Experimental Results of Centre-line Temperature Measurements

For a rod of a specific diameter undergoing air-cooling, the temperature-time response can be calculated from the model by inputting the initial temperature of the rod and the heat-transfer co-efficient which depends on the cooling conditions. In the present study, the appropriate heat-transfer co-efficient has been calculated by the following procedure.

For a given rod diameter and initial temperature, different cooling profiles were generated with the model by using different heat-transfer co-efficients. The time-temperature profile from an experiment was then compared with

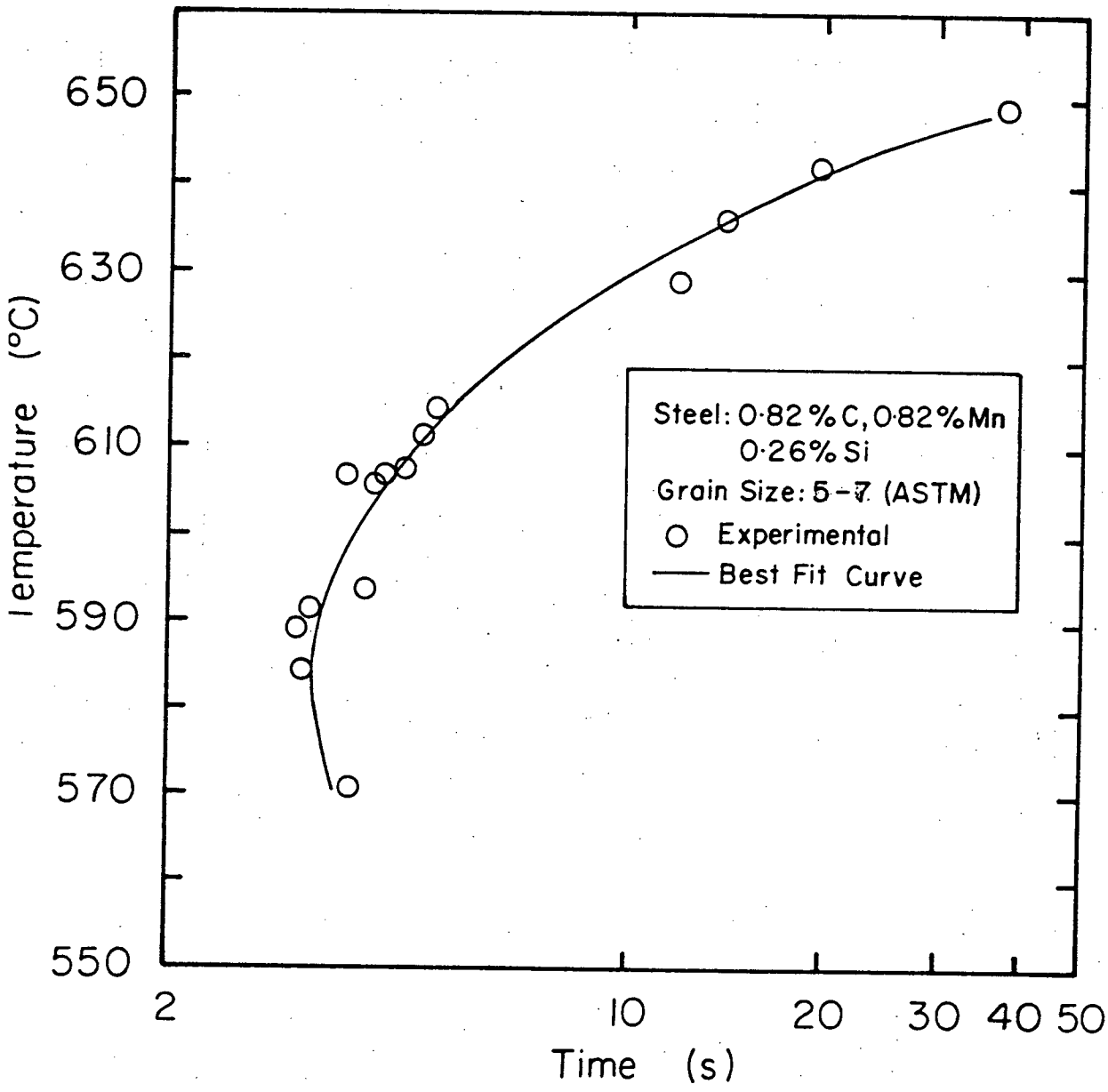


Fig. 6.7 $t_{AV-CCT}$

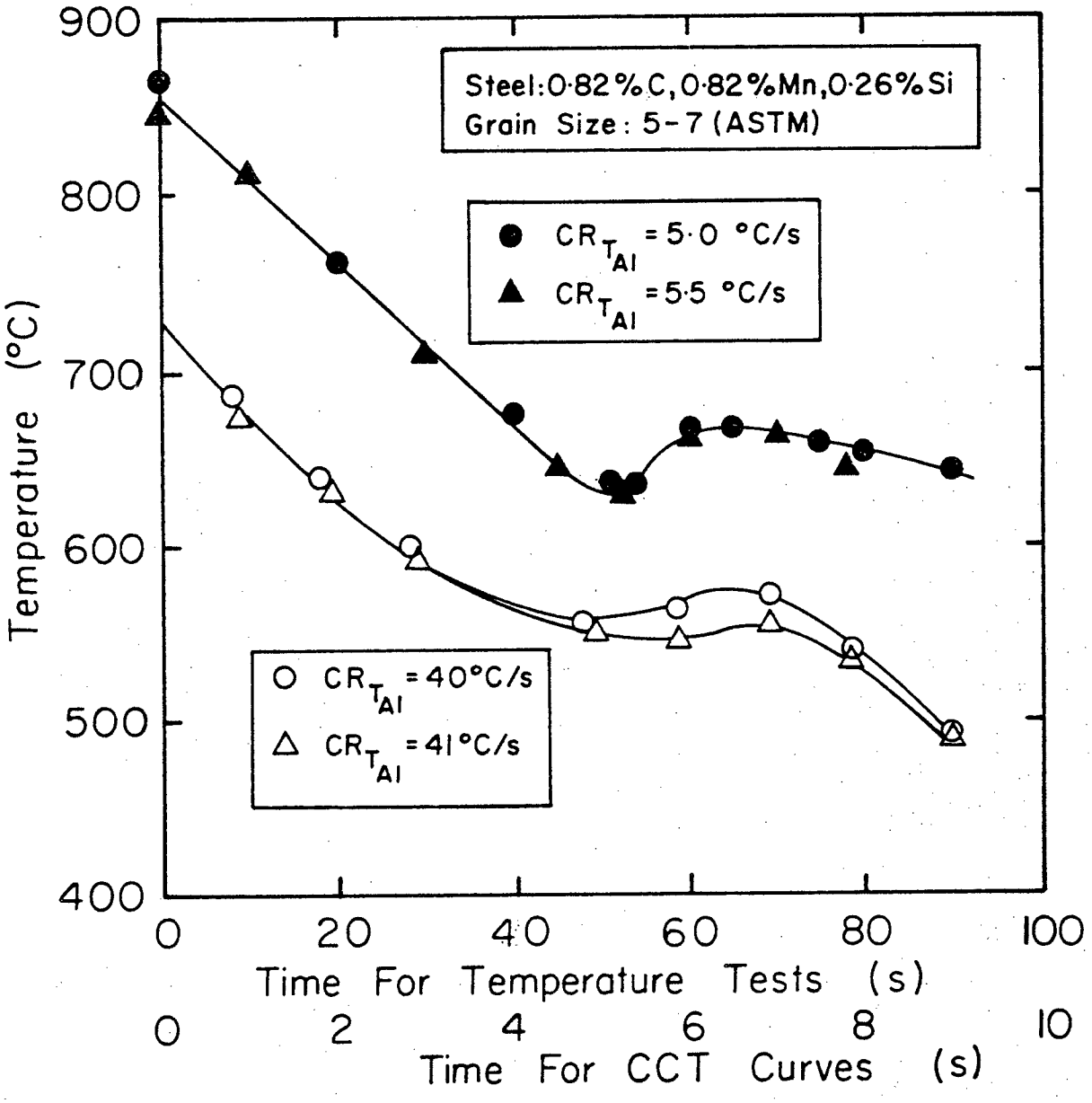


Fig. 6.8 Illustrating the consistency of results observed during CCT and centre-line temperature measurement tests.

the model generated time-temperature profiles to find the value of the heat-transfer co-efficient prior to transformation that best fits the experimental result. Using this value of the heat-transfer co-efficient as the first approximation, the model calcultions were repeated until the model-predicted values agreed with the experimental result for a given value of the heat-transfer co-efficient. The results of the model-predicted and experimental time-temperature profiles are shown in Figs. 6.9 to 6.19 and Table 6.3. As can be seen from these, the model predicted values agree very well with the experimental results.

## 6.4 Model Prediction and Validation with Measured Temperature Data

From the comparison of model-predicted and experimental results of centre-line temperature measurements during air cooling of a steel rod, it is evident that the model calculations are sufficiently accurate for the experimental situations in the present work, particularly so, in the light of the number of different inputs. The accuracy of model calculations is governed by the accuracy of the inputs. In this regard, the heat-transfer co-efficient, h, which has been assumed constant during cooling, merits special consideration. This assumption seems reasonable in the time period prior to transformation because a good fit between predicted and measured temperatures was

Table 6.3 Model Predicted Time-temperature Response at Centre-line of Air-cooled Steel Rods

| Cooling Rate at $T_{A1}$ (°C/s) | $T_{min}$ (°C) | $T_{max}$ (°C) | $t_{min}$ (s) | Amount of Recalescence $T_{max} - T_{min}$ (°C) |
|---|---|---|---|---|
| 4.3 | 636 | 660 | 57 | 24 |
| 5.0 | 638 | 660 | 53 | 22 |
| 5.5 | 636 | 660 | 53.5 | 24 |
| 5.0 | 637 | 660 | 49 | 23 |
| 6.2 | 631 | 656 | 25 | 25 |
| 10.5 | 624 | 652 | 26 | 28 |
| 10.0 | 624 | 651 | 25 | 27 |
| 10.6 | 624 | 652 | 27 | 28 |

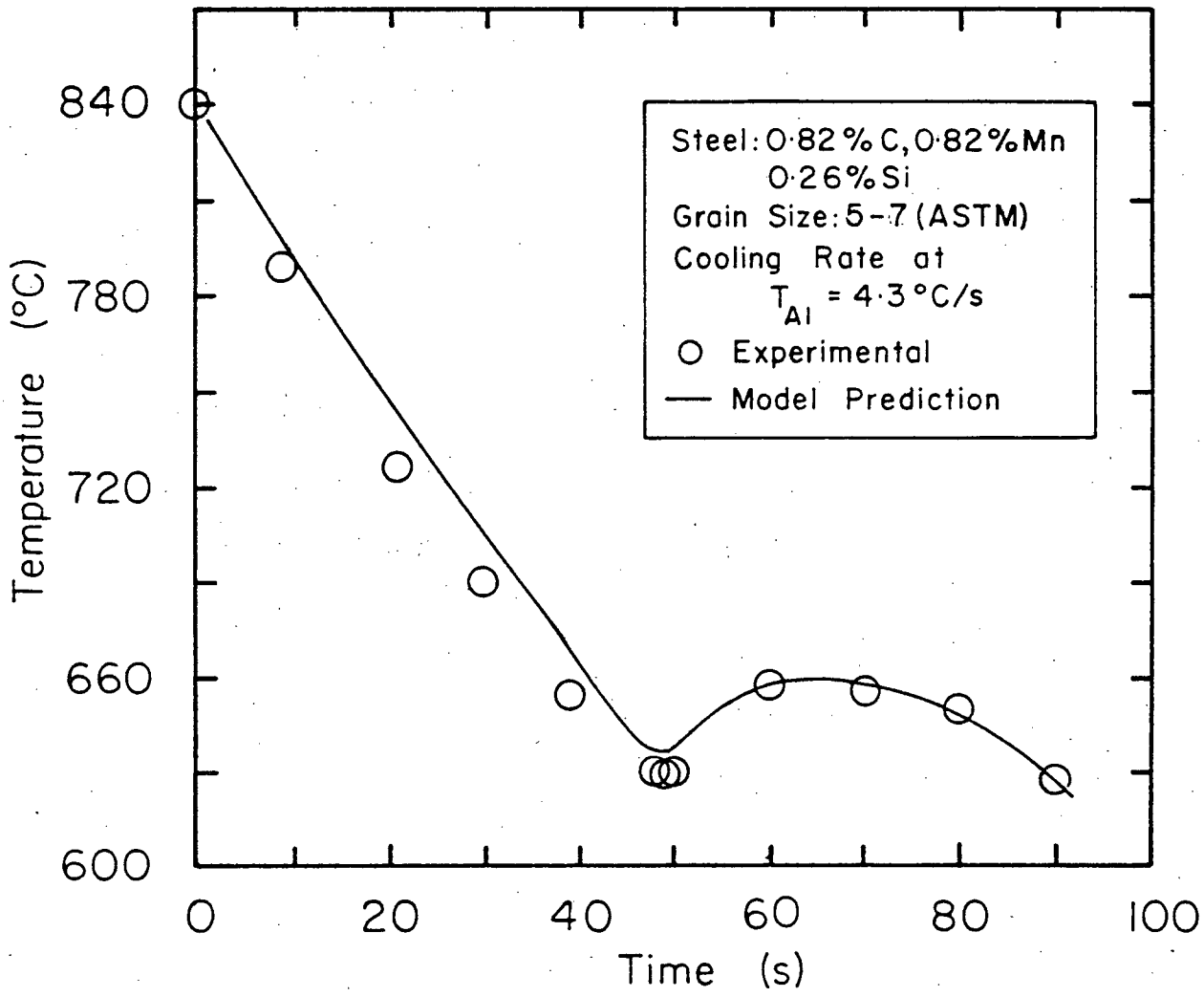


Fig. 6.9 Temperature response at the centre-line of air cooled steel rod (10 mm diameter).

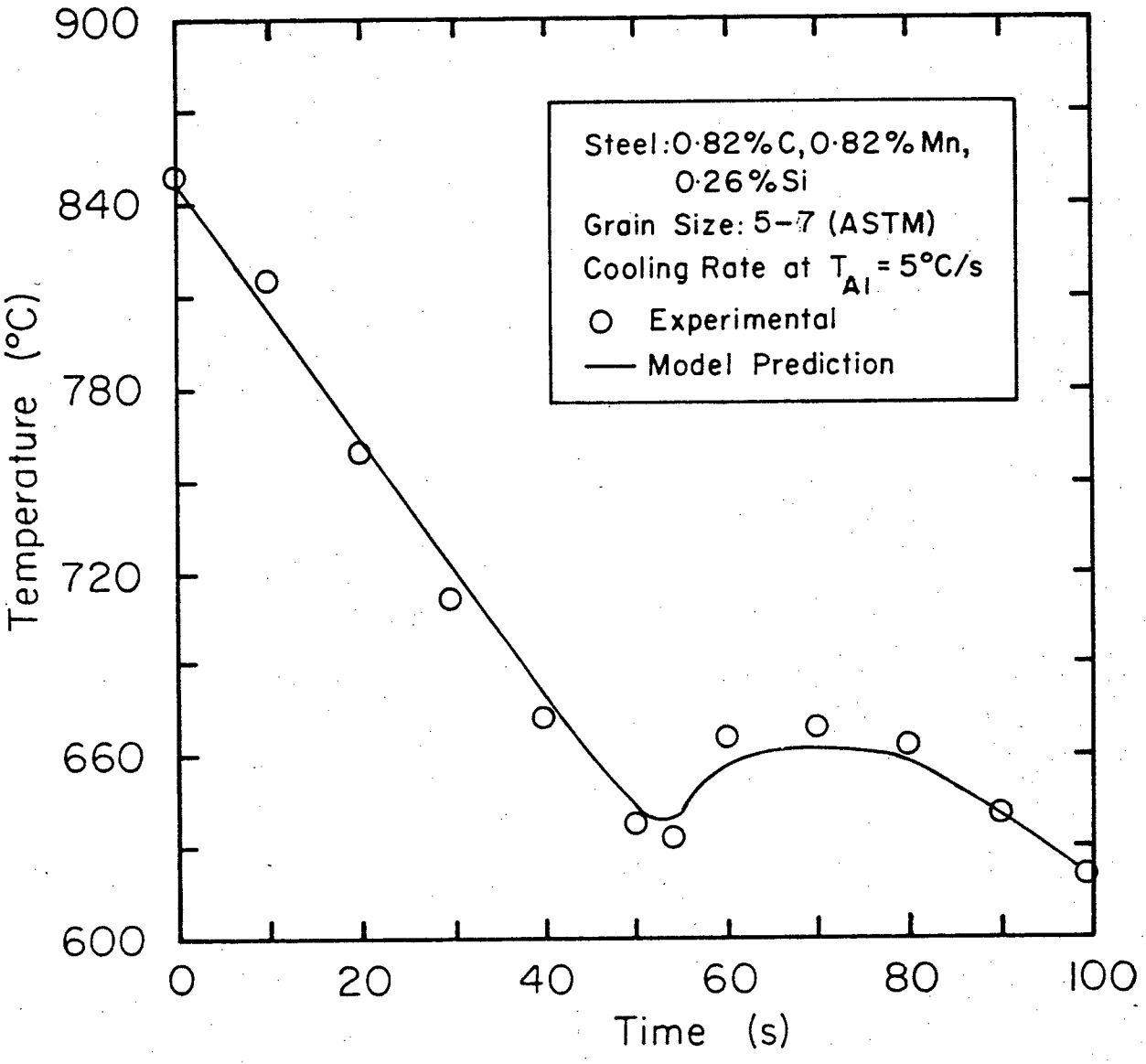


Fig. 6.10 Temperature response at the centre-line of air cooled steel rod (10 mm diameter).

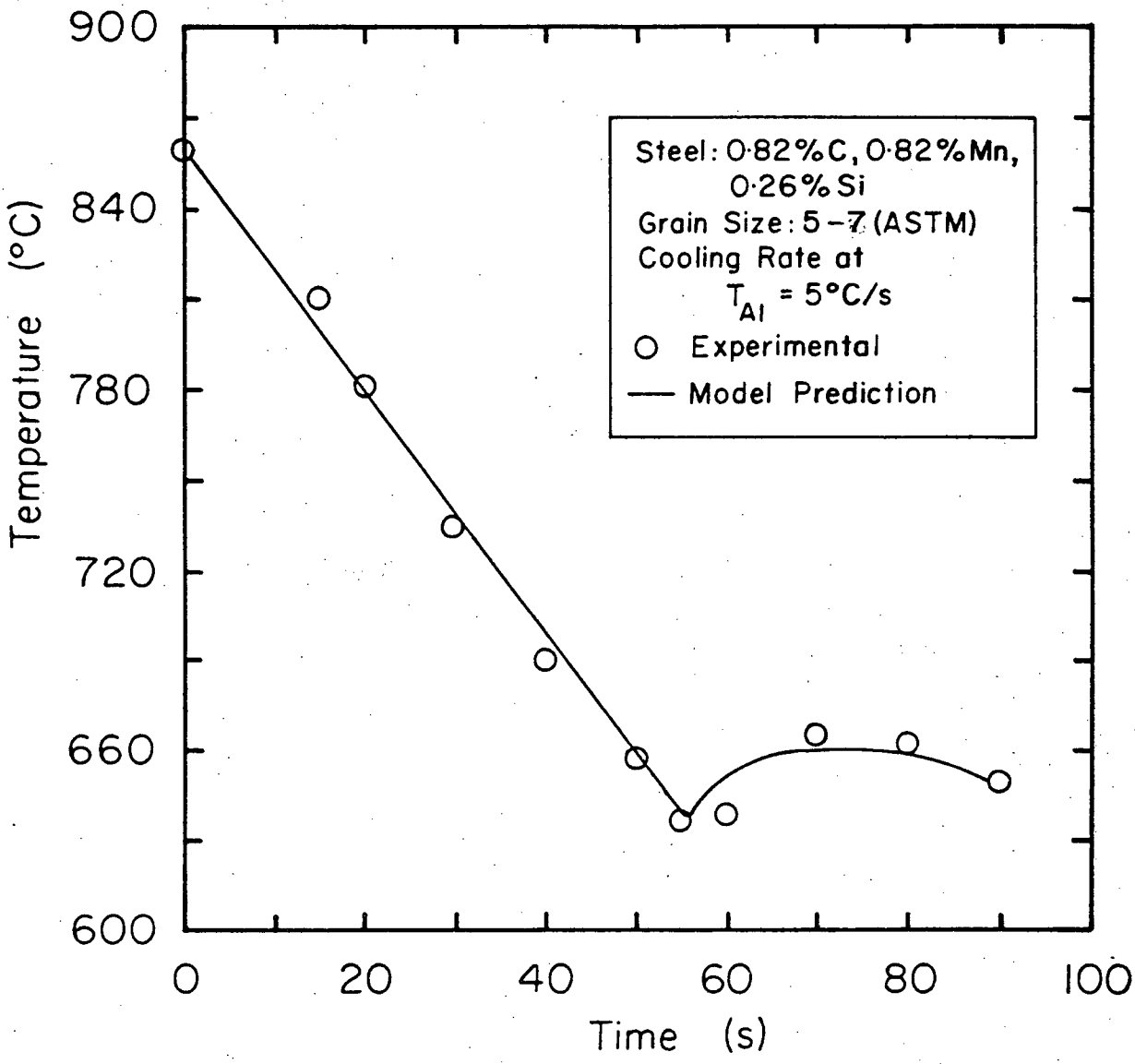


Fig. 6.11 Temperature response at the centre-line of air cooled steel rod (10 mm diameter).

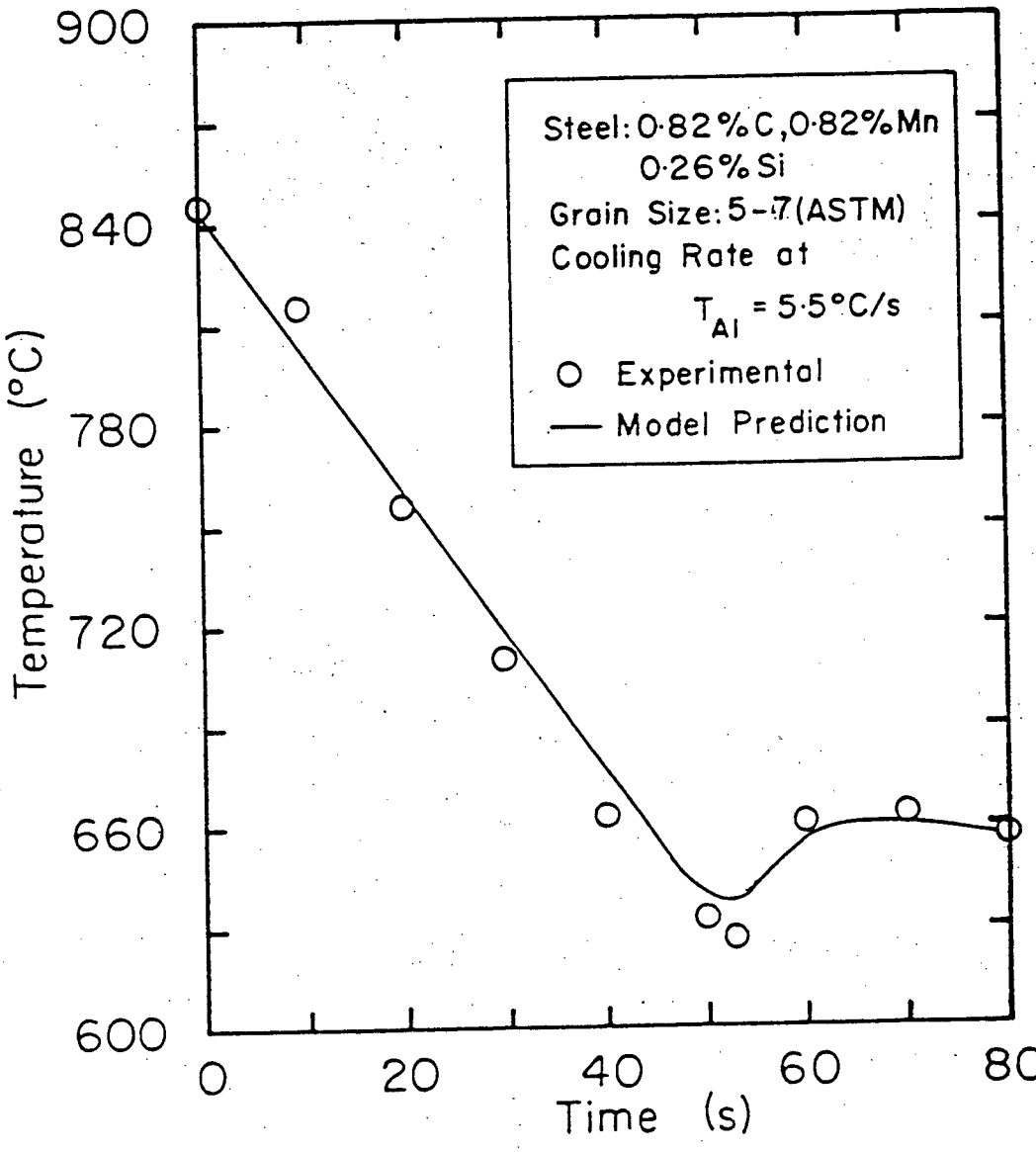


Fig. 6.12 Temperature response at the centre-line of air cooled steel rod (10 mm diameter).

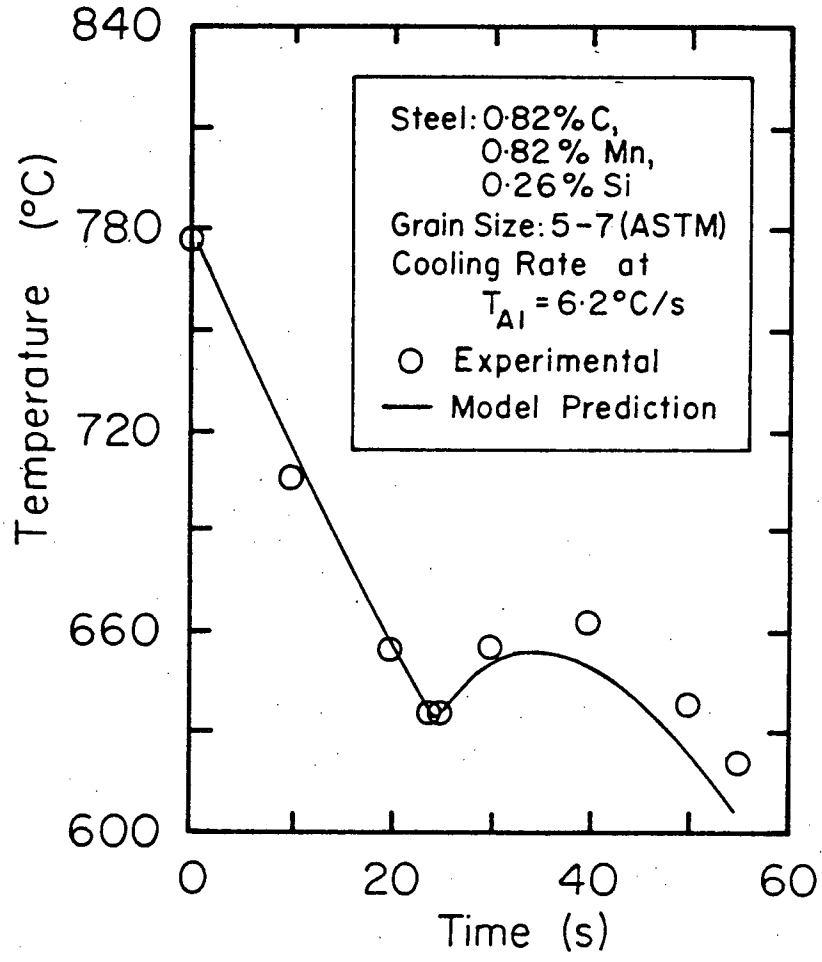


Fig. 6.13 Temperature response at the centre-line of air cooled steel rod (10 mm diameter).

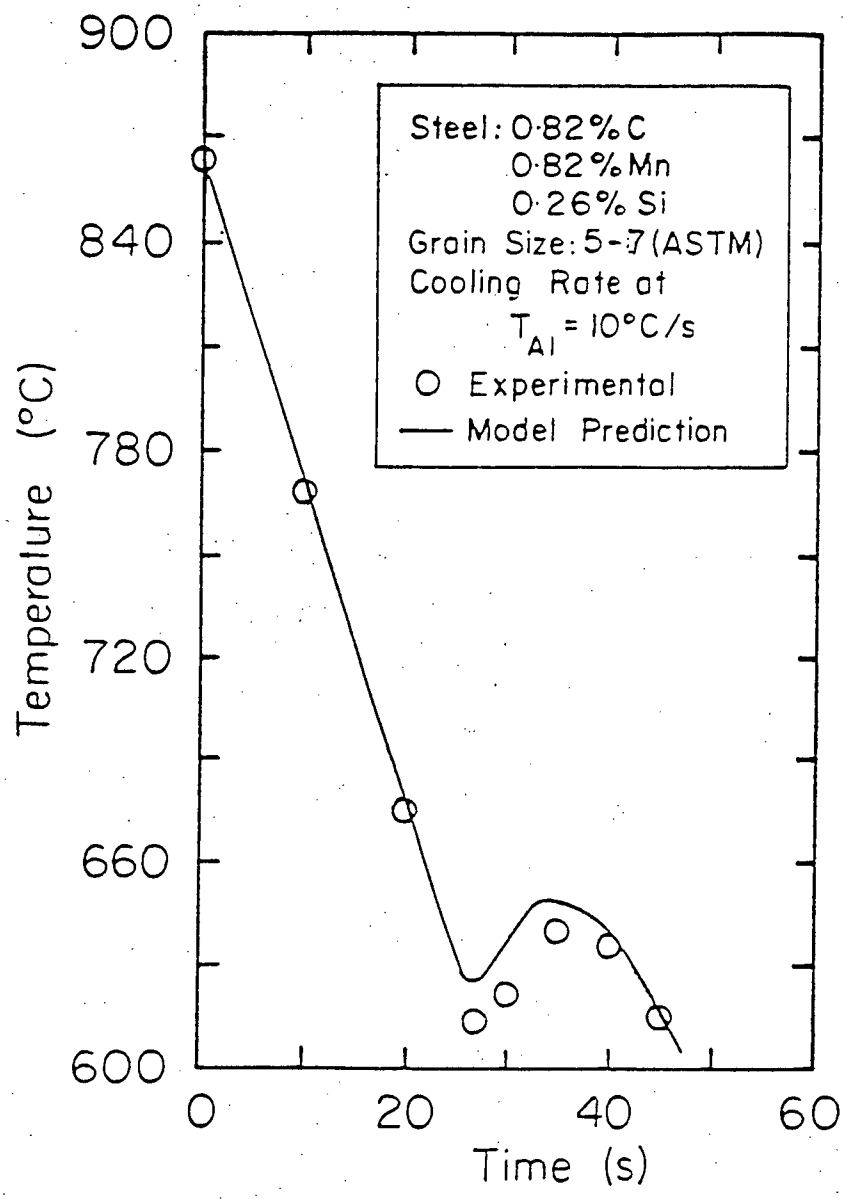


Fig. 6.14 Temperature response at the centre-line of air cooled steel rod (10 mm diameter).

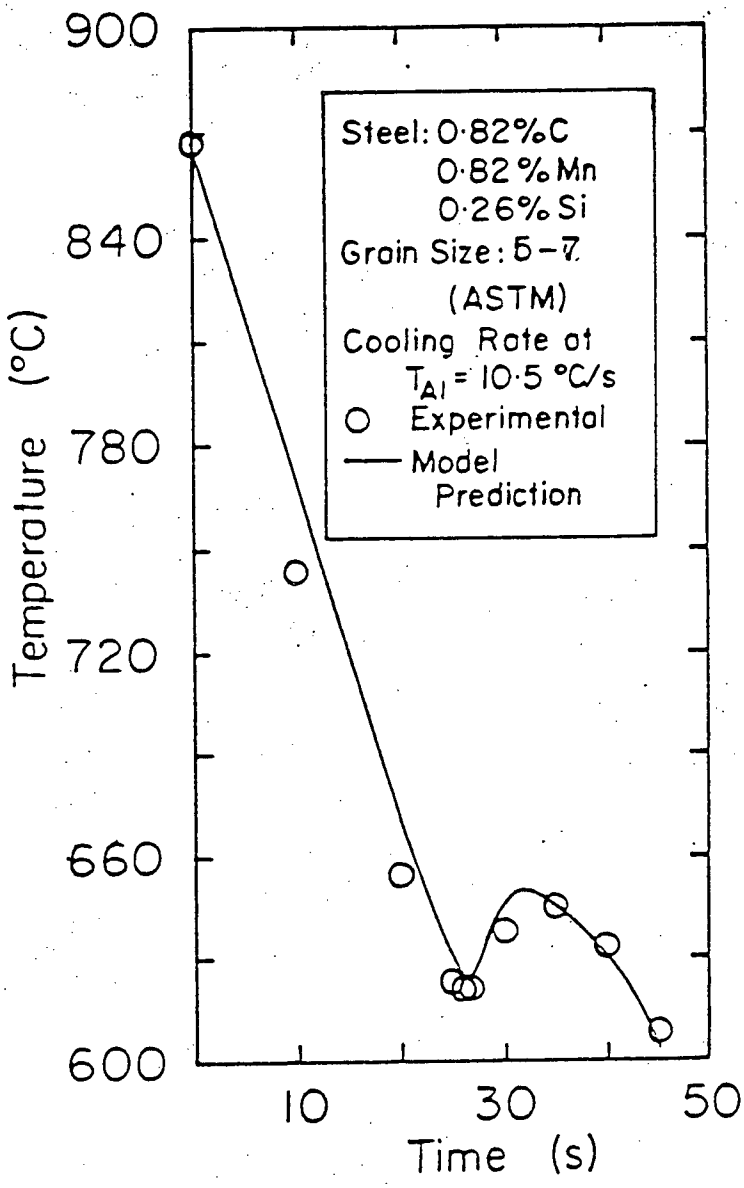


Fig. 6.15 Temperature response at the centre-line of air cooled steel rod (10 mm diameter).

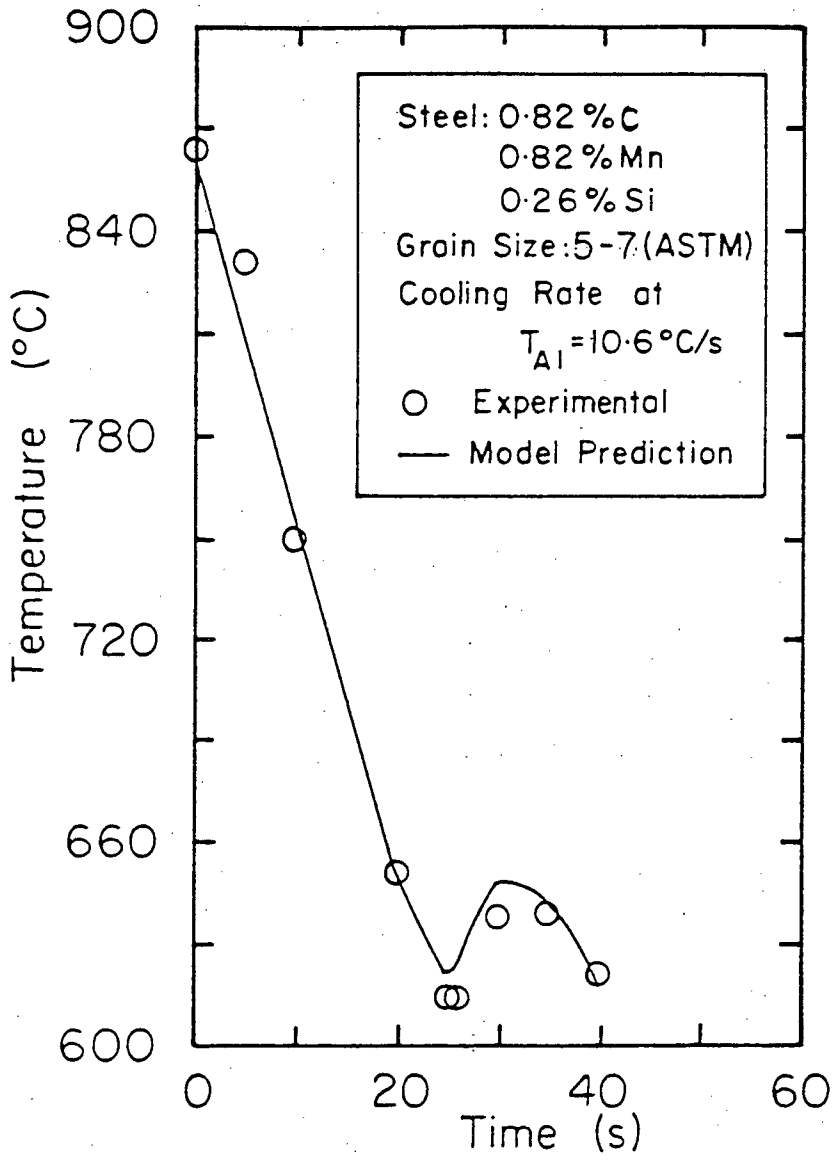


Fig. 6.16 Temperature response at the centre-line of air cooled steel rod (10 mm diameter).

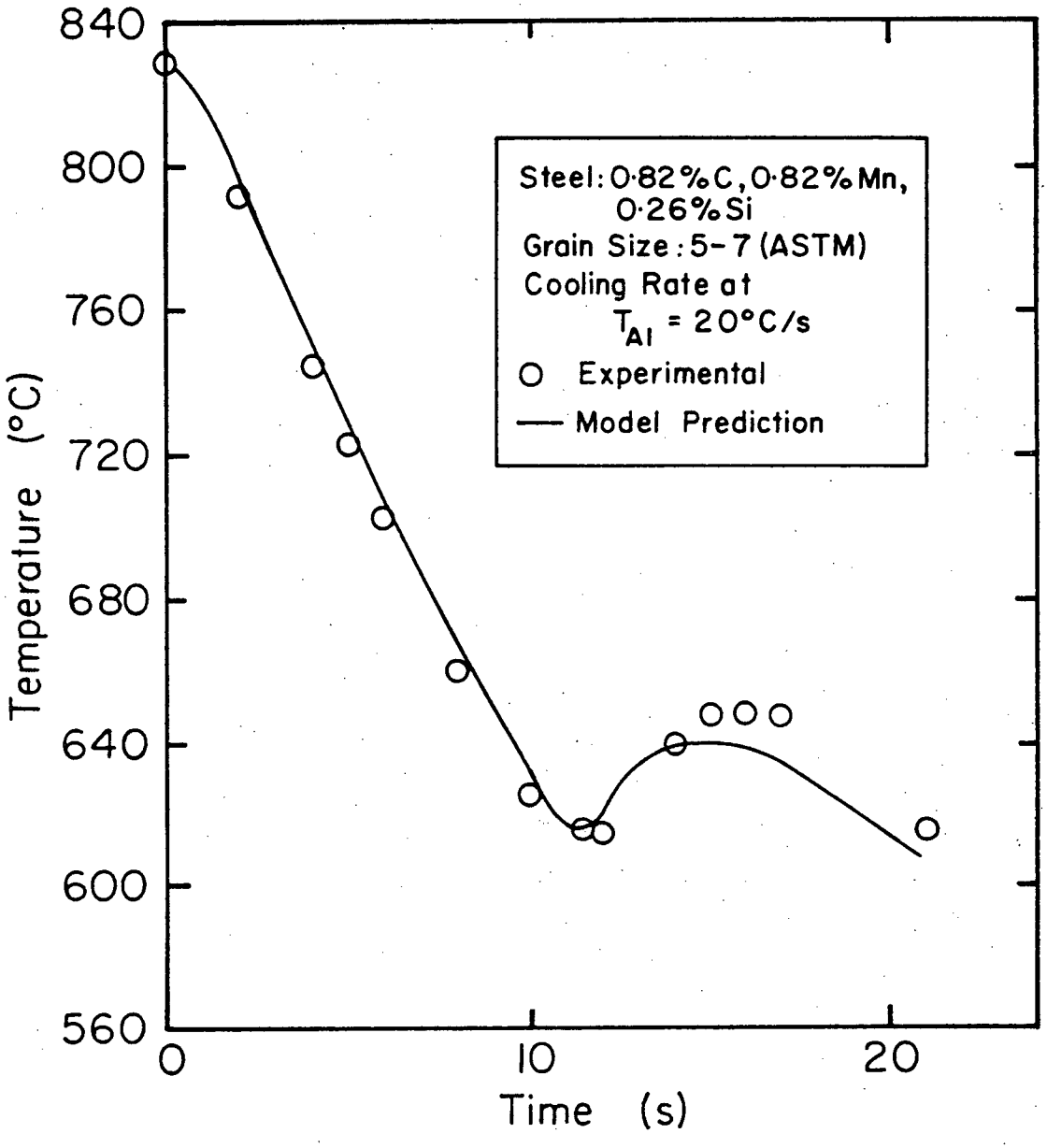


Fig. 6.17 Temperature response at the centre-line of air cooled steel rod (10 mm diameter).

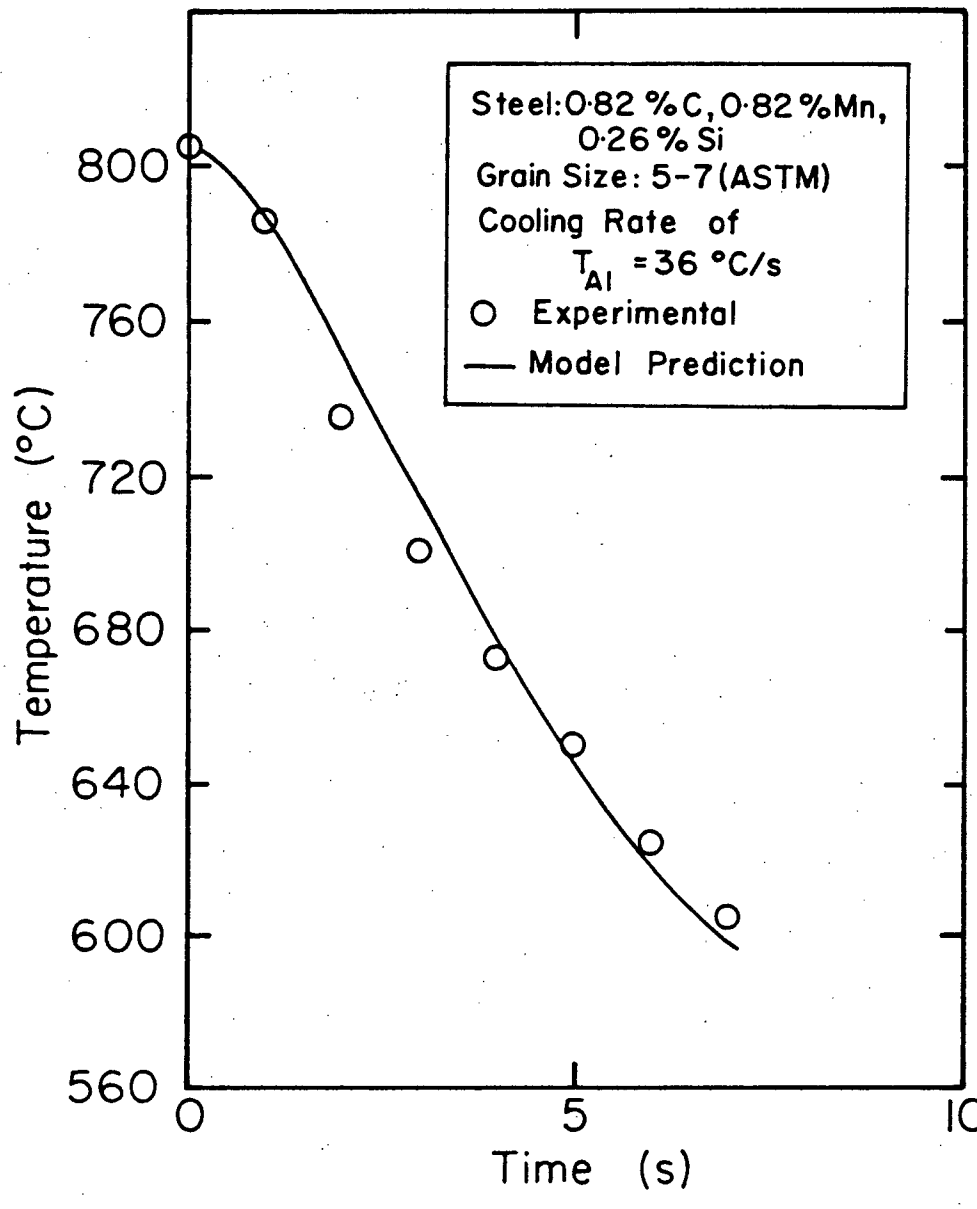


Fig. 6.18 Temperature response at the centre-line of air cooled steel rod (10 mm diameter).

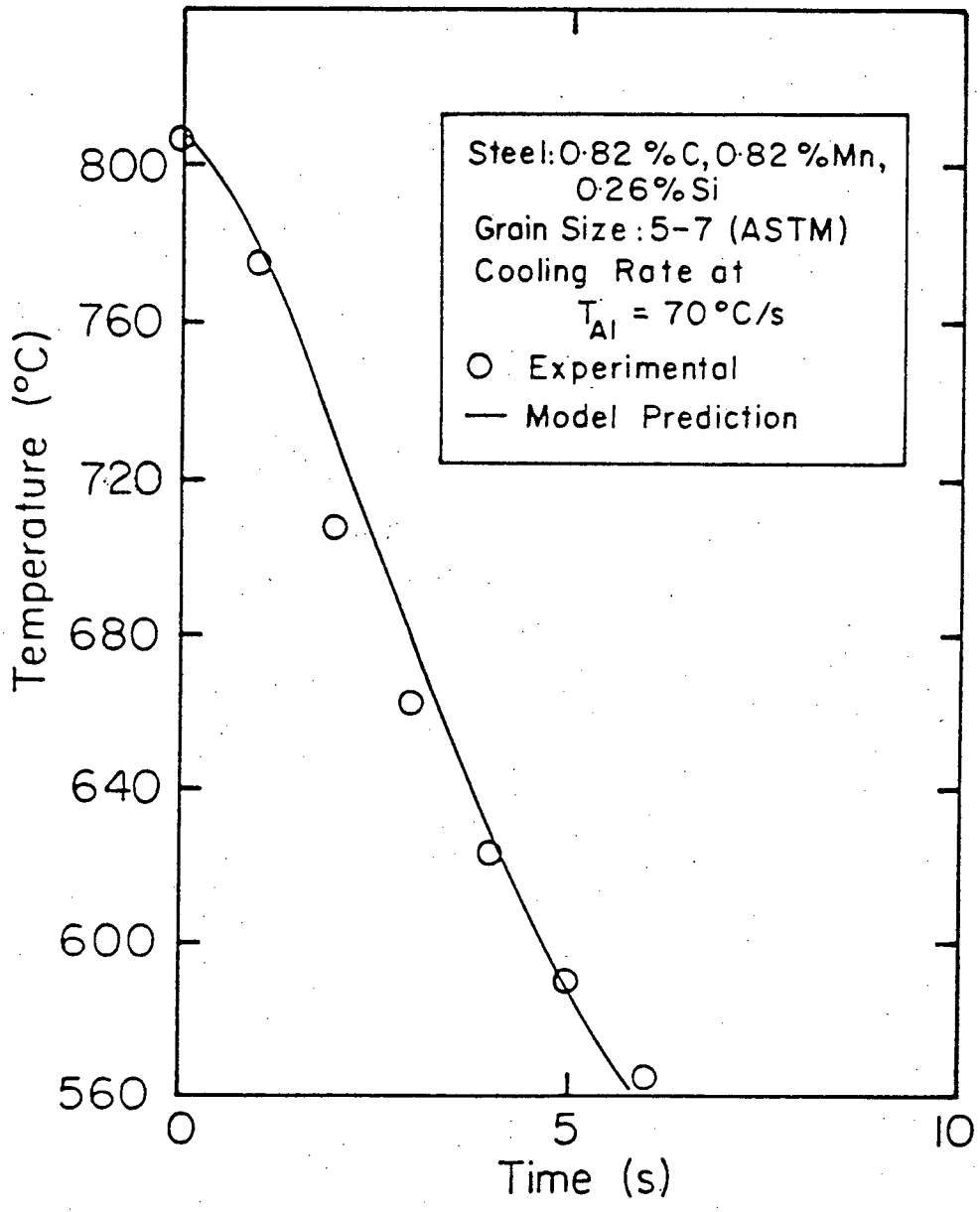


Fig. 6.19 Temperature response at the centre-line of air cooled steel rod (10 mm diameter).

obtained, Figs. 6.9 to 6.19. This is not surprising since the dominant mode of heat transfer is temperature independent convection, especially at higher cooling rates. The temperature dependent term, the radiative heat transfer, is a small portion of the total heat transfer (usually less than 5-10% at higher cooling rates). Hence it is to be expected that 'h' will be roughly constant in the pre-transformation period and the use of a constant 'h' is thus justified.

## 6.5 Discussion

The good agreement of the model predictions with the experimental results is primarily due to the following factors:

i) Accurate inputs, like thermal conductivity, specific heat etc.

ii) Use of $t_{AV\text{-}TTT}$ and $t_{AV\text{-}CCT}$

iii) Validity of the additivity principle for the experimental conditions.

As mentioned earlier, the transformation is assumed to "start" at $t_{AV\text{-}CCT}$ during continuous cooling.[35] The conventional approach is to assume that the transformation starts at $T_{A1}$, even during continuous cooling. In the present work, if n and b are calculated using t = 0 at $T_{A1}$,

the variation in n with temperature is much higher than for the case of t = 0 at $T_{AV}$ (see Table 6.4). The range of values of n (1.9 to 4.8) is in contrast with the work of Tamura et al.[29] and others, who propose a value of 4 for the austenite-pearlite reaction. Also the range is too wide to expect a constant n, as required by additivity. In addition, model calculations using t = 0 at $T_{A1}$ are not in agreement with the time-temperature response of the steel rods measured experimentally, as shown in Table 6.5 and Fig. 6.21. (Nomenclature of terms used in Table 6.5 is shown in Fig. 6.20.)

The value of n calculated by using t = 0 at $t_{AV}$ varies within a narrow range (1.7 to 3), with an average close to 2.5. This is lower than the value expected by Tamura et al.[29] This discrepancy can be partly explained by the effect of inhomogeneity of the reaction in the experimental situations encountered in this work. Due to inhomogeneity, the volumetric growth of the transformed product does not follow the Johnson-Mehl equation (which would mean n = 4). The value of n and b would be determined by the degree of inhomogeneity present in the reaction. Further work is needed to study the nature of this inhomogeneity and its effect on the reaction kinetics.

The model calculations also demonstrate the validity

Table 6.4 Values of n and b for t = 0 at $T_{Al}$

| Temperature (°C) | n | ln b |
|---|---|---|
| 680 | 1.94 | - 11.57 |
| 670 | 2.29 | - 10.72 |
| 660 | 2.91 | - 11.54 |
| 650 | 3.60 | - 10.83 |
| 630 | 4.32 | - 8.96 |
| 623 | 4.63 | - 8.16 |
| 615 | 4.79 | - 7.16 |
| 603 | 4.76 | - 6.98 |

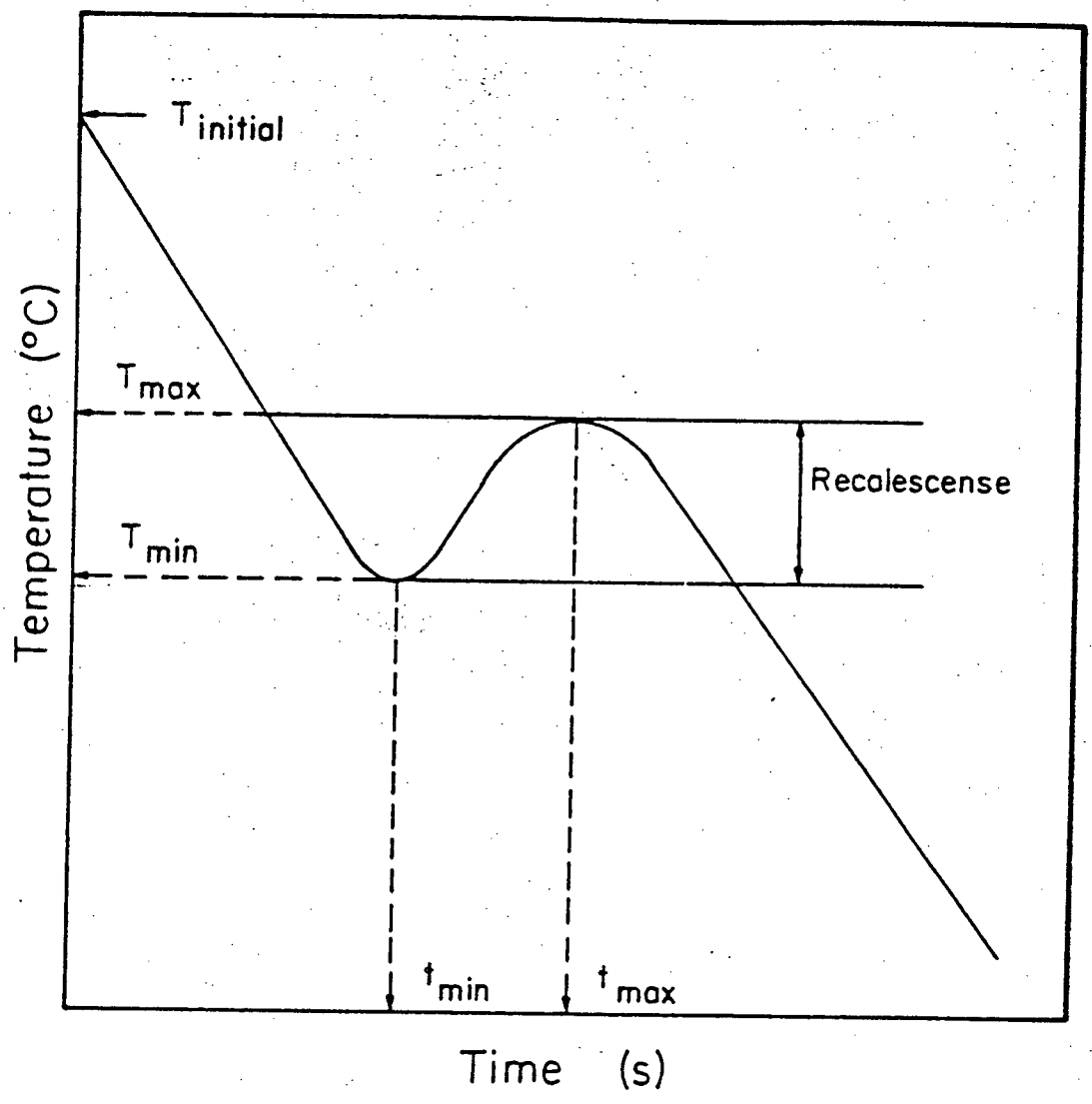


Fig. 6.20 Nomenclature of parameters describing a continuous cooling reaction.

Table 6.5 Comparison of Model Predicted Time-temperature Profiles at Centre-line of Air-cooled Steel Rods Using t = 0 at $t_{AV}$ and t = 0 at $T_{A1}$ with Experimental Results.

| $T_{min}$ (°C) | | | $T_{max}$ (°C) | | | $t_{min}$ (s) | | |
|---|---|---|---|---|---|---|---|---|
| Expt. | Model 1 | Model 2 | Expt. | Model 1 | Model 2 | Expt. | Model 1 | Model 2 |
| 633 | 637 | 645 | 668 | 661 | 661 | 57 | 57 | 56 |
| 629 | 638 | 645 | 660 | 661 | 661 | 53 | 53 | 53 |
| 633 | 636 | 646 | 670 | 661 | 661 | 54 | 53.5 | 54 |
| 629 | 637 | 644 | 660 | 660 | 660 | 49 | 49 | 46 |
| 635 | 631 | 637 | 663 | 656 | 655 | 25 | 25 | 26 |
| 620 | 624 | 630 | 646 | 652 | 651 | 26.5 | 25.6 | 26 |
| 614 | 624 | 629 | 640 | 651 | 649 | 25 | 25 | 24 |
| 614 | 624 | 631 | 640 | 652 | 650 | 27 | 27 | 26 |

Model 1: t = 0 at $t_{AV}$

Model 2: t = 0 at $T_{A1}$

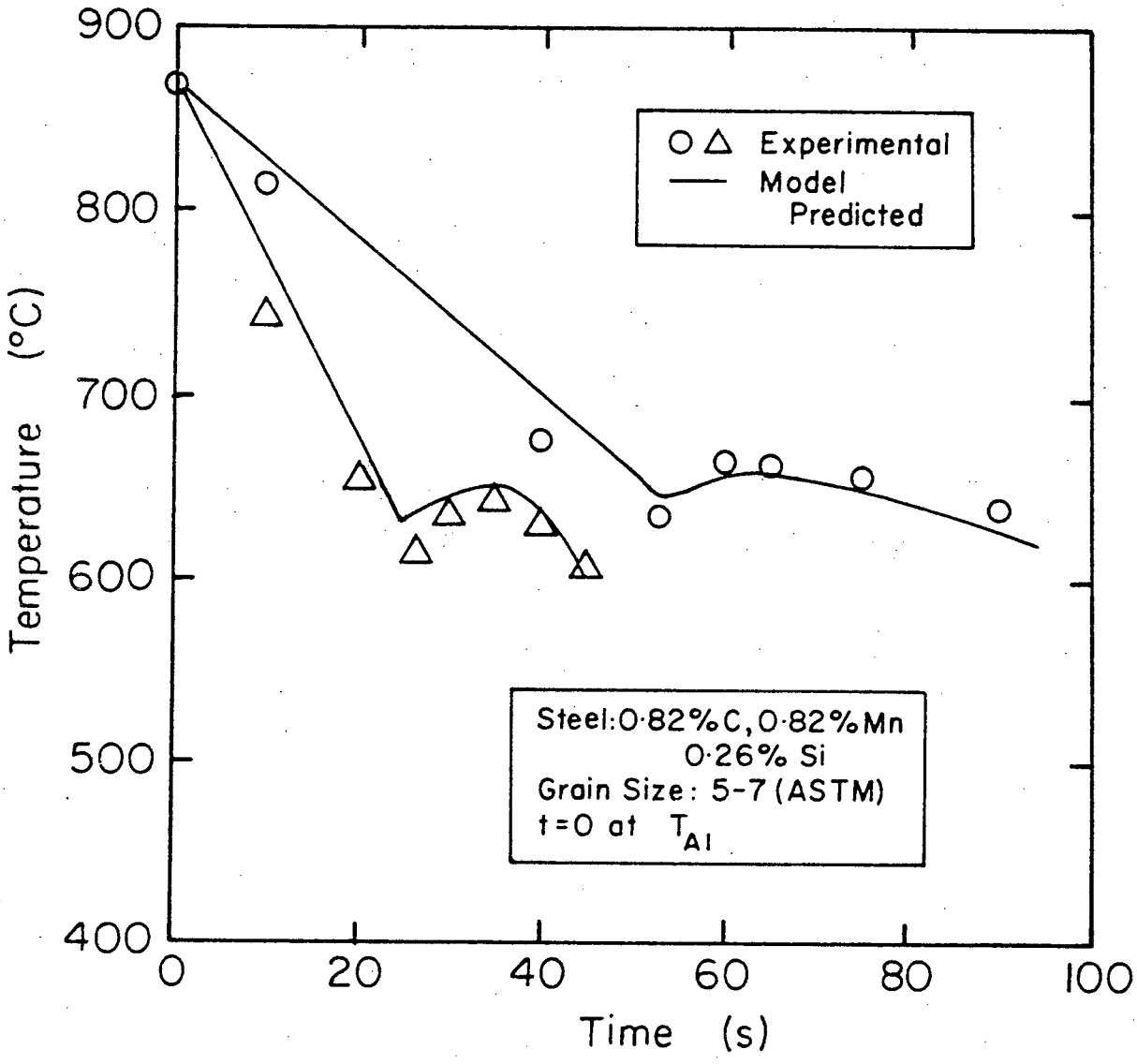


Fig. 6.21 Comparison of typical model predicted (with t = 0 at $T_{A1}$) and experimental results of centre-line temperatures of air-cooled steel rods. (Rod diameter = 10 mm)

of the additivity principle. This principle is derived from a consideration of the fundamental aspects of the nucleation and growth reactions, characterized by nucleation and growth rates. It is important to realise that the concept of nucleation envisioned by Avrami in deriving his equation is different from that of Johnson and Mehl. Avrami treated nucleation in two steps:

i) a probability 'P' of a germ nucleus becoming a growth nucleus

ii) a germ nucleus becoming unavailable for growth due to consumption by the growing phase.

In contrast, Johnson and Mehl defined the nucleation rate, N (a constant) as the number of nuclei nucleating and growing. Evidently Avrami's concept of nucleation is closer to the real situation. Avrami then stated that P/G be constant in the isokinetic range. The Avrami P is the equivalent of the Johnson-Mehl N. Avrami started his derivation by assuming that there are $\overline{N}$ germ nuclei present before the transformation began. (Hence, $P\overline{N} = N$.) This assumption is equivalent to stating that there is an incubation time for each reaction, before the transformation starts, which corresponds to $t_{AV\text{-}TTT}$ and $t_{AV\text{-}CCT}$ used in the present work. The nucleation rate N, used in deriving the effective site saturation condition, is $P\overline{N}$. In

terms of Cahn's site saturation principle, 'P' is very close to unity. The behaviour of 'P' is, indeed, difficult to determine. It is affected by the thermodynamics of the austenite-pearlite reaction, the grain size, the site energy etc. It is closely related to the forces governing atomic behaviour. But the principle of effective site saturation is easier to deal with, and since it is based on the fundamental aspects of reaction mechanism becomes a useful tool to study the effect of these variables on the more easily measurable and important process parameters such as temperature, cooling rate etc.

## 6.6 Scope of Application of the Mathematical Model

By slightly modifying the model in its present form, it is possible to study the effect of segregation on the transformation behaviour of wire rods undergoing cooling in a Stelmor-like process. Due to the segregation of elements like manganese and phosphorus in cast ingots or billets the final product may contain segregated regions at the centre. Due to the higher hardenability associated with the high Mn (and P) contents, the central region in the finished product may have transformed to martensite if the post-rolling controlled cooling parameters are designed for the matrix material. The brittle martensite may fracture during subsequent processing, e.g. when wire rods

are drawn into wires. An example of Mn segregation in a wire rod and the effect on transformation is described in section 6.7.

Finally, but most importantly, the model calculations can be used for evaluating the average mechanical properties of finished steel rods. An example of such calculations is shown in section 6.8.

## 6.7 Effect of Segregation on Phase Transformation

To study the effect of segregation on phase transformation, a plain carbon eutectoid steel of 0.8% C - 1.88% Mn (Grain Size = 5 to 8 ASTM) was chosen as the composition in the segregated region in a matrix composition of 0.82% C - 0.82% Mn (Grain Size = 5 to 7 ASTM). Normally the range of segregation for manganese is about 1.2 to 1.3 times the matrix composition. But no published TTT diagram of a steel with 0.8% C and about 1% Mn could be obtained from the literature. Hence, though the manganese content of 1.88% is too high, the calculations were done with the aim of demonstrating the trends that could be expected in the transformation behaviour due to segregation.

The $T_{AV-TTT}$ for the segregated region has been calculated from published data[45] and is shown in Table 6.6. The

Table 6.6 TTT Data for Segregated Steel

| Temperature (°C) | $t_{AV}$ (s) |
|---|---|
| 675 | 93 |
| 650 | 29 |
| 625 | 13 |
| 600 | 6.2 |
| 575 | 5.4 |
| 550 | 3.5 |
| 525 | 3.4 |
| 500 | 2.9 |
| 475 | 1.9 |
| 450 | 2.5 |
| 425 | 4.2 |
| 400 | 7.5 |

n and b values in the Avrami equation have been calculated from the $t_{AV-TTT}$ and are shown in Table 6.7. The $t_{AV-CCT}$ has been calculated from $t_{AV-TTT}$ by using additivity (Table 6.8). The thermal conductivity, specific heat and density have been assumed to be the same as that of the matrix material since the carbon contents are the same. The $M_s$ temperature for the segregated steel is 180°C.[45]

The program, used for calculations on the 0.82%C steel, has been modified to include the parameters for the segregated composition. The program listing is shown in the Appendix 9. The program logic is the same as before. The only changes are in the $t_{AV-CCT}$ and the n and b values used for calculating the start of transformation and its further course in the segregated regions. Normally, the segregated region at the centre occupies less than 5% of the cross-sectional area of the wire rod. For modelling purposes, two situations have been considered, 1% and 4% of cross-sectional area occupied by segregated material. Due to the presence of the high hardenability material at the core, martensite may be expected to form at the core, depending on the cooling conditions and rod size. The effect of segregation has been investigated for three different rod diameters - 5, 10 and 15 mm. The results of the model calculations are shown in Tables 6.9 to 6.14. The amount of martensite that can be expected to form at the core for the different rod sizes at different cooling rates are

Table 6.7 n and b Values for Segregated Steel

| Temperature (°C) | n | ln b |
|---|---|---|
| 675 | 0.77 | - 6.09 |
| 650 | 0.83 | - 4.60 |
| 624 | 1.28 | - 5.08 |
| 600 | 1.65 | - 5.57 |
| 575 | 1.21 | - 4.00 |
| 550 | 1.10 | - 4.02 |
| 525 | 0.74 | - 2.92 |
| 500 | 0.72 | - 2.98 |
| 475 | 0.85 | - 3.78 |
| 450 | 0.91 | - 3.97 |
| 425 | 0.99 | - 4.38 |
| 400 | 1.06 | - 5.03 |

Table 6.8 CCT Data for Segregated Steel

| Temperature (°C) | $t_{AV-CCT}$ (s) |
|---|---|
| 696 | 3060 |
| 675 | 473 |
| 667 | 286 |
| 641 | 86 |
| 591 | 23 |
| 545 | 11.4 |
| 512 | 8.3 |
| 458 | 5.9 |
| 443 | 5.6 |
| 423 | 5.4 |
| 383 | 5.6 |
| 364 | 5.9 |

Table 6.9 Effect of Cooling Rate on Martensite Formation at Centre of Rod

| Initial Temperature = 850°C<br>Rod Diameter = 5 mm<br>Amount of Segregated Area = 1 % | | | | |
|---|---|---|---|---|
| Cooling Rate at $T_{Al}$ (°C/s) | $T_{min}$ (°C) | $T_{max}$ (°C) | $t_{min}$ (s) | % Martensite formed |
| 6 | 629 | 654 | 36 | < 34 |
| 9 | 620 | 650 | 25 | < 53 |
| 13 | 614 | 646 | 20 | < 62 |
| 61 | - | - | - | 100 |

Table 6.10 Effect of Cooling Rate on Martensite Formation at Centre of Rod

| Initial Temperature = 805°C<br>Rod Diameter = 5 mm<br>Amount of Segregated Area = 4 % | | | | |
|---|---|---|---|---|
| Cooling Rate at $T_{A1}$ (°C/s) | $T_{min}$ (°C) | $T_{max}$ (°C) | $t_{min}$ (s) | % Martensite formed |
| 6 | 628 | 656 | 36 | <33 |
| 9 | 622 | 646 | 25 | <52 |
| 13 | 613 | 642 | 20 | <62 |
| 61 | - | - | - | 100 |

Table 6.11 Effect of Cooling Rate on Martensite Formation at Centre of Rod

| Initial Temperature = 850°C<br>Rod Diameter = 10 mm<br>Amount of Segregated Area = 1 % | | | | |
|---|---|---|---|---|
| Cooling Rate at $T_{A1}$ (°C/s) | $T_{min}$ (°C) | $T_{max}$ (°C) | $t_{min}$ (s) | % Martensite formed |
| 3 | 640 | 662 | 78 | < 5 |
| 4.5 | 631 | 656 | 38 | < 30 |
| 61 | - | - | - | 100 |

Table 6.12 Effect of Cooling Rate on Martensite Formation at Centre of Rod

| Initial Temperature = 850°C<br>Rod Diameter = 10 mm<br>Amount of Segregated Area = 16 % | | | | |
|---|---|---|---|---|
| Cooling Rate at $T_{A1}$ (°C/s) | $T_{min}$ (°C) | $T_{max}$ (°C) | $t_{min}$ (s) | % Martensite Formed |
| 2.5 | 639 | 662 | 85 | < 5 |
| 4.0 | 634 | 657 | 57 | <16 |
| 6.0 | 631 | 655 | 45 | <30 |
| 58.0 | - | - | - | 100 |

Table 6.13 Effect of Cooling Rate on Martensite Formation at Centre of Rod

| Initial Temperature = 850°C<br>Rod Diameter = 15 mm<br>Amount of Segregated Area = 1 % | | | | |
|---|---|---|---|---|
| Cooling Rate at $T_{Al}$ (°C/s) | $T_{min}$ (°C) | $T_{max}$ (°C) | $t_{min}$ (s) | % Martensite Formed |
| 2.0 | 646 | 666 | 99 | < 1 |
| 3.0 | 642 | 663 | 69 | < 4 |
| 4.5 | 638 | 660 | 53 | < 12 |
| 52.0 | - | - | - | 100 |

Table 6.14 Effect of Cooling Rate on Martensite Formation at Centre of Rod

| Initial Temperature = 850°C<br>Rod Diameter = 15 mm<br>Amount of Segregated Area = 16 % | | | | |
|---|---|---|---|---|
| Cooling Rate at $T_{Al}$ (°C/s) | $T_{min}$ (°C) | $T_{max}$ (°C) | $\bar{t}_{min}$ (s) | % Martensite Formed |
| 1.5 | 646 | 664 | 100 | < 0.1 |
| 2.5 | 641 | 660 | 69 | < 1 |
| 4.0 | 638 | 657 | 53 | < 5 |
| 48.0 | - | - | - | 100 |

shown in Fig. 6.22. As expected, the percentage martensite formed in the segregated region is higher for smaller rod diameter and faster cooling rates.

The problem of segregation is not unusual in a wire rod mill. An example of segregation is shown in Fig. 6.23. Many methods have been studied to minimise or eliminate the martensite formation at the centre. One such method, which has been tried in an industrial situation, is described by Van Vuuren.[47] He reports that the cooling rate was reduced to ensure transformation to pearlite at the segregated centre region. But this resulted in a wide scatter in the tensile values and hence the procedure was unacceptable. The procedure which worked successfully was to have a high cooling rate initially followed by slower cooling. This resulted in an initial sharp drop in temperature, but later, the drop was very slow. This procedure allows time for homogenisation of temperature. It is claimed that this procedure helped hold the scatter in the tensile strength values to a minimum while avoiding the formation of martensite. Obviously, this procedure requires good control over the process cooling conditions.

The model calculations can be used to study the effect of such changes in cooling conditions and their effect on

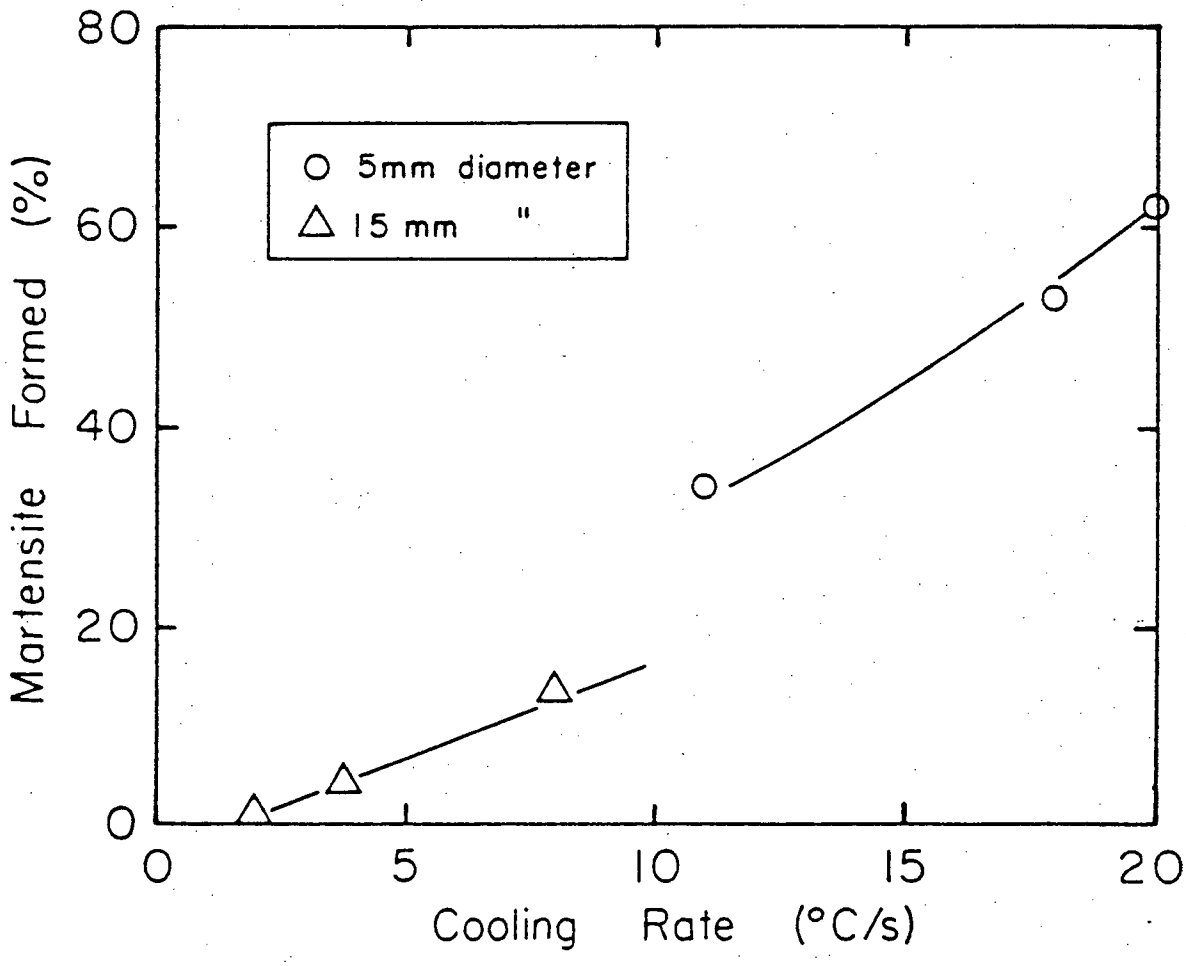


Fig. 6.22 Effect of cooling rate on centre-line martensite formation due to segregation.

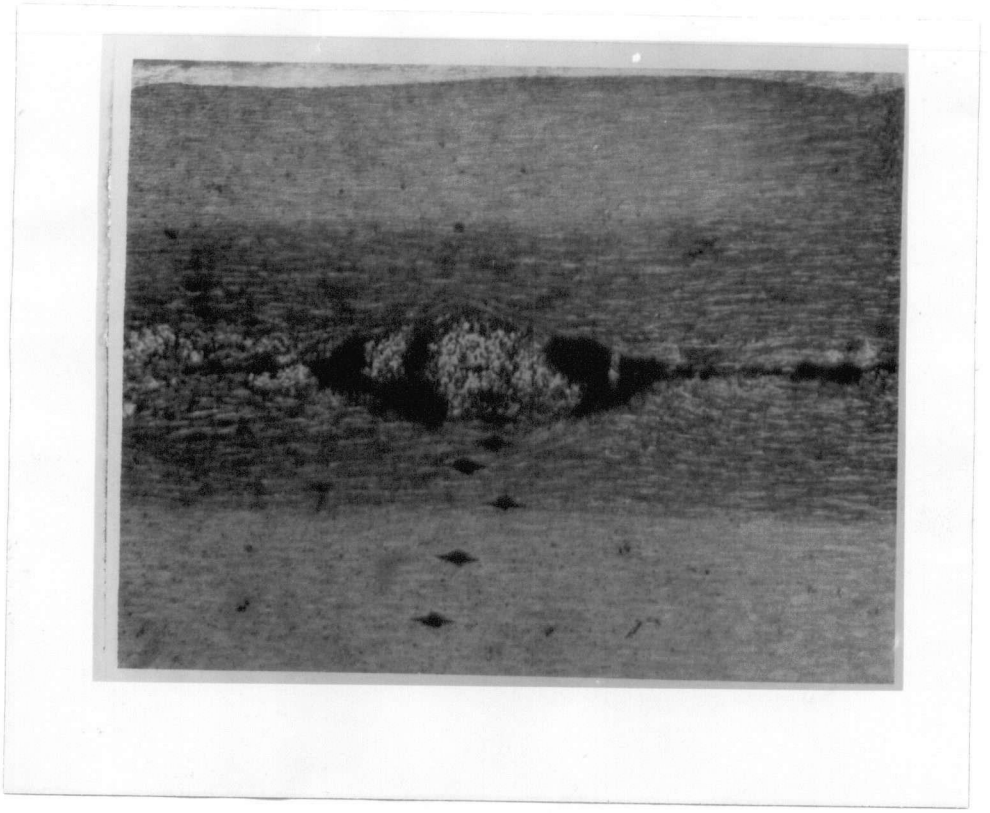

Fig. 6.23 Longitudinal section through a cold drawn rod showing a white centre line martensitic phase fractured during subsequent cold drawing.

the transformation. These then can be used as a guide for designing the process parameters.

## 6.8 Calculation of Mechanical Properties of a Wire Rod

The mechanical properties of plain carbon steel rods depend primarily on:

i) composition (esp. N, Si, Mn and C)

ii) amount of the ferrite phase

iii) pearlite spacing.

For a given steel composition, the amount of ferrite, and more importantly, the pearlite spacing depends on the undercooling during transformation. Frequently, and especially during slow cooling, the steel undergoes recalescence after the start of the austenite-pearlite transformation in the case of a eutectoid steel. This implies that the transformation takes place over a range of temperature. If this range is narrow, then the reaction can be considered isothermal from a practical standpoint. If the rod size and cooling conditions are such that the temperatures at different locations are significantly different, then it is possible that transformations at these locations take place over different temperature ranges. This introduces another difficulty in calculating an average pearlite spacing value for the rod. At this stage, it is not possible

to calculate accurately the effect of such a temperature range on pearlite spacing. However, for illustrative purposes, we can assume that the average undercooling at the centre of the rod determines the pearlite spacing in the rod.

The model calculations are very useful in this regard. The model prediction of the time-temperature response at the centre-line of a rod being cooled can be used to determine the average undercooling. Since the model calculates the temperature and the fraction transformed, it is possible to determine the start and end transformation temperatures as well as the maximum and minimum undercooling values. Using these values, the pearlite spacing for the steel can be determined from published empirical relationships.[54]

The mechanical properties are related to the pearlite spacing and steel chemistry as follows:[54]

$$\text{i)}\quad \sigma_{YS}\,(\text{MPa}) = 15.4\left[\alpha^{\frac{1}{3}}\left\{2.3 + 3.8\,(\%\text{Mn}) + 1.13\,d^{-\frac{1}{2}}\right\} + \left\{(1-\alpha)^{\frac{1}{3}}\left\{11.6 + 0.255\,s_p^{-\frac{1}{2}}\right\} + 4.1\,(\%\text{Si}) + 27.6(\%\text{N})\right] \quad (6.8)$$

$$\text{ii)}\quad \text{UTS(MPa)} = 15.4\left[\alpha^{\frac{1}{3}}\left\{16.0 + 74.2\,(\sqrt{\%\text{N}}) + 1.18\,d^{-\frac{1}{2}}\right\} + (1-\alpha)^{\frac{1}{3}}\left\{46.7 + 0.23 s_p^{-\frac{1}{2}}\right\} + 6.3\,(\%\text{Si})\right] \quad (6.9)$$

$\alpha$ = volume fraction of ferrite

$s_p$ = pearlite spacing (mm)

$d$ = grain diameter (mm)

For illustrative purposes, the mechanical properties for the steel used in the present study have been calculated, for two different rod sizes and two cooling conditions. Pearlite spacings have been calculated by using the procedure mentioned above and are shown in Tables 6.17 and 6.18. For a eutectoid steel, Eq. (6.8) and (6.9) can be rewritten as:

$$\text{i)}\quad \sigma_{YS}\ (\text{MPa}) = 15.4\left\{11.6 + 0.255\, s_p^{-\frac{1}{2}} + 4.1\ (\%\ \text{Si}) + 27.6\ (\%\ \text{N})\right\} \qquad (6.10)$$

$$\text{ii)}\quad \text{UTS}\ (\text{MPa}) = 15.4\left\{46.7 + 0.23\, s_p^{-\frac{1}{2}} + 6.3\ (\%\ \text{Si})\right\} \qquad (6.11)$$

The mechanical properties calculated using Eq. (6.10) and (6.11) are shown in Tables 6.15 to 6.17. This example illustrates applicability of the model to calculating the mechanical properties of the wire rods for different cooling rates. This application can be extended to other materials by suitably modifying the model. It is thus demonstrated that the mechanical properties can be calculated from a knowledge of the reaction kinetics of the transformation. Admittedly, the calculations have been done with simplified assumptions. For example, the effect of the different temperature ranges of transformation at different locations in the rod on the pearlite spacing needs to be studied further. Also the time taken for the transformation at different locations in the rod may also affect pearlite spacing. Nevertheless,

Table 6.15 Pearlite Spacing Calculations

| Rod Diameter = 5 mm<br>Initial Temperature of Rod = 850°C | | |
|---|---|---|
| Air Velocity (m/s) | 0 | 10 |
| Cooling rate at $T_{A1}$ (°C/s) | 4.4 | 18.1 |
| Maximum undercooling (°C) | 83 | 127 |
| Minimum undercooling (°C) | 69 | 82 |
| Average undercooling (°C) | 76 | 104.5 |
| Minimum interlamellar pearlite spacing (Å) | 1000 | 675 |

Table 6.16 Pearlite Spacing Calculations

| Rod Diameter = 15 mm<br>Initial Temperature of Rod = 850°C | | |
|---|---|---|
| Air Velocity (m/s) | 0 | 10 |
| Cooling rate at $T_{A1}$ (°C/s) | 1.2 | 3.7 |
| Maximum undercooling (°C) | 76 | 88 |
| Minimum undercooling (°C) | 57 | 66 |
| Average undercooling (°C) | 67.5 | 77 |
| Minimum interlamellar pearlite spacing (Å) | 1050 | 1000 |

Table 6.17 Mechanical Properties

| Cooling Conditions | $\sigma_{YS}$ (MPa) | UTS (MPa) | RA (%) |
|---|---|---|---|
| Rod dia = 5 mm<br>$CR_{T_{Al}}$ = 4.38 °C/s<br>Air Velocity = 0 m/s | 599 | 1098 | 37 |
| Rod dia = 5 mm<br>$CR_{T_{Al}}$ = 18.13 °C/s<br>Air Velocity = 10 m/s | 675 | 1175 | 40 |
| Rod dia = 15 mm<br>$CR_{T_{Al}}$ = 1.2 °C/s<br>Air Velocity = 0 m/s | 580 | 1090 | 35 |
| Rod dia = 15 mm<br>$CR_{T_{Al}}$ = 3.7 °C/s<br>Air Velocity = 10 m/s | 599 | 1098 | 36 |

these considerations only imply that the calculations need to be more sophisticated than the one attempted in the present study. But they do not in any way bring into doubt the validity of using the model to do such calculations. It has been demonstrated in the present study, albeit in principle, that the model can be used to integrate the reaction kinetics with the macro level variables such as temperature and mechanical properties.

# Chapter 7

## SUMMARY AND CONCLUSIONS

With the ultimate objective of calculating mechanical properties of wire rods in the Stelmor process using phase-transformation data, a mathematical model has been developed. The predictions, made by the model, of the centre-line temperature profiles have been shown to be in good agreement with experimental results for a plain carbon eutectoid steel. Calculations have also been done to derive the mechanical properties of wire rods using model-predicted data. However, these calculations are only illustrative and need to be refined further with the help of experimental data.

The model has been modified to study the effect of centre-segregation on transformation in air-cooled steel rods. Calculations have been carried out with a centre segregation composition of 0.8% C - 1.88% Mn in a matrix of 0.82% C - 0.82% Mn. Though the manganese in the segregated region is higher than would be normally expected, the calculations, nevertheless, give a quantitative estimate of the amount of martensite that can be expected to form

at the centre of the rod. Also the effect of increasing the cooling rate, the rod diameter and the amount of segregation on the amount of martensite formed at the centre can be predicted quantitatively by the model. Experiments are needed to validate the model predictions. However the capability of the model to perform the calculations and give meaningful predictions has been demonstrated. This should help reduce the amount of empirical experimentation to design process parameters, such as cooling rates for different rod sizes, in a Stelmor-line.

The success of the model is primarily due to two factors:

i) use of $t_{AV\text{-}TTT}$ and $t_{AV\text{-}CCT}$ for calculation of n and b in the Avrami equation and the start of transformation during cooling, respectively.

ii) additivity.

The use of $t_{AV\text{-}TTT}$ and $t_{AV\text{-}CCT}$ was proposed by B. Hawbolt et al.[35] and has worked well in the present study. The conditions for additivity proposed by Avrami and Cahn were not obtained in the present work, thereby necessitating further exploration into the mechanics of additive reactions. As a result, two new sufficient conditions for additivity have been derived. These are:

i) additivity range

ii) effective site saturation.

These two sufficient conditions increase the scope of reactions to which the additivity rule becomes applicable (see Table 7.1). The effective site saturation ratio is a simple but effective method of determining additivity for nucleation and growth reactions and can be used for homogeneous and heterogeneous reactions. The reasons for the heterogeneity encountered in the reactions in the present study need to be studied further. The effectively site saturated reactions are growth dominated. To study the deviations of heterogeneous reaction kinetics from the homogeneous, the Inhomogeneity Co-efficient ($I_t$) and the Heterogeneity Co-efficient ($H_t$) have been proposed. Further experiments are needed to study the nature of the heterogeneity and its effect on the co-efficients b and n in the Avrami equation.

Using the additivity rule, a new iterative procedure, called the "additivity method", has been derived to calculate TTT data from CCT. The method has been shown to work successfully for the data in the present study.

Table 7.1 Scope of Reactions Covered by Different Additivity Criteria

| Criterion | Remarks |
|---|---|
| Avrami's Isokinetic Range | 1. $\frac{N}{G}$ must be constant in the temperature range. Also implies that N and G must be constant for an isothermal reaction.<br>2. Normally not encountered for austenite-pearlite reactions in steel. |
| Cahn's Site Saturation | 1. The nucleation event is nearly complete in the early stages of the reaction. The growth rate must be a function of temperature alone (thereby implying that it be constant for an isothermal reaction).<br>2. May hold true for reactions in alloy steels, especially grain-boundary nucleated reactions. |
| Additivity Range | 1. N and G are functions of temperature alone.<br>2. Does not require that $\frac{N}{G}$ be constant. Thus it is less restrictive than the Avrami criterion. Implies that N and G be constant for an isothermal reaction.<br>3. There is evidence in the literature to support N and G are functions of temperature alone. Also, the criterion does not call for physical saturation of nucleation sites. Thus it is less restrictive than Cahn's criterion and includes reactions which are not covered by the Avrami criterion. Applicable to all steels. |
| Effective Site Saturation | 1. G is a function of temperature alone, and hence constant for an isothermal reaction.<br>2. Includes all reactions covered by the Avrami, Cahn and Additivity Range criteria for austenite-pearlite reactions in steel for growth dominated reactions, which is usually the case.<br>3. Also includes reactions with decreasing nucleation rates and heterogeneous reactions.<br>4. The most flexible and practically useful criterion. |

# BIBLIOGRAPHY


1. Morgan Construction Company, "The Stelmor Process", August (1978).

2. Feldman, U. "Controlled Cooling of Wire Surface from the Rolling Heat", Iron and Steel Engineer, Jan., pp. 62-67 (1980).

3. Ammerling, W.J. "Controlled Cooling of Wire Rod from Rolling Temperature", Iron and Steel Engineer, Dec., pp. 99-107 (1970).

4. Schummer, A. "Controlled Cooling Processes for Wire Rod and Structural Shapes", SEAISI Quarterly, Oct., pp. 6-12 (1978).

5. McLean, D.W. "The History of Controlled Cooling of Rod at Stelco", Wire, Vol. 39, pp. 1606-1609 (1964).

6. Dove, A.B. "Wire Manufacturing Using Stelmor Controlled Cooled Rod", Wire, Vol. 39, pp. 1610-1615 (1964).

7. Hitchcock, J.H. "Mechanical Aspects", Wire, Vol. 39, p.1622 (1964).

8. Grattan, E.; Twigg, G.M.; Benson, P. "S-ED-C: An Advance in the Controlled Cooling of Carbon Steel Rod". Iron and Steel International, Oct., pp. 277-280 (1979).

9. Malmgren, N.G.; Tarnblom, S.G. "D-patented Wire Rod", Wire, Vol. 25, pp. 211-218 (1975).

10. Beaujean, R.; Godart, F.; Lambert, M.; Economopoulos, M. "Research for Obtaining the Lead Patenting Structure by Treatment of the Wire Rod Directly after the Rolling Mill", Centre de Reserches Metallurgiques, Vol. 32, pp. 10-33 (1972).

11. Bain, E.C. "On the Rates of Reactions in Solid Steel", Trans. A.I.M.E., Vol. 100, pp. 13-46 (1932).

12. Bain, E.C.; Davenport, E.S., Trans. A.I.M.E., Vol. 90, p. 117 (1930).

13. Brandt, H. Trans. A.I.M.E., Vol. 167, p. 405 (1946).

14. Zener, C. "Kinetics of the Decomposition of Austenite", Trans. A.I.M.E., Vol. 167, p. 550 (1946).

15. Holloman, J.H.; Jaffe, L.D. "Anisothermal Decomposition of Austenite", Trans. A.I.M.E., Vol. 167, p. 419 (1946).

16. Manning, G.K.; Lorig, C.H. "The Relationship Between Transformation at Constant Temperature and Transformation During Cooling", Trans. A.I.M.E., Vol. 167, p. 442 (1946).

17. Scheil, E. "Initiation Time of the Austenite Transformation", Archiv. Eisenhuttenwesen, Vol. 8, pp. 565-567 (1935).

18. Austin, J.B.; Rickett, R.L. Metals Technology, T.P. #964, Sept. (1938).

19. Johnson, W.A.; Mehl, R.F. "Reaction Kinetics in Processes of Nucleation and Growth", Trans. A.I.M.E., Vol. 135, pp. 416-442 (1939).

20. Avrami, M. "Kinetics of Phase Change I", J. of Chem. Physics, Vol. 7, pp. 1103-1112 (1939).

21. Avrami, M. "Kinetics of Phase Change II", J. of Chem. Physics, Vol. 8, pp. 212-224 (1940).

22. Avrami, M. "Kinetics of Phase Change III", J. of Chem. Physics, Vol. 9, pp. 177-183 (1940).

23. Cahn, J.W. "The Kinetics of Grain Boundary Nucleated Reactions", Acta Met., Vol. 4, p. 449 (1956).

24. Cahn, J.W. J. of Metals, Jan., p. 146 (1956).

25. Christian, J.W. "The Theory of Transformations in Metals and Alloys", Pergamon Press, Chapters 1,12 (1965).

26. Shimizu, N.; Tamura, I. Trans. ISIJ, Vol. 18, p. 445 (1978).

27. Sakamoto, Y. et al. Yo Ito Research Labs., Kawasaki Steel Corpn., Chiba, Japan 280.

28. Grange, R.A.; Keifer, J.M. "Transformation of Austenite on Continuous Cooling and its Relation to Transformation at Constant Temperature", Trans. A.S.M., Vol. 29, p. 29 (1941).

29. Shimizu, N.; Tamura, I. Trans. ISIJ, Vol. 17, p. 17 (1977).

30. Umemoto, M.; Tamura, I. "Continuous Cooling Transformation Kinetics of Steels", Trans. ISIJ, Vol. 21, pp. 383-392 (1981).

31. Agarwal, P.K.; Brimacombe, J.K. "Mathematical Model of Heat Flow and Austenite-Pearlite Transformation in Eutectoid Carbon Steel Rods for Wire", Met. Trans. 'B', Vol. 12B, pp. 121-132 (1981).

32. Hildenwall, B. "Prediction of the Residual Stresses Created During Quenching", Linkoping Studies in Science and Technology, Dissertation #39 (1979).

33. Hildenwall, B.; Ericsson, T. "Hardenability Concepts with Application to Steel", The Metallurgical Society of A.I.M.E., Warrendale, Pa. (1978).

34. Kirkaldy, J.S.; Sharma, R.C. "A New Phenomenology for Steel IT and CCT Curves", Scripta Met., Vol. 16, pp. 1193-1198 (1982).

35. Private communication with Dr. Hawbolt, E. B. and Brimacombe, J.K.

36. Brown, D.; Ridley, N. "Kinetics of the Pearlite Reaction in High-purity Nickel Eutectoid Steels", J. of the Iron and Steel Institute, Sept., pp. 1232-1240 (1969).

37. Kuban, B. M.A.Sc. Thesis, University of British Columbia, Vancouver, B.C., Canada (1983).

38. Markowitz, L.M.; Richman, M.H. "The Computation of Continuous Transformation Diagrams from Isothermal Data", Trans. A.I.M.E., Vol. 239, pp. 131-132 (1967).

39. Tzitzelkov, I.; Hogardy, H.P.; Rose, A. "Mathematical Description of the TTT Diagram for Isothermal Transformation and Continuous Cooling", Report #1808 of the Materials Committee of the Association of German Iron and Steel Engineers (1974).

40. Takeo, K. et al. "The Direct Patenting of High Carbon Steel Wire Rod by Film Boiling", Trans. ISIJ, Vol. 15, pp. 422-427 (1975).

41. Cahn, J.W.; Hagel, W.C. "Theory of the Pearlite Reaction", Decomposition of Austenite by Diffusional Processes. Ed. V.F. Zackay and H.I. Aaronson, A.I.M.E. Publication (1962).

42. Scheil, E.; Lange-Weise, A. "Statistiche Ge fugeuntersuchungern", Vol. 2, p. 93 (1937-1938).

43. Hull, F.C.; Colton, R.A.; Mehl, R.F. "Rate of Nucleation and Rate of Growth of Pearlite", Trans. A.I.M.E., Vol. 150, pp. 185-207 (1942).

44. Private Communications with Dr. I. Tamura.

45. Atlas of Isothermal Transformation and Cooling Transformation Diagrams. ASM, Metals Park, Ohio (1977).

46. "Physical Constants of Some Commercial Steels at Elevated Temperatures", BISRA, Scientific Publications, London (1978).

47. Van Vuuren, C.J. "Operating and Quality Control Aspects of the Production of Critical Low and High Carbon Products from Continuously Cast Blooms", South African Iron and Steel Industrial Corporation Ltd., Iscor, Newcastle Works, South Africa.

48 Marder, A.R.; Bramfitt, B.L. "Effect of Continuous Cooling on the Morphology and Kinetics of Pearlite", Met. Trans., Vol. 6A, pp. 2009-2014 (1975).

49. "Grain Size Determination" - Metallography, Structures and Phase Diagrams, A.S.M. Metals Handbook, Vol. 8, 8th Edition, Metals Park, Ohio.

50. Umemoto, M.; Horiuchi, K.; Tamura, I. "Transformation Kinetics of Bainite During Isothermal Cooling and Continuous Cooling", Trans. I.S.I.J., Vol. 22, pp. 854-861 (1982).

51. Carnahan, B. et al. "Applied Numerical Methods", John Wiley (1969).

52. Kreith, F. "Principles of Heat Transfer", 3rd ed., Intext Publishers, New York (1973).

53. B. Hawbolt et al Paper to be published in Met. Trans.

54. Leslie, W.C. "The Physical Metallurgy of Steels", McGraw-Hill Book Co., pp. 164-165 (1981).

# Appendix 1

## THE PRINCIPLE OF ADDITIVITY

[Reference: "The Theory of Transformations in Metals and Alloys", J. W. Christian, 1965, Pergamon, London, pp.545-546.]

Consider the simplest type of non-isothermal transformation, obtained by combining two isothermal transformations. The assembly is transformed at temperature $T_1$, where the kinetic law is $f = f_1(t)$ for a time $t_1$ ($f$ = volume fraction transformed) and is then suddenly transferred to a second temperature $T_2$. If the reaction is additive, the course of the reaction at $T_2$ is exactly the same as if the fraction transformed $f_1(t_1)$ had all been formed at $T_2$. Thus if $t_2$ is the time taken at $T_2$ to produce the same amount of transformation as is produced at $T_1$ in a time $t_1$, we have

$$f_1(t_1) = f_2(t_2)$$

and the course of the whole reaction is

$$\begin{aligned} f &= f_1(t) && t < t_1 \\ &= f_2(t+t_2-t_1) && t > t_1 \end{aligned}$$

Suppose that $t_{a1}$ is the time taken to produce a fixed amount of transformation $f_a$ at $T_1$ and $t_{a2}$ is the corresponding time to produce the same amount of transformation at $T_2$. Then in the composite process above, an amount $f_a$ of transformation will be produced in a time

$$t = t_{a2} - t_2 + t_1$$

if the reaction is additive (see Figure A.1)

$$\therefore \quad t - t_1 + t_2 = t_{a2}$$

$$\therefore \quad \frac{t-t_1}{t_{a2}} + \frac{t_2}{t_{a2}} = 1$$

If $\frac{t_1}{t_{a1}} = \frac{t_2}{t_{a2}}$ then

$$\frac{t-t_1}{t_{a2}} + \frac{t_1}{t_{a1}} = 1 \qquad \text{(A1.1)}$$

For an additive reaction the total time to reach a specified stage of transformation is obtained by adding the fractions of the time to reach this stage isothermally until the sum becomes

Equation A1.1 can be written in the more generalised form as

$$\int_0^t \frac{dt}{t_a(T)} = 1 \qquad \text{(A1.2)}$$

Where $t_a(T)$ are the isothermal transformation times for a fraction transformed 'a' at a temperature T and 't' is the time taken to reach a fraction transfomred 'a' for an a isothermal reaction path.

The derivation of Eq. A1.2 is based on the relationship that, for an additive reaction,

$$t_1 = \frac{t_{a1}}{t_{a2}} \qquad \text{(A1.3)}$$

The above relationship holds if, for a reaction, the reaction rate depends only on the fraction transformed and temperature.

Consider a transformation for which the instantaneous reaction rate may be written

$$\frac{dX}{dt} = \frac{h(T)}{g(X)} \qquad \text{(A1.4)}$$

where:

X = volume fraction transformed

t = time

h(T) = function of temperature

g(X) = function of volume fraction transformed.

Then,

$$\int h(T)\, dt = \int g(X)\, dX \qquad (A1.5)$$

for any transformation path

$$\therefore \quad X = F \int h(T)\, dt \qquad (A1.6)$$

and for an isothermal reaction

$$X = F\left\{h(T)t\right\} \qquad (A1.7)$$

According to A1.7, the volume fraction transformed at any temperature is a function of time and temperature.

From A1.5

$$h(T) = \frac{g(X_a)}{t_a(T)} \qquad (A1.8)$$

Also

$$\frac{dX}{dt} = \frac{h(T)}{g(X)}$$

$$\therefore \quad t_a(T)\, \frac{dX}{dt} = \frac{g(X_a)}{g(X)}$$

$$\therefore \quad \frac{dt}{t_a(T)} = \frac{gX}{g(X_a)}\, dt$$

$$\therefore \quad \int_0^t \frac{dt}{t_a(T)} = \frac{1}{g(X_a)} \int g(X)dX = \frac{g(X)}{g(X_a)} \qquad (A1.9)$$

This is the general additivity rule (Eq. A1.9). In particular, if $X = X_a$, then

$$\int_0^t \frac{dt}{t_a(T)} = \frac{g(X_a)}{g(X_a)} = 1 \qquad \text{(A1.10)}$$

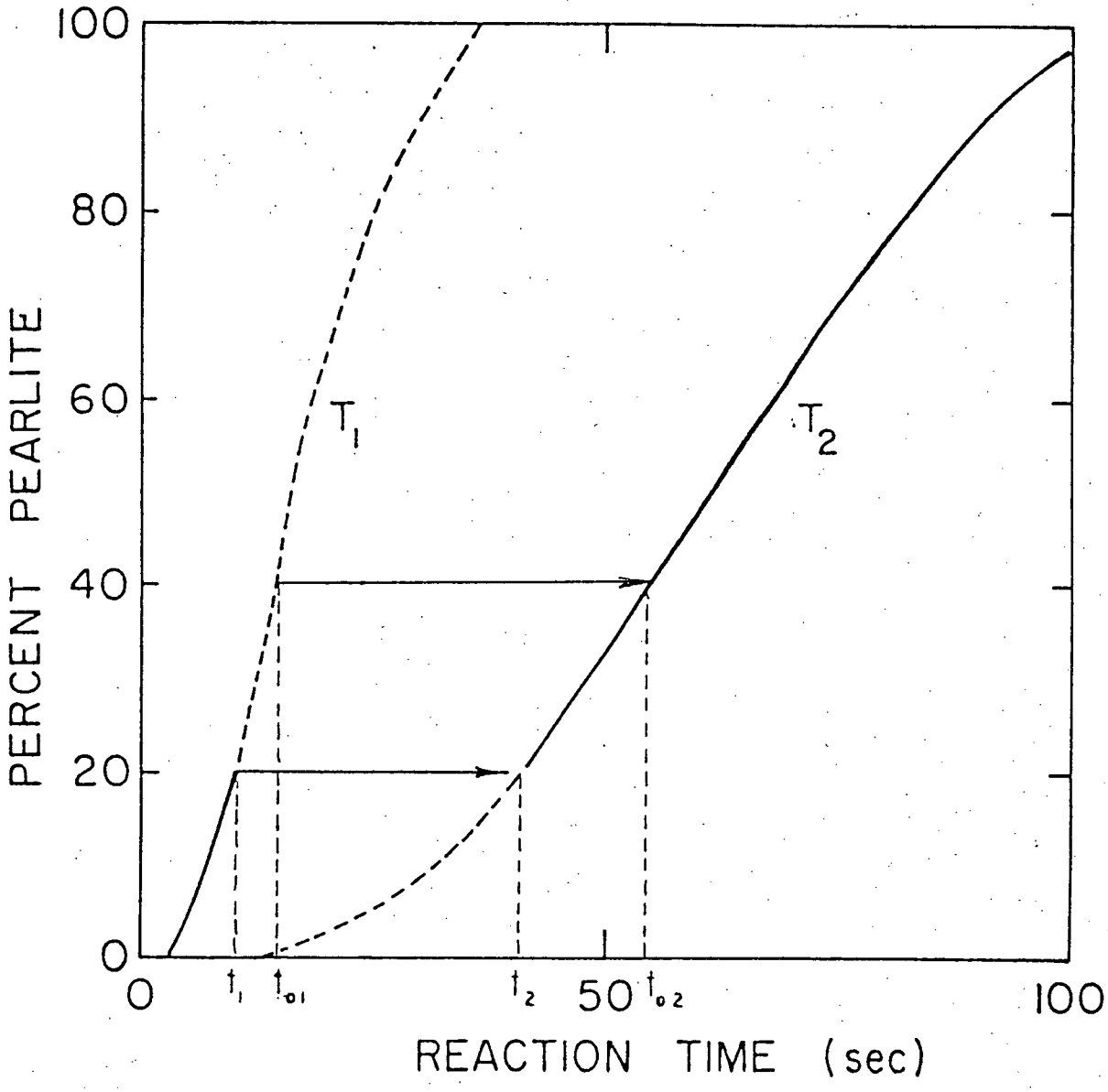


Fig. A 1.1. Additivity Principle.

# Appendix 2

## ADDITIVITY OF THE AVRAMI EQUATION KINETICS

The Avrami equation is:

$$X = 1 - \exp(-bt^n) \tag{A2.1}$$

$$\therefore \log(1-X) = -bt^n \tag{A2.2}$$

$$t = n \frac{\log(1-X)}{-b} \tag{A2.3}$$

Differentiating A2.1 w.r.t. 't',

$$\frac{dX}{dt} = \exp(-bt^n)\,(-nb\,t^{n-1}) \tag{A2.4}$$

$$= (1-X)(-bn)\left[\frac{\log(1-X)}{-b}\right]^{\frac{n-1}{n}} \tag{A2.5}$$

$$= (1-X)(n)(-b)^{\frac{1}{n}}\left[\log(1-X)\right]^{\frac{n-1}{n}} \tag{A2.6}$$

$$= \frac{n\,(-b)^{\frac{1}{n}}}{\left(\frac{1}{1-X}\right)\left[\frac{1}{\log(1-X)}\right]^{\frac{n-1}{n}}} \tag{A2.7}$$

$$= \frac{h(T)}{g(X)}$$

where

$$h(T) = n\,(-b)^{\frac{1}{n}}$$

and

$$g(X) = \frac{1}{1-X}\left[\frac{1}{\log\,(1-X)}\right]^{\frac{n-1}{n}}$$

# Appendix 3

## INDEPENDENCE OF N(T) AND G(T) w.r.t. TIME

Consider the equation

$$V_{ex}^{\tau} = \int_0^t \left\{\frac{1}{T_\tau - T_0}\int_{T_0}^{T_\tau} G(T)dT\right\}^3 \left\{\frac{1}{T_\tau - T_0}\int_{T_0}^{T_\tau} N(T)dT\right\}^3 (\tau - t)^3 dt \qquad (A3.1)$$

Since $G(T)$ and $N(T)$ are functions of temperature alone, Eq. (A4.1) can be written as:

$$V_{ex}^{\tau} = \left\{\frac{1}{T_\tau - T_0}\int_{T_0}^{T_\tau} G(T)dT\right\}^3 \cdot \left\{\frac{1}{T_\tau - T_0}\int_{T_0}^{T_\tau} N(T)dT\right\}^3 \cdot \int_0^{\tau} (\tau - t)^3 dt \qquad (A3.2)$$

In the case of a continuous cooling reaction, since the temperature is a function of time (which is given by the cooling rate), it would seem that

$$T = f(t) \qquad (A3.3)$$

$$\therefore N(T) = N\{f(t)\} = N_1(t) \qquad (A3.4)$$

$$G(T) = G\{f(t)\} = G_1(t) \qquad (A3.5)$$

But this is not true, as can be seen from Fig. A3.1. The figure is a three-dimensional representation of t, G(T) and T. As can be seen, the G(T) for three different reactions can be

obtained, independent of the time. The G(T) for a reaction depends only on the temperature path of the reaction. The time of the reaction can then be brought in, and when multiplied by the temperature averaged growth rate for the reaction, gives the total growth of one particle during the time interval. This should be multiplied by the number of particles growing to give the total growth. Thus, it can be demonstrated that if G is a function of temperature alone, it can be calculated, independent of time, for any reaction path. The same is true for N.

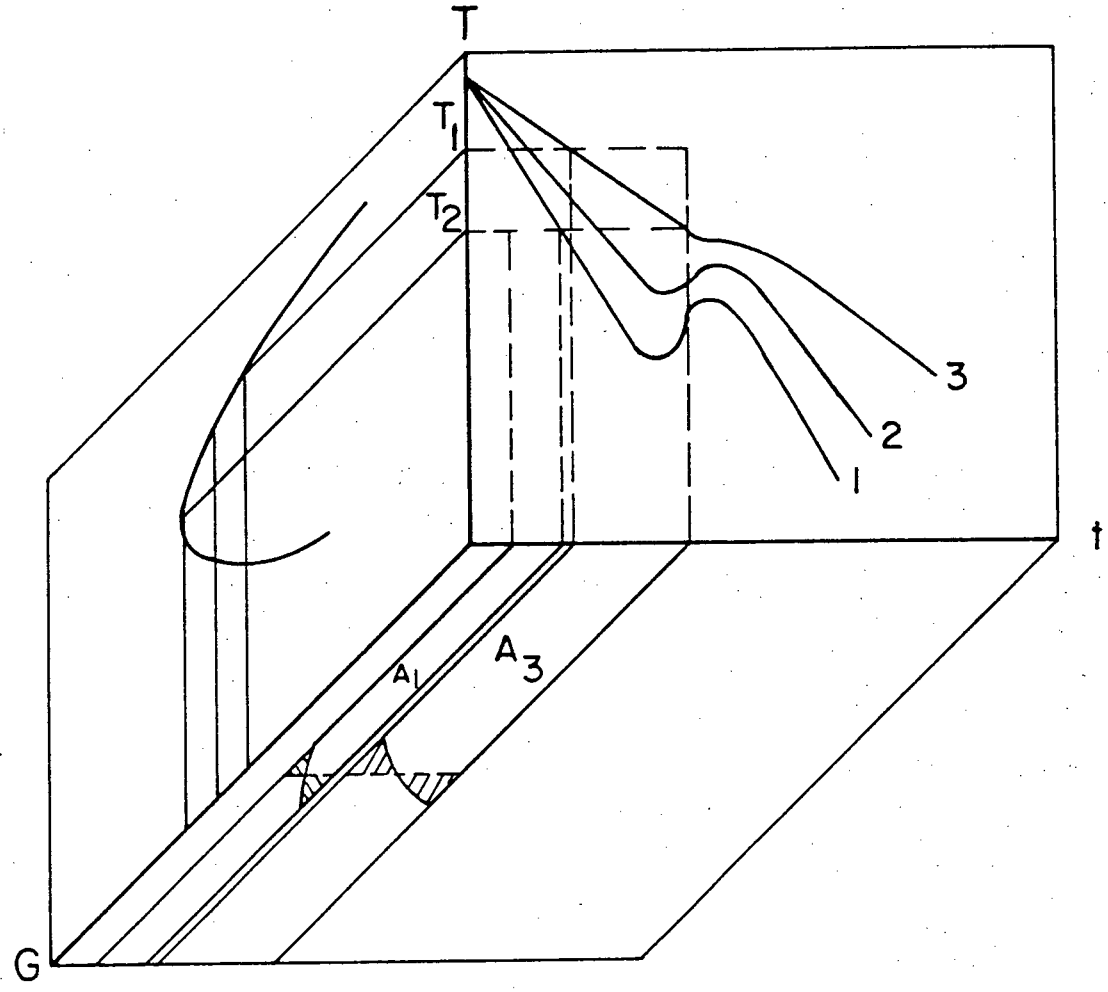


Fig. A3.1 Demonstrating the independence of G(T) and N(T) with respect to time.

# Appendix 4

## CALCULATION OF $t_{AV-TTT}$ FROM $t_{AV-CCT}$ BY THE ADDITIVITY METHOD

The additivity method has been used to calculate the $t_{AV-TTT}$ for the steel used in the present work from the experimentally determined $t_{AV-CCT}$. By using a multiple regression procedure, a first approximation for $t_{AV-TTT}$ was determined from the experimentally determined $t_{AV-TTT}$ data. This is shown in Table A4.1. By successive iterations, the best approximation for $t_{AV-TTT}$ to the experimental data was calculated by the additivity method. The results of the iterations are shown in Table A4.2. The comparison of the $t_{AV-TTT}$ values predicted by the additivity method and the experimental data is shown in Table 3.5.

Table A4.1 Comparison of Experimental and First Approximation of $T_{AV-TTT}$

| Temperature (°C) | $t_{AV-TTT}$ (s) | |
|---|---|---|
| | Experimental | First Approximation |
| 680 | 43 | 58 |
| 670 | 5.6 | 12 |
| 660 | 6.2 | 6.3 |
| 650 | 3.0 | 4.0 |
| 630 | 1.8 | 2.1 |
| 623 | 1.6 | 2.0 |
| 615 | 1.5 | 1.9 |
| 603 | 1.9 | 1.7 |

Table A4.2 Iteration Results

| Approximation Number | Co-efficient in the Equation for $t_{AV-TTT}$* | | |
|---|---|---|---|
| | log a | b | c |
| 1 | 40.00 | -10.00 | 0.100 |
| 2 | 39.85 | -10.39 | 0.087 |
| 3 | 45.75 | -12.32 | 0.117 |
| 4 | 43.66 | -11.60 | 0.103 |
| 5 | 44.12 | -11.74 | 0.105 |
| 6 | 43.86 | -11.66 | 0.104 |

*$\log t_{AV-TTT} = \log a + b \log x + cx$

$x = 728-T$

# Appendix 5

## LISTING OF COMPUTER PROGRAM TO CALCULATE TTT DATA FROM CCT BY THE ADDITIVITY METHOD

```
      1     C ***********************************************************
      2     C This program calculates the additivity integral value
      3     C upto a time t(AV-CCT)for a given cooling rate.The first
      4     C approximation for t(AV-TTT) is to be input by replacing
      5     C the values in statement no.34.The cooling rate is to be
      6     C specified by replacing the value in statement no.23 by an
      7     C appropriate temperature value.The t(AV-CCT) for the steel
      8     C must be input by replacing the values in statement no.24.
      9     C The time step value is specified in statement no.29 and the
     10     C T(A1) temperature is specified by statement no.30.The program
     11     C calculates the additivity integral value for the given
     12     C cooling rate and prepares the input data for the next
     13     C iteration.These values are then used as input to the
     14     C multiple regression package available in the general MTS
     15     C system as *STRP.The  *STRP program gives the next
     16     C approximation for the t(AV-TTT).Thais is input to this
     17     C program for the next run.Thus the program must be run
     18     C repetitively,along with *STRP,till the required t(AV-TTT)
     19     C is obtained.
     20     C ***************************************************************
     21           IMPLICIT REAL*8(A-H,O-Z)
     22           DIMENSION A(100),B(100),C2(100)
     23           A1=600.0D0
     24           TAVCCT=41.4594D0+0.0698528D0*(728.0D0-A1)-10.0961D0*
     25          1(DLOG(728.0D0-A1))
     26           TAVCCT=DEXP(TAVCCT)
     27           CR=(728.0D0-A1)/TAVCCT
     28           C=0.0D0
     29           DT=0.10D0
     30           T=727.0D0
     31           C1=1.0D0/CR
     32           DO 100 I=1,30000
     33           IF (T.LE.A1) GO TO 500
     34           T1=40.4817D0-10.6052D0*DLOG(728.0D0-T)+0.088608  D0*
     35          1(728.0D0-T)
     36           T1=DEXP(T1)
     37           C=C1*(DT/T1)+C
     38     100   T=T-DT
     39     500   T=700.0D0
     40           PRINT,C
     41           DO 10  I=1,30
     42           T2=40.478   D0-10.6132   D0*DLOG(728.0D0-T)+0.0889042 D0*
     43          1(728.0D0-T)
     44           T2=DEXP(T2)
     45           IF (T.GE.A1) T2=T2*C
     46           A(I)=DLOG(T2)
     47           B(I)=728.0D0-T
     48           C2(I)=DLOG(B(I))
     49           WRITE(6,200) A(I),B(I),C2(I)
     50     200   FORMAT(F20.10,F20.10,F20.10)
     51     10    T=T-5.0D0
     52           STOP
     53           END
End of file
```

Appendix 6

# DERIVATION OF IMPLICIT FINITE DIFFERENCE EQUATIONS

i) Node Arrangement

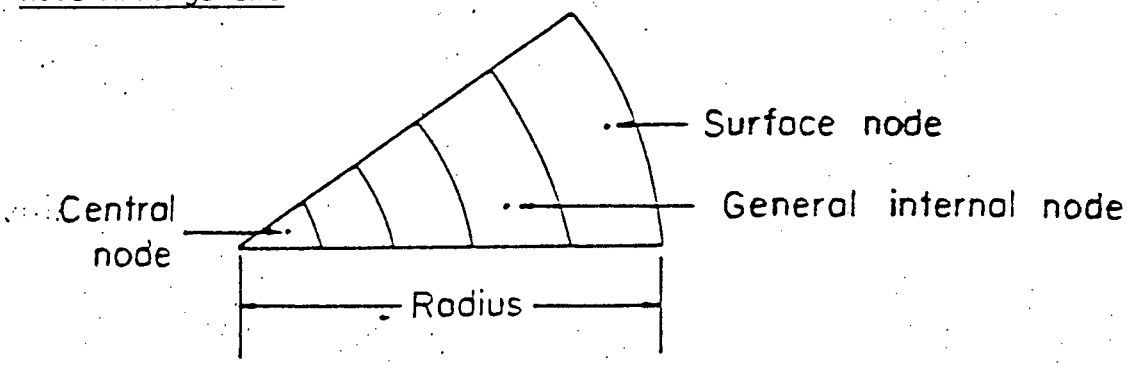


ii) Heat Flow Equations

a) Central Node

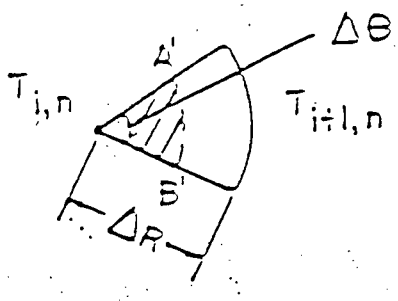


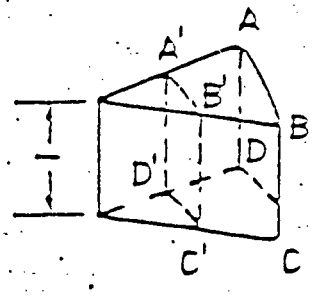

Heat flow across A'B'C'D' is:

$$-K_{i,i+1} \frac{\Delta R}{2} \Delta\theta \cdot 1 \frac{T_{i+1,n} - T_{i,n}}{\Delta R}$$

Rate of heat accumulation is:

$$\rho C_p \frac{T_{i,n+1} - T_{i,n}}{\Delta t} \frac{1}{2} \left(\frac{\Delta R}{2}\right)^2 \Delta\theta \cdot 1$$

$$\therefore -K_{i,i+1} \frac{T_{i,n+1} - T_{i,n}}{2} = \rho \frac{C_p \Delta R^2}{8\Delta t} T_{i,n+1} - T_{i,n}$$

$$\therefore T_{i,n} \left\{1 + \rho \cdot \frac{C_p \Delta R^2}{4K_{i,i+1}\Delta t}\right\} - T_{i+1,n}$$

$$= \rho \frac{C_p \Delta R^2}{4K_{i,i+1}\Delta t} \cdot T_{i,n+1}$$

The rate of latent heat generated due to transformation is:

$$\dot{q}_{AP} = H \cdot \rho \frac{\Delta F}{\Delta t} \frac{1}{2} \left(\frac{\Delta R}{2}\right)^2 \Delta\theta \cdot 1$$

$$\therefore T_{i,n} \left[1 + \rho \frac{C_p \Delta R^2}{4K_{i,i=1}\Delta t}\right] - T_{i+1,n}$$

$$= \rho \frac{C_p \Delta R^2}{4K_{i,i+1}\Delta t} \cdot T_{i,n+1} + H\rho \frac{\Delta F}{\Delta t} \frac{\Delta R^2}{4K_{i,i+1}}$$

b) General Internal Node

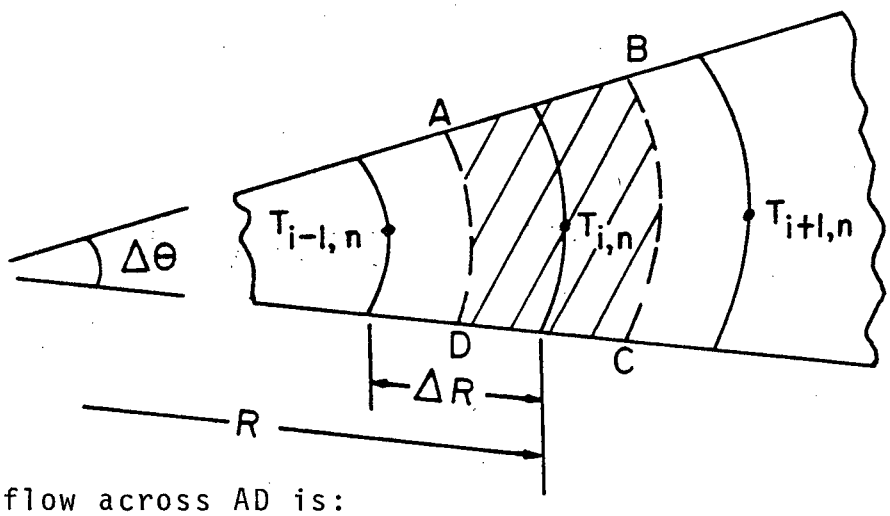


Inflow across AD is:

$$- \frac{K_{i-1,n} + K_{i,n}}{2} \left\{R - \frac{\Delta R}{2}\right\} \Delta\theta \quad \frac{T_{i,n} - T_{i-1,n}}{\Delta R}$$

Outflow across BC is:

$$- \frac{K_{i+1,n} + K_{i,n}}{2} \left\{R + \frac{\Delta R}{2}\right\} \Delta\theta \quad \frac{T_{i+1,n} - T_{i,n}}{\Delta R}$$

Rate of accumulation is:

$$\rho C_p \frac{T_{i,n+1} - T_{i,n}}{\Delta t} \quad R \; \Delta\theta \; \Delta R$$

Rate of outflow - Rate of Inflow

= Rate of accumulation +

Rate of generation.

Rate of heat generation (due to latent heat liberation during transformation) is:

$$\dot{q}_{AP} = H\rho \frac{\Delta F}{\Delta t} \quad R\ \Delta\theta\ \Delta R$$

$$\therefore \quad T_{i-1,n}\ K_{i-1,i}\ \frac{\Delta R - 2R}{2} +$$

$$T_{i,n}\left[\left\{K_{i+1,i}\ \frac{2R + \Delta R}{2} + K_{i,i-1}\ \frac{2R - \Delta R}{2}\right\} + \rho\ \frac{C_p R \Delta R^2}{\Delta t}\right] +$$

$$T_{i+1,n}\left\{-K_{i+1,i}\ \frac{\Delta R + 2R}{2}\right\}$$

$$= T_{i,n+1}\ \rho\ \frac{C_p R \Delta R^2}{t} + H\rho\ \frac{\Delta F}{\Delta t}\ R\Delta R^2$$

c) Surface Node

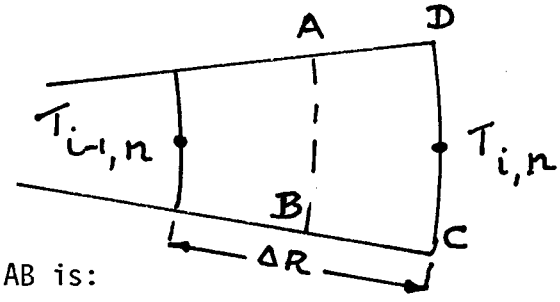


Inflow across AB is:

$$-K_{i-1,i}\left[R_0 - \frac{\Delta R}{2}\right]\Delta\theta 1\ \ \frac{T_{i,n} - T_{i-1,n}}{\Delta R}$$

Outflow across CD is:

$$h\left[T_a - T_{i,n}\right]\ R_0\Delta\theta$$

Rate of heat generation due to latent heat of transformation is:

$$\dot{q}_{AP} = H\rho \frac{\Delta F}{\Delta t} \left[R_0 - \frac{\Delta R}{2}\right] \Delta\theta \cdot 1 \cdot \frac{\Delta R}{2}$$

Rate of heat accumulation is:

$$\rho C_p \frac{T_{i,n+1} - T_{i,n}}{\Delta t} \left[R_0 - \frac{\Delta R}{2}\right] \Delta\theta \cdot 1 \cdot \frac{\Delta R}{2}$$

$$\therefore \quad T_{i-1,n} \; K_{i-1,i} \; \frac{\Delta R - 2R}{2\Delta R} +$$

$$T_{i,n} \; K_{i-1,i} \; \frac{2R - \Delta R}{2\Delta R} + hR_0 =$$

$$\rho \frac{C_p \Delta R \; (4R_0 - \Delta R)}{8\Delta t}$$

$$= hR_0T_a + \Delta RH\rho \frac{\Delta F}{\Delta t} \; (4R_0 - \Delta R) +$$

$$\rho \frac{C_p \Delta R}{8\Delta t} \; (4R_0 - \Delta R) \cdot T_{i,n}$$

# Appendix 7

## COMPARISON OF MODEL PREDICTION WITH ANALYTICAL SOLUTION OF EQ. (4.1)

For a body with negligible internal resistance, Eq. (4.1) can be re-written as:

$$V\rho C_p \frac{dT}{dt} = hA(T-T_a) \qquad (A7.1)$$

$$\therefore \quad \frac{\theta(t)}{\theta_0} = e^{-\frac{hA}{\rho V C_p} t} \qquad (A7.2)$$

where

$\theta(t) = T(t) - T_\infty$

$\theta_0 = T_0 - T_\infty$

$T(t)$ = temperature of body at any time t

$T_\infty$ = temperature of body at time = $\infty$

$T_0$ = initial temperature of the body

$h$ = convective heat-transfer co-efficient

$A$ = surface area

$\rho$ = density

$V$ = volume

$C_p$ = specific heat

$t$ = time

Using the above equation, the values of $T_t$ were calculated for rods of dia 5.5, 8.5, 13.5 and 25 mm with a value of $h = 250\ W/m^2\ °C$. The model predictions using the same h value were calculated. The values of $T_t$ predicted by the model for the surface of the rod were then compared with the analytical solution values. A sample computer output showing the comparison is shown in Fig. A7.1. For a 5.5 mm dia rod, the maximum difference between the two solutions is less than 1% in the pre-transformation period, the region where the comparison is meaningful.

## Summary of Comparison Results

(All comparisons made before the Start of the Transformation.)

| Rod diameter (mm) | Maximum difference between model predicted and analytical solution values of temperature (%) |
|---|---|
| 5.5 | 1.0 |
| 8.5 | 0.9 |
| 13.5 | 1.4 |
| 25 | 2.6 |

COMPARISON OF ANALYTICAL AND CALCULATED
VALUES OF TEMPERATURE FOR 0.8%C STEEL ROD

DIAMETER OF ROD= 5.5 MM

| TIME(SECONDS) | % DIFFERENCE |
|---|---|
| 0.10 | 0.395115344578634 |
| 0.20 | 0.505964762365217 |
| 0.30 | 0.550808718128153 |
| 0.40 | 0.569784433443964 |
| 0.50 | 0.577463027588642 |
| 0.60 | 0.578311603873660 |
| 0.70 | 0.576850442366463 |
| 0.80 | 0.574224223074626 |
| 0.90 | 0.569262148676523 |
| 1.00 | 0.566578789140192 |
| 1.10 | 0.561543548630365 |
| 1.20 | 0.555303321342505 |
| 1.30 | 0.550182225960195 |
| 1.40 | 0.543847722637660 |
| 1.50 | 0.537470009879105 |
| 1.60 | 0.531036110455511 |
| 1.70 | 0.524558328991617 |
| 1.80 | 0.516841917661739 |
| 1.90 | 0.510258825212505 |
| 2.00 | 0.502428403952435 |
| 2.10 | 0.493338134677705 |
| 2.20 | 0.486594560740012 |
| 2.30 | 0.477376003093878 |
| 2.40 | 0.468094394994059 |
| 2.50 | 0.458737923146185 |
| 2.60 | 0.449317476984690 |
| 2.70 | 0.438601864670495 |
| 2.80 | 0.427807486631018 |
| 2.90 | 0.418172622645464 |
| 3.00 | 0.407223576883559 |
| 3.10 | 0.396199465938024 |
| 3.20 | 0.383843670941287 |
| 3.30 | 0.372653719659355 |
| 3.40 | 0.360127487640224 |
| 3.50 | 0.348774253660875 |
| 3.60 | 0.336070751737211 |
| 3.70 | 0.322008113590259 |
| 3.80 | 0.309120976974933 |
| 3.90 | 0.296141228730804 |
| 4.00 | 0.281787557798469 |
| 4.10 | 0.267331568259515 |
| 4.20 | 0.252772762445194 |
| 4.30 | 0.239407821518229 |
| 4.40 | 0.223347617192569 |
| 4.50 | 0.208479920777633 |
| 4.60 | 0.192199573761493 |
| 4.70 | 0.175804568294831 |
| 4.80 | 0.160612962255957 |
| 4.90 | 0.143991334099522 |
| 5.00 | 0.127255133286501 |
| 5.10 | 0.110401702580471 |
| 5.20 | 0.093430501054428 |
| 5.30 | 0.076340989754242 |
| 5.40 | 0.057788708355173 |

| | |
|---|---|
| 5.50 | 0.040456893180318 |
| 5.60 | 0.021651172546309 |
| 5.70 | 0.002715730871076 |
| 5.80 | -0.014988009592328 |
| 5.90 | -0.032814230437934 |
| 6.00 | -0.052134782131489 |
| 6.10 | -0.071588859672065 |
| 6.20 | -0.089795128959617 |
| 6.30 | -0.109512323601988 |
| 6.40 | -0.129364306579489 |
| 6.50 | -0.149351646357633 |
| 6.60 | -0.169477281640425 |
| 6.70 | -0.189737319222494 |
| 6.80 | -0.210137364962064 |
| 6.90 | -0.229263667369554 |
| 7.00 | -0.248516004430685 |
| 7.10 | -0.270747834017325 |
| 7.20 | -0.290273686618808 |
| 7.30 | -0.309930696052692 |
| 7.40 | -0.329719378572555 |
| 7.50 | -0.351085040598724 |
| 7.60 | -0.369699166364627 |
| 7.70 | -0.391341034071401 |
| 7.80 | -0.411672822294564 |
| 7.90 | -0.430674577016040 |
| 8.00 | -0.451271497868586 |
| 8.10 | -0.470536175234161 |
| 8.20 | -0.489920369438442 |
| 8.30 | -0.509438726254661 |
| 8.40 | -0.529084757887836 |
| 8.50 | -0.547363383483388 |
| 8.60 | -0.565768740151578 |
| 8.70 | -0.587287484753110 |
| 8.80 | -0.607434270172263 |
| 8.90 | -0.629216890304000 |
| 9.00 | -0.655682838148267 |
| 9.10 | -0.683823304942449 |
| 9.20 | -0.718223583460949 |
| 9.30 | -0.760462115160079 |
| 9.40 | -0.810602558175372 |
| 9.50 | -0.873288200562619 |
| 9.60 | -0.951701903403813 → Transformation Start. |
| 9.70 | -1.048983651395537 |
| 9.80 | -1.171394301914426 |
| 9.90 | -1.322094747522043 |
| 10.00 | -1.505746227816433 |
| 10.10 | -1.723840987020306 |
| 10.20 | -1.977839422006990 |
| 10.30 | -2.270624578570190 |
| 10.40 | -2.595793403077311 |
| 10.50 | -2.949940405244339 |
| 10.60 | -3.326696662329319 |
| 10.70 | -3.722737528202555 |
| 10.80 | -4.131765590017377 |
| 10.90 | -4.544530137822069 |
| 11.00 | -4.961002829053284 |
| 11.10 | -5.375185445459516 |
| 11.20 | -5.784053674520205 |
| 11.30 | -6.186274204109633 |
| 11.40 | -6.583374875373876 |

# Appendix 8

LISTING OF COMPUTER PROGRAM TO CALCULATE TEMPERATURE RESPONSE OF A STEEL ROD UNDERGOING COOLING.

Steel: 0.82% C - 0.82% Mn - 0.26% Si
(Plain carbon eutectoid)

Grain Size: 5 - 7 ASTM

Austenitising Conditions: 850°C - 5 minutes

```
1     C ****************************************************************
2     C This program calculates the temperature (in *C) inside a
3     C cylindrical rod of 0.82%C-0.82%Mn-0.26%Si steel undergoing
4     C cooling.It takes into account the effect of the latent heat
5     C of transformation of austenite to pearlite generated,during
6     C cooling,on the temperature of the rod.Calculations are
7     C based on a 1-D Implicit Finite Difference Unsteady State
8     C Heat Transfer Model.The model has been written for a constant
9     C node distance.Density is considered constant.Variations of Thermal
10    C Conductivity and Specific Heat have been incorporated into the
11    C model by using BISRA data.
12    C     ************************************************************
13
14
15
16
17          IMPLICIT REAL*8 (A-H,O-Z)
18          REAL*8 KK
19
20
21
22    C ********************************************************
23    C Data for this program is:
24    C ******************************
25    C DX           = Node distance,Meters
26    C DT           = Time increment,Seconds
27    C TOTTIM       = Total time counter,Seconds(Initial Value=0)
28    C H            = Convective Heat transfer coefficient at the rod
29    C                surface,W/m *C
30    C R            = Radius of rod,Meters
31    C TATMOS       = Atmospheric temperature at rod surface,*C
32    C XX           = Distance of node from the rod centre,Meters
33    C M            = Number of nodes+1
34    C DD           = Density of steel,Kg/cubic Meter
35    C T1           = Maximum time upto which calculations are to
36    C                be done
37    C FRMAX        = Maximum Fraction transformed after which
38    C                check for transformation at the node is
39    C                terminated.
40    C ************************************************************
41
42
43
44    C ************************************************************
45    C DATA FOR THIS PROGRAM IS ENTERED BY INPUTTING APPROPRIATE
46    C VALUES OF THE VARIABLES IN THE STATEMENT NO.62.IF THE
47    C PROGRAM IS TO BE RUN WITH A CONSTANT HEAT TRANSFER
48    C COEFFICIENT,THEN INSERT THE FOLLOWING AFTER THE
49    C STATEMENT NO.167:
50    C GO TO 220
51    C INSERT AFTER STATEMENT NO.221
52    C H=PRESELECTED VALUE.
53    C BY THE ABOVE PROCEDURE THE CALCULATION OF THE HEAT
54    C TRANSFER COEFFICIENT FOR A GIVEN AIR VELOCITY,EMISSIVITY,
55    C ETC. IS BYPASSED.(THE PROGRAM DOES NOT EXECUTE STATEMENT
56    C NOS.175 TO 221)
57    C ************************************************************
58
59
60
```

```
      DATA DX,DT,T1,DD,TATMOS,R,XX,M,FRMAX/ 0.0075D0,0.1D0,100.0D0,
     17650.0D0,20.0D0,0.015D0,0.0D0,11,0.99D0/
      VEL=20.0D0
      EMISS=0.3D0
      TOTTIM=0.0D0
      J1=0
      K9=0
      K1=0

C ****************************************************************
C Matrix Identification
C **********************
C AA,BB,C          *   Contain coefficients of the Tridiagonal
C                     system at each time step
C D                *   Contains the RHS of the tridiagonal system
C T                *   Contains the temperature of each node at
C                      each time step
C KK,CP            *   Contain Thermal Conductivity and Specific
C                      Heat of each node at each time step
C THERM1,THERM2    *   Contain coefficients of the Polynomial used
C                      to calculate Thermal Conductivity as a function
C                      of temperature for Ferrite and Austenite
C                      respectively
C CP1,CP2          *   Contain coefficients of the polynomial used
C                      to calculate Specific Heat as a function of
C                      temperature for Austenite and Pearlite resply
C F                *   Contains total fraction transformed for each
C                      node at each time step
C DF               *   Contains the incremental fraction transformed
C                      for each node at each time step
C AN,ALB           *   Contains the coefficients of the Polynomial
C                      used to calculate 'n' and 'Log b' as a
C                      function of temperature.The data for these
C                      was generated at the Metallurgy Dept.of UBC.
C JJ               *   Contains the information on whether a node
C                      has started transformation.If JJ(i)=i, then
C                      the 'i'th node has started transforming.If
C                      not,JJ(i)=0
C TAVRAM           *   Contains the Avrami time for each node at
C                      each time step.The data for this has been
C                      generated at the Metallurgy Dept. of UBC
C BETA,GAMMA       *   Are dummy matrices used for calculating the
C                      temperature of each node at each time step
C ****************************************************************
C                  *   UNITS   *
C                  *************
C Time                    *          Seconds
C Distance                *          Meters
C Specific Heat           *          W/Kg *C
C Thermal Conductivity    *          W/M *C
C Convection Heat
C Transfer Coefficient    *          W/m2 *C
C Density                 *          Kg/m3
C Note on Dimensioning of Matrices
C *********************************
C Matrices AA,BB,C,D,T,TT,DF,KK,CP,JJ,F,TAVRAM,BETA,GAMMA should
C be dimensioned at least M (=no. of nodes+1)
C ****************************************************************
```

```
121
122
123
124
125           DIMENSION AA(30),BB(30),C(30),D(30),T(30),TT(30),DF(30),
126          1KK(30),CP(30),ALB(10),AN(5),THERM1(10),THERM2(10),F(50,2),JJ(3
127          1CP1(10),CP2(10),TAVRAM(30),H1(20),BETA(30),GAMMA(30)
128           DIMENSION K5(100),TAV(100),TA1(100),TI(100)
129           CALL THER(THERM1)
130           CALL THERMA(THERM2)
131           CALL CEEPE2(CP2)
132           CALL CEEPE1(CP1)
133           CALL LOGB(ALB)
134           CALL EXPONT(AN)
136           DO 3001 I=1,M
137      3001 K5(I)=0
138
139
140      C ************************************************************
141      C Initialisation of Temperature at all nodes at TOTTIM=0.The
142      C fraction transformed matrix F and the JJ matrix are also
143      C initialised to 0.
144      C ************************************************************************
145
146
147
148           DO 10 I=1,M
149           F(I,1)=0.0D0
150           F(I,2)=0.0D0
151           JJ(I)=0
152      10   T(I)=850.0D0
153
154
155
156      C ****************************************************************
157      C Starting with TOTTIM=0 the time is incremented in steps of
158      C DT.The calculations will stop when TOTTIM value is Greater
159      C than or Equal to a prespecified value
160      C ************************************************************
161
162
163
164
165      25    TOTTIM=TOTTIM+DT
166           IF (TOTTIM.GE.T1) GO TO 1001
167           K7=0
168
169
170
171      C ************************************************************
172      C Calculation of convective heat transfer coefficient by
173      C using air velocity
174      C ************************************************************
175           TEM=((T(M)+TATMOS)/2.0D0)*1.8D0+32.0D0
176           IF (TEM.GT.900.0D0) AIRK=(1.617D-05*TEM+1.575D-02)/2419.0D0
177           IF (TEM.LE.900.0D0) AIRK=(1.860D-05*TEM+1.372D-02)/2419.0D0
178           IF (VEL.LE.(0.1D-8).AND.VEL.GE.(-0.1D-8)) GO TO 130
179           IF (TEM.GT.1000.0D0) AIRNU=(1.233D-06*TEM-3.060D-04)*9.2894D-02
180           IF (TEM.LE.1000.0D0.AND.TEM.GT.800.0D0)
181          1AIRNU=(1.0D-06*TEM-8.3D-05)*9.2894D-02
```

```
      IF (TEM.LE.800.0D0) AIRNU=(8.475D-07*TEM+3.9D-05)*9.2894D-02
      RE=(VEL*2.0D0*R)/AIRNU
      IF (RE.GE.0.4D0.AND.RE.LT.4.0D0)            VC=0.891D0
      IF (RE.GT.0.4D0.AND.RE.LT.4.0D0)            VN=0.33D0
      IF (RE.GT.4.0D0.AND.RE.LT.40.0D0)           VC=0.821D0
      IF (RE.GT.4.0D0.AND.RE.LT.40.0D0)           VN=0.385D0
      IF (RE.GT.40.0D0.AND.RE.LT.4000.0D0)        VC=0.615D0
      IF (RE.GT.40.0D0.AND.RE.LT.4000.0D0)        VN=0.466D0
      IF (RE.GT.4000.0D0.AND.RE.LT.40000.0D0)     VC=0.174D0
      IF (RE.GT.4000.0D0.AND.RE.LT.40000.0D0)     VN=0.618D0
      IF (RE.GT.40000.0D0.AND.RE.LT.400000.0D0)   VC=0.0239D0
      IF (RE.GT.40000.0D0.AND.RE.LT.400000.0D0)   VN=0.805D0
      H=(VC*AIRK/(2.0D0*R))*(RE**VN)+1.366D-11*EMISS*(((T(M)
     1+273.0D0)**4)-((TATMOS+273.0D0)**4))/(T(M)-TATMOS)
      GO TO 230


C ************************************************************
C Calculation of the radiative heat transfer coefficient
C ************************************************************


130   D2=(T(M)-TATMOS)*1.8D0
      IF (TEM.GT.1000.0D0) GR=(335.29345D0*(10.0D0**(TEM
     1*(-0.00110218D0))))*1000.0D0
      IF (TEM.LE.1000.0D0.AND.TEM.GT.800.0D0) GR=(621.10241D0
     1*(10.0D0**(TEM*(-0.00136992D0))))*1000.0D0
      IF (TEM.LE.800.0D0.AND.TEM.GT.500.0D0) GR=(1100.7197D0
     1*(10.D0**(TEM*(-0.00168056D0))))*1000.0D0
      IF (TEM.LE.500.0D0.AND.TEM.GT.300.0D0) GR=(2071.8664D0
     1*(10.D0**(TEM*(-0.00222993D0))))*1000.0D0
      IF (TEM.LE.300.0D0) GR=(4200.0D0*(10.D0**(TEM*(-0.00325289D0)
     1)))*1000.0D0
      D1=(2.0D0*R)*3.2808399D0
      NUS=0.53D0*((GR*(D1**3.0D0)*D2*0.7D0)**0.25D0)
      H=((AIRK*2419.0D0*NUS/D1)/737.3D0)+
     11.366D-11*EMISS*(((T(M)+273.0D0)**4)-
     1((TATMOS+273.0D0)**4))/(T(M)-TATMOS)
230   H=H*1000.0D0
      H=4.186D0*H
220   H=50.0D0

C ************************************************************
C Loop 60
C *******
C In this loop ,the values of Thermal Conductivity and Specific
C Heat for Austenite are calculated for each node at each time
C step
C Loop 70
C *******
C In this loop,values of Thermal Conductivity and Specific
C Heat of Ferrite are calculated for each node at each
C time step.
C Loop 55
C *******
C In this loop the values of Fraction Transformed for each node
C at each time step are checked to find whether transformation
C of Austenite to Pearlite is complete at all nodes.If so,
C control is directed to Loop 70 wherein the values of
C Thermal Conductivity and Specific Heat are calculated.On
```

```
242     C entering Loop 70 a counter J1 is set equal to 1.For all
243     C future time steps control is directed to Loop 70 without
244     C going through Loop 55.On complete transformation at all
245     C nodes, from Loop 70 control is directed to statement no.820
246     C wherein the appropriate Tridiagonal System coefficients
247     C are calculated,bypassing Loop 501.
248     C ***************************************************************
249
250
251
252           IF (J1.EQ.1) GO TO 70
253           L=0
254           DO 55 I=1,M
255           IF (F(I,1).LT.FRMAX) GO TO 55
256           L=L+1
257     55    CONTINUE
258           IF (L.EQ.M) GO TO 70
259           DO 60 I=1,M
260           KK(I)=THERM2(1)+THERM2(2)*T(I)
261           KK(I)=418.6D0*KK(I)
262           CP(I)=CP1(1)+CP1(2)*T(I)+CP1(3)*(T(I)**2)+CP1(4)*(T(I)**3)
263          1+CP1(5)*(T(I)**4)+CP1(6)*(T(I)**5)
264           CP(I)=4186.0D0*CP(I)
265     60    CONTINUE
266           GO TO 700
267     70    DO 600 I=1,M
268           KK(I)=THERM1(1)+THERM1(2)*T(I)+THERM1(3)*(T(I)**2)
269          1+THERM1(4)*(T(I)**3)+THERM1(5)*(T(I)**4)
270           KK(I)=KK(I)*418.6D0
271           CP(I)=CP2(1)+CP2(2)*T(I)+CP2(3)*(T(I)**2)
272           CP(I)=CP(I)*4186.0D0
273     600    CONTINUE
274           J1=1
275           GO TO 820
276     C ***************************************************************
277
278
279
280     C Loop 501
281     C *********
282     C In this loop,each node is checked,at each time step for
283     C transformation start.At each time step,for each node, the
284     C Avrami time is calculated.If the TOTTIM value is Greater
285     C than or Equal to the Avrami time the node will start
286     C transforming.Once a node starts transforming,JJ(node) is
287     C set equal to node number.For all future time steps this
288     C node will not be checked again for transformation start.
289     C When a node starts transforming,control is directed to
290     C statement no.500 wherein 'n','log b' for that node
291     C temperature are calculated.The fraction transformed is
292     C then calculated.The Specific Heat and Thermal Conductivity
293     C of the transforming node is then calculated by using the
294     C formula
295     C Specific Heat=%Transformed*Specific Heat of Ferrite +
296     C                (1-%transformed)*Specific Heat of Austenite
297     C                 at the node temperature
298     C When the fraction transformed of the node is equal to 1
299     C control is transferred to statement no. 8000 where the
300     C Specific Heat and Thermal Conductivity values of Ferrite
301     C are used for further calculations.
```

```
C ***********************************************************
700   DO 501 I=1,M
      IF(T(I).GT.728.0D0) GO TO 501
      IF (F(I,1).GE.FRMAX) GO TO 501
      IF (JJ(I).NE.0) GO TO 500
      IF(K5(I).EQ.1) GO TO 229
      TAV(I)=TOTTIM
      K5(I)=1
229   IF (T(I).GE.700.0D0) GO TO 501
      TAVRAM(I)=62.7348D0+0.105339D0*(728.0D0-T(I))-15.4325D0
     1*(DLOG(728.0D0-T(I)))
      TAVRAM(I)=DEXP(TAVRAM(I))
       TA1(I)=TOTTIM-TAV(I)
      IF (TA1(I).LT.TAVRAM(I)) GO TO 501
      JJ(I)=I
500   EN=AN(1)+AN(2)*T(I)+AN(3)*(T(I)**2)+AN(4)*(T(I)**3)
      TT(I)=728.0D0-T(I)
      ALOGB=ALB(1)+ALB(2)*(TT(I))+ALB(3)*((TT(I))**2)+
     1ALB(4)*((TT(I))**3)
      ALOGB=DEXP(ALOGB)
      THETA=DT+(DLOG(1.0D0/(1.0D0-F(I,1)))/ALOGB)**(1.0D0/EN)
      F(I,2)=1.0D0-DEXP(-ALOGB*(THETA**EN))
      DF(I)=F(I,2)-F(I,1)
      FK=THERM1(1)+THERM1(2)*T(I)+THERM1(3)*(T(I)**2)+THERM1(4)*
     1(T(I)**3)+THERM1(5)*(T(I)**4)
      FK=FK*418.6D0
      FCP=CP2(1)+CP2(2)*T(I)+CP2(3)*(T(I)**2)
      FCP=FCP*4186.0D0
      KK(I)=(F(I,2)*FK+(1.0D0-F(I,2))*KK(I))
      CP(I)=(F(I,2)*FCP+(1.0D0-F(I,2))*CP(I))
501   CONTINUE


C ***********************************************************
C Loop 7000
C *********
C This loop calculates the appropriate values of the Tridiagonal
C System Coefficients AA,BB,C,D
C ***********************************************************


820   XX=-DX
      DO 7000 I=1,M
      XX=XX+DX
7050  IF(I.GT.1) GO TO 7051
      AK1=(KK(1)+KK(2))/2.0D0
      BB(1)=1.0D0+((DD*CP(1)*(DX**2))/(4.0D0*AK1*DT))
      C(1)=-1.0D0
      IF ((F(I,1).LE.0.0D0).OR. (F(I,1).GE.FRMAX)) GO TO 450
      D(1)=((DX**2)/(4.0D0*AK1))*
     1(DD*80000.0D0*DF(1)/DT)+((DD*CP(1)*(DX**2)*T(I))/
     1(4.0D0*AK1*DT))
      GO TO 7000
450   D(1)=(BB(1)-1.0D0)*T(1)
```

```
      GO TO 7000
7051  IF (I.EQ.M) GO TO 7052
      AK2=(KK(I-1)+KK(I))/(2.0D0)
      AA(I)=AK2*((DX-2.0D0*XX)/(2.0D0*DX))
      AK3=AK2*(2.0D0*XX-DX)/(2.0D0*DX)
      AK4=(KK(I)+KK(I+1))/(2.0D0)
      AK4=AK4*(2.0D0*XX+DX)/(2.0D0*DX)
      BB(I)=AK3+AK4+((DD*CP(I)*XX*DX)/(DT))
      AK4=(KK(I)+KK(I+1))/(2.0D0)
      C(I)=-AK4*((2.0D0*XX+DX)/(2.0D0*DX))
      IF ((F(I,1).LE.0.0D0).OR.(F(I,1).GE.FRMAX)) GO TO 451
      D(I)=(XX*DX*(DD*80000.0D0*DF(I)/DT))+(DD*CP(I)*XX*DX*T(I)/DT)
      GO TO 7000
451   D(I)=(DD*CP(I)*XX*DX*T(I))/DT
      GO TO 7000
7052  IF ((F(I,1).LE.0.0D0).OR.(F(I,1).GE.FRMAX)) GO TO 350
      D(M)=((DX)*(4.0D0*R-DX)*
     1(80000.0D0*DD*DF(M)/DT))/(8.0D0)+(H*TATMOS*R)+
     1((DD*CP(M)*DX*(4.0D0*R-DX)*T(M))/(8.0D0*DT))
      GO TO 351
350   D(M)=(H*R*TATMOS)+((DD*CP(M)*DX*(4.0D0*R-DX)*T(M))/
     1(8.0D0*DT))
351   AK5=(KK(M-1)+KK(M))/(2.0D0)
      AA(M)=AK5*((DX-2.0D0*R)/(2.0D0*DX))
      BB(M)=AK5*((2.0D0*R-DX)/(2.0D0*DX))+(H*R)+((DD*CP(M)*DX*
     1(4.0D0*R-DX))/(8.0D0*DT))
7000  CONTINUE

C ***************************************************************
C This part of the program calculates the temperature of each node
C at each time step.The algorithm used is the solution of a
C Tridiagonal System of Simultaneous Equations described in the
C book 'Applied Numerical Methods' by Carnahan,Luther and Wilkes.
C T(M) is the temperature of the surface node and T(1) is the
C temperature of the Centre of the rod.After the calculations of
C temperature for one time step are completed control is
C transferred to statement no. 25 where the TOTTIM is incremented
C by DT and the calculation of the Tridiagonal System coefficients
C etc. is repeated.
C ***************************************************************



      BETA(1)=BB(1)
      GAMMA(1)=D(1)/BETA(1)
      DO 110 I=2,M
      BETA(I)=BB(I)-AA(I)*C(I-1)/BETA(I-1)
110   GAMMA(I)=(D(I)-AA(I)*GAMMA(I-1))/BETA(I)
      TI(M)=GAMMA(M)
      MAST=M-1
      DO 120 J=1,MAST
      I=M-J
120   TI(I)=GAMMA(I)-C(I)*TI(I+1)/BETA(I)



C ***************************************************************
C If transformation starts at any node,the latent heat
```

```
C liberated due to the transformation is calculated by an
C iterative procedure.K7 is controls the number of iterations
C to be performed.
C ************************************************************


      IF (K7.GE.3) GO TO 6002
      IF (JJ(M).EQ.0) GO  TO 6002
      IF (J1.EQ.1) GO TO 6002
      DO 6003 II=1,M
      TI(II)=(TI(II)+T(II))/2.0D0
      IF (JJ(II).EQ.0) GO TO 6600
      IF (F(II,2).GE.FRMAX) GO TO 6005
      EN=AN(1)+AN(2)*TI(II)+AN(3)*(TI(II)**2)+AN(4)*(TI(II)**3)
      TT(II)=728.0D0-T(II)
      ALOGB=ALB(1)+ALB(2)*(TT(II))+ALB(3)*((TT(II))**2)+
     1ALB(4)*((TT(II))**3)
      ALOGB=DEXP(ALOGB)
      THETA=DT+(DLOG(1.0D0/(1.0D0-F(II,1)))/ALOGB)**(1.0D0/EN)
      F(II,2)=1.0D0-DEXP(-ALOGB*(THETA**EN))
      DF(II)=F(II,2)-F(II,1)
6005  FK=THERM1(1)+THERM1(2)*T(II)+THERM1(3)*(T(II)**2)+THERM1(4)*
     1(T(II)**3)+THERM1(5)*(T(II)**4)
      FK=FK*418.6D0
      FCP=CP2(1)+CP2(2)*T(II)+CP2(3)*(T(II)**2)
      FCP=FCP*4186.0D0
      KK(II)=(F(II,2)*FK+(1.0D0-F(II,2))*KK(II))
      CP(II)=(F(II,2)*FCP+(1.0D0-F(II,2))*CP(II))
      GO TO 6003
6600  KK(II)=THERM2(1)+THERM2(2)*TI(II)
      KK(II)=418.6D0*KK(II)
      CP(II)=CP1(1)+CP1(2)*T(II)+CP1(3)*(T(II)**2)+CP1(4)*(T(II)**3)
     1+CP1(5)*(T(II)**4)+CP1(6)*(T(II)**5)
      CP(II)=4186.0D0*CP(II)
6003  CONTINUE
      K7=K7+1
      GO TO 820
6002  DO 6004 I1=1,M
      F(I1,1)=F(I1,2)
6004  T(I1)=TI(I1)
      K9=K9+1
      IF (K9.LE.9) GOTO 325
      K9=0
      WRITE(6,730) TOTTIM,T(M),T(1)
730   FORMAT(5X,F8.2,5X,F6.2,5X,F6.2)
325    GO TO 25


C ********************************************************************
C Calculation of temperature for all nodes for the current time
C step is complete.Control is now transferred to statement no.25
C for incrementing the TOTTIM value by DT and further calculations.
C ********************************************************************


1001  STOP
      END
```

```
482
483     C ***************************************************************
484     C End of main program.Start of subroutines.
485     C ***************************************************************
486
487
488           SUBROUTINE THER(THERM1)
489
490
491     C ***************************************************************************
492     C In this subroutine a Polynomial of the 4th degree is fitted to
493     C Thermal Conductivity values of Ferrite in the temperature range
494     C 50*C to 750*C,the data for which has been obtained from the
495     C BISRA report.This Polynomial is the best fit for the data used
496     C and calculates Thermal Conductivity values in the temperature
497     C range within 0.5% of the experimental values.
498     C ***************************************************************************
499
500
501
502           IMPLICIT REAL*8 (A-H,O-Z)
503           DIMENSION X(25),Y(25),YF(25),YD(25),WT(25),S(20),A(20),B(20),
504          1SIGMA(20),P(20),THERM1(10)
505           DATA K,N/4,14/
506           X(1)=50.0D0
507           DO 3300 I=2,14
508     3300  X(I)=X(I-1)+50.0D0
509           DATA (Y(I),I=1,14)/0.118D0,0.115D0,0.112D0,0.108D0,0.103D0,
510          10.099D0,0.096D0,0.091D0,0.087D0,0.084D0,0.081D0,0.078D0,
511          10.075D0,0.072D0/
512           LOGICAL LK
513           LK= .TRUE.
514           NWT=0
515           CALL DOLSF(K,N,X,Y,YF,YD,WT,NWT,S,SIGMA,A,B,SS,LK,P)
516           DO 3400 I=1,5
517     3400  THERM1(I)=P(I)
518           RETURN
519           END
520     C ***************************************************************
521
522
523
524           SUBROUTINE THERMA(THERM2)
525     C ***************************************************************************
526     C In this subroutine a Polynomial of 1st degree is fitted to the
527     C Thermal Conductivity data of Austenite.The prediction error is
528     C less than 0.8%.
529     C ***************************************************************************
530
531
532
533           IMPLICIT REAL*8(A-H,O-Z)
534           DIMENSION X(25),Y(25),YF(25),YD(25),WT(25),S(20),A(20),B(20)
535          1,SIGMA(20),P(20)
536          1,THERM2(4)
537           DATA K,N/1,11/
538           X(1)=700.0D0
539           DO 2100 I=2,11
540     2100  X(I)=X(I-1)+50.0D0
541           DATA (Y(I),I=1,11)/0.053D0,0.055D0,0.057D0,0.059D0,0.061D0,
```

```
      10.063D0,
     10.064D0,0.066D0,0.068D0,0.070D0,0.072D0/
      LOGICAL LK
      LK= .TRUE.
      NWT=0
      CALL DOLSF(K,N,X,Y,YF,YD,WT,NWT,S,SIGMA,A,B,SS,LK,P)
      DO 2110 I=1,2
2110  THERM2(I)=P(I)
      RETURN
      END
C *******************************************************


      SUBROUTINE CEEPE2(CP2)
C ***************************************************************************
C In this subroutine a Polynomial of 2nd degree is fitted to the
C Specific Heat data of Ferrite.The prediction error is less than
C 1.0%.
C ***************************************************************************



      IMPLICIT REAL*8(A-H,O-Z)
      DIMENSION X(25),Y(25),YF(25),YD(25),WT(25),S(20),SIGMA(20),
     1A(20),B(20),P(20),CP2(3)
      DATA K,N/2,13/
      X(1)=75.0D0
      DO 4000 I= 2,13
4000  X(I)=X(I-1)+50.0D0
      DATA (Y(I),I=1,13)/0.117D0,0.124D0,0.127D0,0.131D0,0.135D0,
     10.140D0,0.145D0,0.150D0,0.160D0,0.166D0,0.172D0,0.172D0,
     10.184D0/
      LOGICAL LK
      LK= .TRUE.
      NWT=0
      CALL DOLSF(K,N,X,Y,YF,YD,WT,NWT,S,SIGMA,A,B,SS,LK,P)
      DO 4010 I=1,3
4010  CP2(I)=P(I)
      RETURN
      END
C *******************************************************



      SUBROUTINE CEEPE1(CP1)
C ************************************************************
C In this subroutine a Polynomial of 5th degree is fitted to
C the Specific Heat values of Austenite.The prediction error
C is less then 0.9%.
C ***************************************************************



      IMPLICIT REAL*8(A-H,O-Z)
      DIMENSION X(25),Y(25),YF(25),YD(25),S(20),WT(25),SIGMA(20),
     1A(20),B(20),P(20),CP1(10)
      DATA K,N/5,13/
      X(1)=675.0D0
      DO 5000 I=2,13
5000  X(I)=X(I-1)+50.0D0
```

```
      DATA (Y(I),I=1,13)/0.139D0,0.141D0,0.143D0,0.145D0,0.148D0,
     10.149D0,0.151D0,0.154D0,0.156D0,0.158D0,0.160D0,0.162D0,
     10.162D0/
      LOGICAL LK
      LK= .TRUE.
      NWT=0
      CALL DOLSF(K,N,X,Y,YF,YD,WT,NWT,S,SIGMA,A,B,SS,LK,P)
      DO 5010 I=1,6
5010  CP1(I)=P(I)
      RETURN
      END
C ***********************************************************


      SUBROUTINE LOGB(ALB)
C ***************************************************************
C In this subroutine a polynomial of 6th degree is fitted to
C the data of 'Log b' values obtained for 0.82%C-0.82%Mn-
C 0.26%Si steel in the Department of Metallurgy at UBC.
C ***************************************************************



      IMPLICIT REAL*8(A-H,O-Z)
      DIMENSION X(25),Y(25),YF(25),YD(25),WT(25),S(20),A(20),B(20)
     1,SIGMA(20),P(20),ALB(10)
      DATA K,N/3,8/
      DATA(X(I),I=1,8)/58.0D0,48.0D0,68.0D0,78.0D0,98.0D0,105.0D0,
     1113.0D0,125.0D0/
      DATA(Y(I),I=1,8)/-9.8133D0,-9.44464D0,-9.47115D0,-8.3921D0,
     1-5.7279D0,-4.51327D0,-3.1385D0,-2.04103D0/
      LOGICAL LK
      LK= .TRUE.
      NWT=0
      CALL DOLSF(K,N,X,Y,YF,YD,WT,NWT,S,SIGMA,A,B,SS,LK,P)
      DO 6100 I=1,4
6100  ALB(I)=P(I)
      RETURN
      END
C ***********************************************************



      SUBROUTINE EXPONT(AN)
C ***************************************************************
C In this subroutine a Polynomial of 1st degree is fitted to the
C data of 'n' values obtained for 0.82%C-0.82%Mn-0.26%Si steel in
C the Department of Metallurgy at UBC.
C ***************************************************************



      IMPLICIT REAL*8 (A-H,O-Z)
      DIMENSION X(25),Y(25),YF(25),YD(25),WT(25),S(20),A(20),B(20)
     1,SIGMA(20),P(20),AN(5)
      DATA K,N/3,8/
      DATA(X(I),I=1,8)/670.0D0,680.0D0,660.0D0,650.0D0,630.0D0,
     1623.0D0,615.0D0,603.0D0/
      DATA(Y(I),I=1,8)/2.125109D0,1.618956D0,2.467576D0,2.946133D0,
     13.166861D0,3.147945D0,2.922434D0,2.346407D0/
```

```
      LOGICAL LK
      LK= .TRUE.
      NWT=0
      CALL DOLSF(K,N,X,Y,YF,YD,WT,NWT,S,SIGMA,A,B,SS,LK,P)
      DO 6200 I=1,4
 6200 AN(I)=P(I)
      RETURN
      END
C ***************************************************************************
End of file
```

# Appendix 9

## LISTING OF COMPUTER PROGRAM TO CALCULATE THE TEMPERATURE RESPONSE OF A CENTRE-SEGREGATED STEEL ROD UNDERGOING COOLING

Matrix Steel: 0.82% C - 0.82% Mn - 0.26% Si

Grain Size: 5 - 7 ASTM

Segregated Steel: 0.8% C - 1.88% Mn

Grain Size: 5 - 8 ASTM

Austenitising Conditions: 850°C - 5 minutes

```
1     C ****************************************************************
2     C This program calculates the temperature (in *C) inside a
3     C cylindrical rod of 0.82%C-0.82%Mn-0.26%Si steel with a
4     C centre segregation of composition 0.8%C-1.88%Mn.It takes
5     C into account the effect of the transformational heat
6     C liberated,during cooling,on the temperature of the rod.It
7     C is assumed that the segregated region transforms to either
8     C pearlite or martensite,depending on the cooling rate.It is
9     C further assumed that no heat is liberated during the
10    C austenite to martensite transformation.
11    C                                                Calculations are
12    C based on a 1-D Implicit Finite Difference Unsteady State
13    C Heat Transfer Model.The model has been written for a constant
14    C node distance.Density is considered constant.Variations of Thermal
15    C Conductivity and Specific Heat have been incorporated into the
16    C model by using BISRA data.(it is assumed that the thermal
17    C conductivity and specific heat of the matrix material and the
18    C segregated material are the same.)
19    C     ****************************************************************
20
21
22
23
24          IMPLICIT REAL*8 (A-H,O-Z)
25          REAL*8 KK
26
27
28
29    C ********************************************************
30    C Data for this program is:
31    C ******************************
32    C DX           = Node distance,Meters
33    C DT           = Time increment,Seconds
34    C TOTTIM       = Total time counter,Seconds
35    C H            = Convective Heat transfer coefficient at the rod
36    C                surface,W/m *C
37    C R            = Radius of rod,Meters
38    C TATMOS       = Atmospheric temperature at rod surface,*C
39    C XX           = Distance of node from the rod centre,Meters
40    C M            = Number of nodes+1
41    C DD           = Density of steel,Kg/cubic Meter
42    C T1           = Maximum time upto which calculations are to
43    C                be done
44    C ************************************************************
45
46
47
48
49
50    C ********************************************************
51    C Data for this program must be input by replacing the
52    C values in statement no.60 by appropriate values.
53    C The no. of nodes segregated is given by the value of
54    C the variable IS.Before running the program, the appropriate
55    C value of this variable must be input.The appropriate
56    C heat transfer coefficient value must be input by replacing
57    C statement no.63
58    C ********************************************************
59
60          DATA DX,DT,TOTTIM,T1,DD,TATMOS,R,XX,M/0.00075D0,1.0D0,0.0D0,
```

```
      1400.0D0,7650.0D0,20.0D0,0.0075D0,0.0D0,11/
       K1=0
       H=1200.0D0
       IS=2


C ****************************************************************
C Matrix Identification
C ***********************
C AA,BB,C          *   Contain coefficients of the Tridiagonal
C                      system at each time step
C D                *   Contains the RHS of the tridiagonal system
C T                *   Contains the temperature of each node at
C                      each time step
C KK,CP            *   Contain Thermal Conductivity and Specific
C                      Heat of each node at each time step
C THERM1,THERM2    *   Contain coefficients of the Polynomial used
C                      to calculate Thermal Conductivity as a function
C                      of temperature for Ferrite and Austenite
C                      respectively
C CP1,CP2          *   Contain coefficients of the polynomial used
C                      to calculate Specific Heat as a function of
C                      temperature for Austenite and Pearlite resply
C F                *   Contains total fraction transformed for each
C                      node at each time step
C DF               *   Contains the incremental fraction transformed
C                      for each node at each time step
C AN,ALB           *   Contains the coefficients of the Polynomial
C                      used to calculate 'n' and 'Log b' as a
C                      function of temperature.The data for these
C                      was generated at the Metallurgy Dept.of UBC.
C JJ               *   Contains the information on whether a node
C                      has started transformation.If JJ(i)=i, then
C                      the 'i'th node has started transforming.If
C                      not,JJ(i)=0
C TAVRAM           *   Contains the Avrami time for each node at
C                      each time step.The data for this has been
C                      generated at the Metallurgy Dept. of UBC
C BETA,GAMMA       *   Are dummy matrices used for calculating the
C                      temperature of each node at each time step
C ****************************************************************
C                  *   UNITS   *
C                  *************
C Time                     *          Seconds
C Distance                 *          Meters
C Specific Heat            *          W/Kg *C
C Thermal Conductivity     *          W/M *C
C Convection Heat
C Transfer Coefficient     *          W/m2 *C
C Density                  *          Kg/m3
C Note on Dimensioning of Matrices
C ********************************
C Matrices AA,BB,C,D,T,TT,DF,KK,CP,JJ,F,TAVRAM,BETA,GAMMA should
C be dimensioned at least M (=no. of nodes+1)
C ****************************************************************
```

```
      DIMENSION AA(30),BB(30),C(30),D(30),T(30),TT(30),DF(30),
     1KK(30),CP(30),ALB(10),AN(5),THERM1(10),THERM2(10),F(50,2),JJ(3(
     1CP1(10),CP2(10),TAVRAM(30),H1(20),BETA(30),GAMMA(30)
      DIMENSION K5(100),TAV(100),TA1(100),
     1ALB1(10),ALB2(10),AL1(10),AL2(10)
      CALL THER(THERM1)
      CALL THERMA(THERM2)
      CALL CEEPE2(CP2)
      CALL CEEPE1(CP1)
      CALL LOGB(ALB)
      CALL EXPONT(AN)
      CALL LOB(ALB2)
      CALL EXPO(ALB1)
      CALL EXP(AL1)
      CALL EX(AL2)
      J1=0
      DO 3001 I=1,M
3001  K5(I)=0

C ************************************************************
C Initialisation of Temperature at all nodes at TOTTIM=0.The
C fraction transformed matrix F and the JJ matrix are also
C initialised to 0.
C ************************************************************************



      DO 10 I=1,M
      F(I,1)=0.0D0
      F(I,2)=0.0D0
      JJ(I)=0
10    T(I)=850.0D0


C ****************************************************************
C Starting with TOTTIM=0 the time is incremented in steps of
C DT.The calculations will stop when TOTTIM value is Greater
C than or Equal to a prespecified value
C ************************************************************



25     TOTTIM=TOTTIM+DT
      IF (TOTTIM.GE.T1) GO TO 1001


C ****************************************************************
C Loop 60
C *******
C In this loop ,the values of Thermal Conductivity and Specific
C Heat for Austenite are calculated for each node at each time
C step
C Loop 70
C *******
C In this loop,values of Thermal Conductivity and Specific
C Heat of Ferrite are calculated for each node at each
```

```
C time step.
C Loop 55
C *******
C In this loop the values of Fraction Transformed for each node
C at each time step are checked to find whether transformation
C of Austenite to Pearlite is complete at all nodes.If so,
C control is directed to Loop 70 wherein the values of
C Thermal Conductivity and Specific Heat are calculated.On
C entering Loop 70 a counter J1 is set equal to 1.For all
C future time steps control is directed to Loop 70 without
C going through Loop 55.On complete transformation at all
C nodes, from Loop 70 control is directed to statement no.820
C wherein the appropriate Tridiagonal System coefficients
C are calculated,bypassing Loop 501.
C ***************************************************************



      IF (J1.EQ.1) GO TO 70
      L=0
      DO 55 I=1,M
      IF (F(I,1).LT.1.0D0) GO TO 55
      L=L+1
55    CONTINUE
      IF (L.EQ.M) GO TO 70
      DO 60 I=1,M
      KK(I)=THERM2(1)+THERM2(2)*T(I)
      KK(I)=418.6D0*KK(I)
      CP(I)=CP1(1)+CP1(2)*T(I)+CP1(3)*(T(I)**2)+CP1(4)*(T(I)**3)
     1+CP1(5)*(T(I)**4)+CP1(6)*(T(I)**5)
      CP(I)=4186.0D0*CP(I)
60    CONTINUE
      GO TO 700
70    DO 600 I=1,M
      KK(I)=THERM1(1)+THERM1(2)*T(I)+THERM1(3)*(T(I)**2)
     1+THERM1(4)*(T(I)**3)+THERM1(5)*(T(I)**4)
      KK(I)=KK(I)*418.6D0
      CP(I)=CP2(1)+CP2(2)*T(I)+CP2(3)*(T(I)**2)
      CP(I)=CP(I)*4186.0D0
600    CONTINUE
      J1=1
      GO TO 820
C ***************************************************************



C Loop 501
C *********
C In this loop,each node is checked,at each time step for
C transformation start.At each time step,for each node, the
C Avrami time is calculated.If the TOTTIM value is Greater
C than or Equal to the Avrami time the node will start
C transforming.Once a node starts transforming,JJ(node) is
C set equal to node number.For all future time steps this
C node will not be checked again for transformation start.
C When a node starts transforming,control is directed to
C statement no.500 wherein 'n','log b' for that node
C temperature are calculated.The fraction transformed is
C then calculated.The Specific Heat and Thermal Conductivity
C of the transforming node is then calculated by using the
```

```
C formula
C Specific Heat=%Transformed*Specific Heat of Ferrite +
C               (1-%transformed)*Specific Heat of Austenite
C                at the node temperature
C When the fraction transformed of the node is equal to 1
C control is transferred to statement no. 8000 where the
C Specific Heat and Thermal Conductivity values of Ferrite
C are used for further calculations.
C ********************************************************


700    DO 501 I=1,M
       IF (F(I,1).GE.0.99999D0) GO TO 501
       IF(T(I).GT.728.0D0) GO TO 501
       IF (I.GT.IS) GO TO 240
       IF (JJ(I).NE.0) GO TO 400
       IF (K5(I).EQ.1) GO TO 230
       TAV(I)=TOTTIM
       K5(I)=1
230    IF (T(I).GE.700.0D0) GO TO 501
       IF (T(I).GE.475.0D0) GO TO 4001
       TAVRAM(I)=35.2807D0-7.07259D0*(DLOG(728.0D0-T(I)))+0.0225313D0*
      1(728.0D0-T(I))
       GO TO 4002
4001   TAVRAM(I)=22.4126D0+0.0123409D0*(728.0D0-T(I))-
      14.27291D0*(DLOG(728.0D0-T(I)))
4002   TAVRAM(I)=DEXP(TAVRAM(I))
       TA1(I)=TOTTIM-TAV(I)
       IF (TA1(I).LT.TAVRAM(I)) GO TO 501
       JJ(I)=1
400    IF (T(I).GE.625.0D0) GO TO 4003
       IF (T(I).LT.500.0D0) GO TO 4004
       EN=AL1(1)+AL1(2)*T(I)+AL1(3)*(T(I)**2)
       GO TO 4005
4003   EN=ALB1(1)+ALB1(2)*T(I)
       GO TO 4005
4004   EN=AL2(1)+AL2(2)*T(I)
4005   ALOGB=ALB2(1)+ALB2(2)*(728.0D0-T(I))+ALB2(3)*
      1((728.0D0-T(I))**2)+ALB2(4)*((728.0D0-T(I))**3)
       ALOGB=DEXP(ALOGB)
       GO TO 410
240    IF (JJ(I).NE.0) GO TO 500
       IF(K5(I).EQ.1) GO TO 229
       TAV(I)=TOTTIM
       K5(I)=1
229    IF (T(I).GE.700.0D0) GO TO 501
       TAVRAM(I)=62.7348D0+0.105339D0*(728.0D0-T(I))-15.4325D0
      1*(DLOG(728.0D0-T(I)))
       TAVRAM(I)=DEXP(TAVRAM(I))
        TA1(I)=TOTTIM-TAV(I)
       IF (TA1(I).LT.TAVRAM(I)) GO TO 501
       JJ(I)=I
500    EN=AN(1)+AN(2)*T(I)+AN(3)*(T(I)**2)+AN(4)*(T(I)**3)
       TT(I)=728.0D0-T(I)
       ALOGB=ALB(1)+ALB(2)*(TT(I))+ALB(3)*((TT(I))**2)+
      1ALB(4)*((TT(I))**3)
       ALOGB=DEXP(ALOGB)
410    THETA=DT+(DLOG(1.0D0/(1.0D0-F(I,1)))/ALOGB)**(1.0D0/EN)
       F(I,2)=1.0D0-DEXP(-ALOGB*(THETA**EN))
```

```
301           DF(I)=F(I,2)-F(I,1)
302           F(I,1)=F(I,2)
303           FK=THERM1(1)+THERM1(2)*T(I)+THERM1(3)*(T(I)**2)+THERM1(4)*
304          1(T(I)**3)+THERM1(5)*(T(I)**4)
305           FK=FK*418.6D0
306           FCP=CP2(1)+CP2(2)*T(I)+CP2(3)*(T(I)**2)
307           FCP=FCP*4186.0D0
308           KK(I)=(F(I,1)*FK+(1.0D0-F(I,1))*KK(I))
309           CP(I)=(F(I,1)*FCP+(1.0D0-F(I,1))*CP(I))
310      501  CONTINUE
311
312
313
314      C ************************************************************
315      C Loop 7000
316      C *********
317      C This loop calculates the appropriate values of the Tridiagonal
318      C System Coefficients AA,BB,C,D
319      C ************************************************************************
320
321
322
323
324      820  XX=-DX
325           DO 7000 I=1,M
326           XX=XX+DX
327      7050 IF(I.GT.1) GO TO 7051
328           AK1=(KK(1)+KK(2))/2.0D0
329           BB(1)=1.0D0+((DD*CP(1)*(DX**2))/(4.0D0*AK1*DT))
330           C(1)=-1.0D0
331           IF ((F(I,1).LE.0.0D0).OR. (F(I,1).GE.0.99999D0)) GO TO 450
332           D(1)=((DX**2)/(4.0D0*AK1))*
333          1(DD*80000.0D0*DF(1)/DT)+((DD*CP(1)*(DX**2)*T(I))/
334          1(4.0D0*AK1*DT))
335           GO TO 7000
336      450  D(1)=(BB(1)-1.0D0)*T(1)
337           GO TO 7000
338      7051 IF (I.EQ.M) GO TO 7052
339           AK2=(KK(I-1)+KK(I))/(2.0D0)
340           AA(I)=AK2*((DX-2.0D0*XX)/(2.0D0*DX))
341           AK3=AK2*(2.0D0*XX-DX)/(2.0D0*DX)
342           AK4=(KK(I)+KK(I+1))/(2.0D0)
343           AK4=AK4*(2.0D0*XX+DX)/(2.0D0*DX)
344           BB(I)=AK3+AK4+((DD*CP(I)*XX*DX)/(DT))
345           AK4=(KK(I)+KK(I+1))/(2.0D0)
346           C(I)=-AK4*((2.0D0*XX+DX)/(2.0D0*DX))
347           IF ((F(I,1).LE.0.0D0).OR.(F(I,1).GE.0.99999D0)) GO TO 451
348           D(I)=(XX*DX*(DD*80000.0D0*DF(I)/DT))+(DD*CP(I)*XX*DX*T(I)/DT)
349           GO TO 7000
350      451  D(I)=(DD*CP(I)*XX*DX*T(I))/DT
351           GO TO 7000
352      7052 IF ((F(I,1).LE.0.0D0).OR.(F(I,1).GE.0.99999D0)) GO TO 350
353           D(M)=((DX)*(4.0D0*R-DX)*
354          1(80000.0D0*DD*DF(M)/DT))/(8.0D0)+(H*TATMOS*R)+
355          1((DD*CP(M)*DX*(4.0D0*R-DX)*T(M))/(8.0D0*DT))
356           GO TO 351
357      350  D(M)=(H*R*TATMOS)+((DD*CP(M)*DX*(4.0D0*R-DX)*T(M))/
358          1(8.0D0*DT))
359      351   AK5=(KK(M-1)+KK(M))/(2.0D0)
360           AA(M)=AK5*((DX-2.0D0*R)/(2.0D0*DX))
```

```
362           1(4.0D0*R-DX))/(8.0D0*DT))
363       7000  CONTINUE
364
365
366       C ***************************************************************
367       C This part of the program calculates the temperature of each node
368       C at each time step.The algorithm used is the solution of a
369       C Tridiagonal System of Simultaneous Equations described in the
370       C book 'Applied Numerical Methods' by Carnahan,Luther and Wilkes.
371       C T(M) is the temperature of the surface node and T(1) is the
372       C temperature of the Centre of the rod.After the calculations of
373       C temperature for one time step are completed control is
374       C transferred to statement no. 25 where the TOTTIM is incremented
375       C by DT and the calculation of the Tridiagonal System coefficients
376       C etc. is repeated.
377       C ***************************************************************
378
379
380
381
382             BETA(1)=BB(1)
383             GAMMA(1)=D(1)/BETA(1)
384             DO 110 I=2,M
385             BETA(I)=BB(I)-AA(I)*C(I-1)/BETA(I-1)
386       110   GAMMA(I)=(D(I)-AA(I)*GAMMA(I-1))/BETA(I)
387             T(M)=GAMMA(M)
388             WRITE(6,6301)TOTTIM,T(M)
389       6301  FORMAT(10X,F8.2,',',F6.2)
390             MAST=M-1
391             DO 120 J=1,MAST
392             I=M-J
393       120   T(I)=GAMMA(I)-C(I)*T(I+1)/BETA(I)
394             WRITE(6,6001)TOTTIM,T(1)
395       6001  FORMAT(10X,F8.2,',',F6.2)
396             PRINT,F(1,1),F(10,1)
397              GO TO 25
398
399
400
401       C ***************************************************************
402       C Calculation of temperature for all nodes for the current time
403       C step is complete.Control is now transferred to statement no.25
404       C for incrementing the TOTTIM value by DT and further calculations.
405       C ***************************************************************
406
407
408
409       1001  STOP
410             END
411
412
413       C ***************************************************************
414       C End of main program.Start of subroutines.
415
416
417
418       C ***************************************************************
419       C The Subroutines Ther,Therma,Ceepe2,Ceepe1,Logb,Expont are
420       C described in the program used for calculation of the
```

```
C temperature without segregation.Subroutine Lob calculates
C the coefficients of the polynomial used to find the value
C of 'b'at different temperatures.Subroutines Expo,Exp and
C Ex calculate the coefficients of the polynomials used to
C find the values of 'n' in the temperature ranges 700 to 625*C,
C 625 to 500*C,<500*C respectively for the segregated steel.
C ***************************************************************


      SUBROUTINE THER(THERM1)




      IMPLICIT REAL*8 (A-H,O-Z)
      DIMENSION X(25),Y(25),YF(25),YD(25),WT(25),S(20),A(20),B(20),
     1SIGMA(20),P(20),THERM1(10)
      DATA K,N/4,14/
      X(1)=50.0D0
      DO 3300 I=2,14
3300  X(I)=X(I-1)+50.0D0
      DATA (Y(I),I=1,14)/0.118D0,0.115D0,0.112D0,0.108D0,0.103D0,
     10.099D0,0.096D0,0.091D0,0.087D0,0.084D0,0.081D0,0.078D0,
     10.075D0,0.072D0/
      LOGICAL LK
      LK= .TRUE.
      NWT=0
      CALL DOLSF(K,N,X,Y,YF,YD,WT,NWT,S,SIGMA,A,B,SS,LK,P)
      DO 3400 I=1,5
3400  THERM1(I)=P(I)
      RETURN
      END
C ***********************************************************


      SUBROUTINE THERMA(THERM2)



      IMPLICIT REAL*8(A-H,O-Z)
      DIMENSION X(25),Y(25),YF(25),YD(25),WT(25),S(20),A(20),B(20)
     1,SIGMA(20),P(20)
     1,THERM2(4)
      DATA K,N/1,11/
      X(1)=700.0D0
      DO 2100 I=2,11
2100  X(I)=X(I-1)+50.0D0
      DATA (Y(I),I=1,11)/0.053D0,0.055D0,0.057D0,0.059D0,0.061D0,
     10.063D0,
     10.064D0,0.066D0,0.068D0,0.070D0,0.072D0/
      LOGICAL LK
      LK= .TRUE.
      NWT=0
      CALL DOLSF(K,N,X,Y,YF,YD,WT,NWT,S,SIGMA,A,B,SS,LK,P)
      DO 2110 I=1,2
2110  THERM2(I)=P(I)
      RETURN
      END
```

```
C ********************************************************
C
C
      SUBROUTINE CEEPE2(CP2)
C
C
C
      IMPLICIT REAL*8(A-H,O-Z)
      DIMENSION X(25),Y(25),YF(25),YD(25),WT(25),S(20),SIGMA(20),
     1A(20),B(20),P(20),CP2(3)
      DATA K,N/2,13/
      X(1)=75.0D0
      DO 4000 I= 2,13
4000  X(I)=X(I-1)+50.0D0
      DATA (Y(I),I=1,13)/0.117D0,0.124D0,0.127D0,0.131D0,0.135D0,
     10.140D0,0.145D0,0.150D0,0.160D0,0.166D0,0.172D0,0.172D0,
     10.184D0/
      LOGICAL LK
      LK= .TRUE.
      NWT=0
      CALL DOLSF(K,N,X,Y,YF,YD,WT,NWT,S,SIGMA,A,B,SS,LK,P)
      DO 4010 I=1,3
4010  CP2(I)=P(I)
      RETURN
      END
C ********************************************************
C
C
C
      SUBROUTINE CEEPE1(CP1)
C
C
C
      IMPLICIT REAL*8(A-H,O-Z)
      DIMENSION X(25),Y(25),YF(25),YD(25),S(20),WT(25),SIGMA(20),
     1A(20),B(20),P(20),CP1(10)
      DATA K,N/5,13/
      X(1)=675.0D0
      DO 5000 I=2,13
5000  X(I)=X(I-1)+50.0D0
      DATA (Y(I),I=1,13)/0.139D0,0.141D0,0.143D0,0.145D0,0.148D0,
     10.149D0,0.151D0,0.154D0,0.156D0,0.158D0,0.160D0,0.162D0,
     10.162D0/
      LOGICAL LK
      LK= .TRUE.
      NWT=0
      CALL DOLSF(K,N,X,Y,YF,YD,WT,NWT,S,SIGMA,A,B,SS,LK,P)
      DO 5010 I=1,6
5010  CP1(I)=P(I)
      RETURN
      END
C ********************************************************
C
C
      SUBROUTINE LOGB(ALB)
C
C
C
      IMPLICIT REAL*8(A-H,O-Z)
      DIMENSION X(25),Y(25),YF(25),YD(25),WT(25),S(20),A(20),B(20)
```

```
      1,SIGMA(20),P(20),ALB(10)
       DATA K,N/3,8/
       DATA(X(I),I=1,8)/58.0D0,48.0D0,68.0D0,78.0D0,98.0D0,105.0D0,
      1113.0D0,125.0D0/
       DATA(Y(I),I=1,8)/-9.8133D0,-9.44464D0,-9.47115D0,-8.3921D0,
      1-5.7279D0,-4.51327D0,-3.1385D0,-2.04103D0/
       LOGICAL LK
       LK= .TRUE.
       NWT=0
       CALL DOLSF(K,N,X,Y,YF,YD,WT,NWT,S,SIGMA,A,B,SS,LK,P)
       DO 6100 I=1,4
 6100  ALB(I)=P(I)
       RETURN
       END
C ************************************************************



       SUBROUTINE EXPONT(AN)



       IMPLICIT REAL*8 (A-H,O-Z)
       DIMENSION X(25),Y(25),YF(25),YD(25),WT(25),S(20),A(20),B(20)
      1,SIGMA(20),P(20),AN(5)
       DATA K,N/3,8/
       DATA(X(I),I=1,8)/670.0D0,680.0D0,660.0D0,650.0D0,630.0D0,
      1623.0D0,615.0D0,603.0D0/
       DATA(Y(I),I=1,8)/2.125109D0,1.618956D0,2.467576D0,2.946133D0,
      13.166861D0,3.147945D0,2.922434D0,2.346407D0/
       LOGICAL LK
       LK= .TRUE.
       NWT=0
       CALL DOLSF(K,N,X,Y,YF,YD,WT,NWT,S,SIGMA,A,B,SS,LK,P)
       DO 6200 I=1,4
 6200  AN(I)=P(I)
       RETURN
       END
       SUBROUTINE HEAT(H1)
       IMPLICIT REAL*8(A-H,O-Z)
       DIMENSION X(25),Y(25),YF(25),YD(25),WT(25),S(20),A(20),
      1B(20),SIGMA(20),P(20),H1(20)
       DATA K,N/6,10/
       DATA (Y(I),I=1,10)/81.94D0,165.67D0,195.48D0,200.91D0,223.82D0,
      1231.82D0,236.57D0,252.67D0,244.06D0,238.85D0/
       DATA (X(I),I=1,10)/890.0D0,860.0D0,830.0D0,805.0D0,770.0D0,
      1740.0D0,712.0D0,675.0D0,658.0D0,640.0D0/
       LOGICAL LK
       LK=.TRUE.
       NWT=0
       CALL DOLSF(K,N,X,Y,YF,YD,WT,NWT,S,SIGMA,A,B,SS,LK,P)
       DO 6300 I=1,7
 6300  H1(I)=P(I)
       RETURN
       END
C ************************************************************


       SUBROUTINE LOB(ALB2)

```

```
601
602
603           IMPLICIT REAL*8(A-H,O-Z)
604           DIMENSION X(25),Y(25),YF(25),YD(25),WT(25),S(20),A(20),B(20)
605          1,SIGMA(20),P(20),ALB2(10)
606           DATA K,N/3,12/
607           DATA(X(I),I=1,12)/53.0D0,78.0D0,103.0D0,128.0D0,153.0D0,
608          1178.0D0,203.0D0,228.0D0,253.0D0,276.0D0,303.0D0,328.0D0/
609           DATA(Y(I),I=1,12)/-6.09954D0,-4.60211D0,-5.08256D0,
610          1-5.57406D0,-4.00138D0,-4.02453D0,-2.9204D0,-2.97626D0,
611          1-3.78062D0,-3.9678D0,-4.37844D0,-5.02969D0/
612           LOGICAL LK
613           LK= .TRUE.
614           NWT=0
615           CALL DOLSF(K,N,X,Y,YF,YD,WT,NWT,S,SIGMA,A,B,SS,LK,P)
616           DO 6100 I=1,4
617      6100 ALB2(I)=P(I)
618           RETURN
619           END
620      C ***********************************************************
621
622
623           SUBROUTINE EXPO(ALB1)
624
625
626
627           IMPLICIT REAL*8(A-H,O-Z)
628           DIMENSION X(25),Y(25),YF(25),YD(25),WT(25),S(20),A(20),B(20)
629          1,SIGMA(20),P(20),ALB1(10)
630           DATA K,N/1,3/
631           DATA(X(I),I=1,3)/675.0D0,650.0D0,625.0D0/
632           DATA(Y(I),I=1,3)/0.770414D0,0.825272D0,1.276907D0/
633           LOGICAL LK
634           LK= .TRUE.
635           NWT=0
636           CALL DOLSF(K,N,X,Y,YF,YD,WT,NWT,S,SIGMA,A,B,SS,LK,P)
637           DO 6100 I=1,2
638      6100 ALB1(I)=P(I)
639           RETURN
640           END
641      C ***********************************************************
642
643
644           SUBROUTINE EXP(AL1)
645
646
647
648           IMPLICIT REAL*8(A-H,O-Z)
649           DIMENSION X(25),Y(25),YF(25),YD(25),WT(25),S(20),A(20),B(20)
650          1,SIGMA(20),P(20),AL1(10)
651           DATA K,N/2,5/
652           DATA(X(I),I=1,5)/600.0D0,575.0D0,550.0D0,525.0D0,500.0D0/
653           DATA(Y(I),I=1,5)/1.648218D0,1.205357D0,1.103574D0,0.74475D0,
654          10.715708D0/
655           LOGICAL LK
656           LK= .TRUE.
657           NWT=0
658           CALL DOLSF(K,N,X,Y,YF,YD,WT,NWT,S,SIGMA,A,B,SS,LK,P)
659           DO 6100 I=1,3
660      6100 AL1(I)=P(I)
```

```
      RETURN
      END
C ***********************************************************
C
C
      SUBROUTINE EX(AL2)
C
C
C
      IMPLICIT REAL*8(A-H,O-Z)
      DIMENSION X(25),Y(25),YF(25),YD(25),WT(25),S(20),A(20),B(20)
     1,SIGMA(20),P(20),AL2(10)
      DATA K,N/1,4/
      DATA(X(I),I=1,4)/475.0D0,450.0D0,425.0D0,400.0D0/
      DATA(Y(I),I=1,4)/0.851409D0,0.905354D0,0.987884D0,1.057347D0/
      LOGICAL LK
      LK= .TRUE.
      NWT=0
      CALL DOLSF(K,N,X,Y,YF,YD,WT,NWT,S,SIGMA,A,B,SS,LK,P)
      DO 6100 I=1,2
 6100 AL2(I)=P(I)
      RETURN
      END
End of file
```